1-1-2016

The Role Of Alarmins, Invariant Nkt Cells And Senescence In The Pathophysiology Of Sterile Intra-Amniotic Inflammation

Olesya Plazyo
Wayne State University,

THE ROLE OF ALARMINS, INVARIANT NKT CELLS AND SENESCENCE IN THE PATHOPHYSIOLOGY OF STERILE INTRA-AMNIOTIC INFLAMMATION

by

OLESYA PLAZYO

DISSERTATION

Submitted to the Graduate School

of Wayne State University,

Detroit, Michigan

in partial fulfillment of the requirements

for the degree of

DOCTOR OF PHILOSOPHY

2016

MAJOR: PHYSIOLOGY

Approved By:

_____

Advisor Date

_____

Co-Advisor

_____

_____

_____

DEDICATION

This dissertation is dedicated to my son Ian. Dear son, always seek knowledge.

ACKNOWLEDGEMENTS

Many people have helped me on the path towards my Doctorate degree. The invaluable support and vision of my advisor and mentor Dr. Nardhy Gomez-Lopez must be acknowledged first. She taught me how to remain strong in the face of challenges and how to quickly adapt to the changing environment. Her passion for science is truly contagious.

I would also like to thank Drs. Roberto Romero and Sonia S Hassan for their support and Drs. Yi Xu and Yang Jiang for teaching me the laboratory techniques. I am also grateful to all my lab mates for being there for me and for making our working environment exciting and peaceful.

Finally, I would like to thank my co-advisor Dr. Steven Cala and my other committee members Drs. Harley Y. Tse, James Rillema, and Bhanu Jena for their guidance. I am also grateful to Dr. Douglas Yingst and Christine Cupps for their assistance with the intricacies of the Physiology Department Graduate program and to Dr. Miriam Greenberg for her supervision of my Master's studies.

This work was supported by the Wayne State University Perinatal Initiative in Maternal, Perinatal, and Child Health, as well as by the Perinatology Research Branch, Division of Intramural Research, Eunice Kennedy Shriver National Institute of Child Health and Human Development, National Institutes of Health, U.S. Department of Health and Human Services.

TABLE OF CONTENTS

LIST OF TABLES

LIST OF FIGURES

CHAPTER 1 - INTRODUCTION

Preterm birth (PTB) is defined as occurring prior to 37 weeks of gestation (1). With a rate of 11.39% in the United States (2), PTB is the leading cause of perinatal mortality (3). The infants that survive PTB have increased risk of developing short-term and lifelong complications (4-6), which greatly increases the number of years they lose due to illness, disability or early death (7). Preterm birth is a syndrome of multiple etiologies (8), which makes studying its pathophysiological mechanisms more challenging. However, the common factor of inflammation underlies many of these etiologies, including decidual senescence, infection, stress, allergy, and breakdown of fetal-maternal tolerance.

Inflammation at the maternal-fetal interface during labor has been well substantiated by the documented increased bioavailability of cytokines and chemokines and an influx of immune cells, including macrophages, neutrophils, and T cells, into the reproductive tissues (9-11). Inflammation has been shown to promote initiation of the common pathway of parturition (12) (Figure 1) via up-regulation of matrix metalloproteinases (13-18) and prostaglandins (19, 20). Sterile intraamniotic inflammation occurring in the absence of detectable microorganisms is more prevalent than microbial-associated intraamniotic inflammation in patients with preterm labor and intact fetal membranes (21). Innate immune response initiates sterile inflammation when endogenous danger signals derived from necrosis or cellular stress (22), referred to as damage-associated molecular pattern molecules (DAMPs) (23) or alarmins (24), bind to their respective pattern recognition receptors (PRRs) and trigger pro-inflammatory cascade.

We aimed to determine 1) whether alarmins are capable of inciting sterile

inflammation of the chorioamniotic membranes leading to pro-labor changes. In addition to initiating innate immune response, alarmins can also activate adaptive immunity (25, 26). We hypothesized that the release of alarmins activates invariant natural killer (iNKT) cells (27) – unique immune cells that have characteristics of both innate and adaptive immunity – leading to labor. Therefore, our next aim was to determine whether 2) activation of iNKT cells leads to sterile inflammation and precipitates labor. Secretion of alarmins is one of the hallmarks of senescent cells (28-30), which have been implicated in the process of murine parturition (31). Thus, our final aim was 3) to investigate whether chorioamniotic membranes obtained from women who underwent preterm labor exhibit cellular senescence.

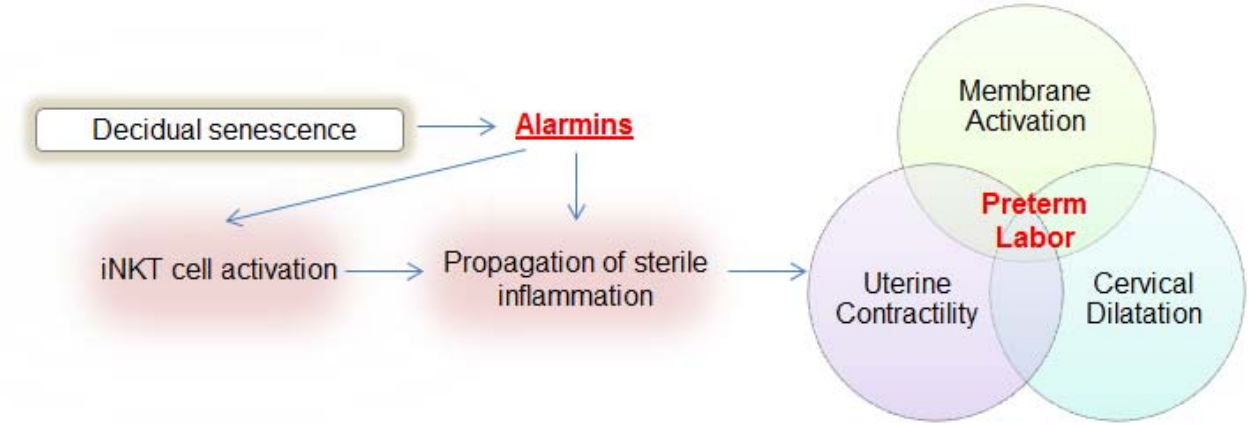

Figure 1: Inflammation as a common factor of multiple etiologies of preterm birth. We propose that decidual senescence, among other pro-inflammatory conditions, causes the release of alarmins at the maternal-fetal interface which induces iNKT cell activation and sterile inflammation initiating the common pathway of parturition.

CHAPTER 2 - HMGB1 INDUCES STERILE INFLAMMATION AT THE MATERNAL-FETAL INTERFACE

Introduction

Innate immune response can initiate sterile inflammation when danger signals (32) are sensed by pattern recognition receptors (PRRs) (33), which leads to activation of the inflammasome complex and caspase-1-mediated maturation of IL1β (34-39). Expression of the inflammasome components is upregulated in the chorioamniotic membranes of patients who underwent spontaneous term labor when compared to term delivery without labor (40). Concentration of caspase-1 is elevated in the amniotic fluid of patients with spontaneous preterm labor and intraamniotic infection/inflammation when compared to patients who delivered preterm without intraamniotic infection/inflammation or those who delivered at term (41). Finally, elevated amniotic fluid IL1 β in term spontaneous labor was demonstrated over two decades ago (42-45). However, the danger signals that initiate the inflammasome-mediated release of IL1β in the chorioamniotic membranes remain unknown.

High mobility group box 1 (HMGB1) is an evolutionary conserved protein that stabilizes nucleosome formation and facilitates gene transcription while localized to the nucleus, but acts as an alarmin when released extracellularly (46). HMGB1 can be either passively released during cell necrosis or actively exocytosed by immune cells to initiates pro-inflammatory intracellular signaling in multiple cell types by binding their cell surface PRRs – RAGE, TLR2, and TLR4 (47, 48). In macrophages, HMGB1 was shown to stimulate production of TNF, IL8, IL6, and IL1β (49). In neutrophils, HMGB1 increases levels of TNF, IL8, and IL1β (50), enhances adhesion and migration (51), and upregulate NF-κB (50). HMGB1 also upregulates NF-κB and induces secretion of TNF,

IL8, and IL6 in dendritic cells (52), and promotes Th1 differentiation in both dendritic cells and T cells (52). Finally, HMGB1 was demonstrated to upregulate expression of VCAM-1, ICAM-1, RAGE and NF-κB and to increase production of TNF and IL8 in endothelial cells (53).

Transcriptomic profiling has identified HMGB1 as a predicted upstream regulator of the inflammatory response in the choriodecidua during term labor (54). Sterile intra-amniotic inflammation in patients with preterm labor and intact membranes is associated with elevated levels of HMGB1 in the amniotic fluid (21). Amniotic fluid HMGB1 concentration is also increased in patients at term with clinical chorioamnionitis (55) and in patients with preterm prelabor rupture of membranes (PPROM) (56). Furthermore, extranuclear expression of HMGB1 is upregulated in the preterm cervix (57), extracellular HMGB1 promotes migration of cord blood $CD34^+$ cells (58), and tracheal aspirates from premature infants that develop bronchopulmonary dysplasia contain elevated HMGB1 (59). Therefore, we hypothesized that HMGB1 can induce sterile inflammation of the chorioamniotic membranes leading to preterm labor and neonatal complications. In support of this hypothesis, our recent findings demonstrate that intraamniotic injections of HMGB1 increase the rate of preterm birth and neonatal mortality in mice (60). Herein, we aimed to explore the molecular mechanisms behind these adverse effects of HMGB1, specifically whether HMGB1 is capable of inducing sterile inflammation of the human chorioamniotic membranes via inflammasome-mediated release of IL1β.

Materials and Methods

Human subjects

Chorioamniotic membranes were obtained from women who underwent elective

caesarian sections without labor and were provided with written informed consent. Samples were collected from the Bank of Biological Specimens of the Perinatology Research Branch, an intramural program of the Eunice Kennedy Shriver National Institute of Child Health and Human Development, National Institutes of Health, U. S. Department of Health and Human Services (NICHD/NIH/DHHS), Wayne State University, and The Detroit Medical Center (Detroit, MI, USA). The Institutional Review Boards of NICHD and Wayne State University (Detroit, MI, USA) approved the collection and use of biological materials for research purposes. Non-laboring status was confirmed by the absence of regular uterine contractions at a frequency of at least two contractions every 10 minutes and the lack of cervical dilatation. Patients with multiple pregnancies or with deliveries prior to 37 weeks of gestation were excluded. The detailed patient demographics information is contained in Table 1.

Table 1: The demographical data of patients whose samples were used for the HMGB1 study

Age (years)	25 (19-33)
Body mass index (kg/m2)	31.5 (20.4-42-.5)
Gestational age at delivery (weeks)	38.93 (39.4-37.1)
Newborn weight (g)	3225 (2745-3880)
Race	
African-American	91.4% (21/23)
Caucasian	8.6% (2/23)
Hispanic	0% (0/23)
Asian	0% (0/23)
Other	0% (0/23)
Primiparity	17.4% (4/23)
C-section	100% (23/23)
Absence of chorioamnionitis	100% (23/23)
Smoking During Pregnancy	17.4% (4/23)

Age, body mass index, gestational age at delivery, and newborn weight are shown as mean (min-max). Race, primiparity, C-section, absence of chorioamnionitis, and smoking during pregnancy are shown as percent (positive/total).

In vitro HMGB1 treatment

Chorioamniotic membrane samples obtained from non-laboring, term deliveries, were spread out flat onto a sterile cutting board. A dermatological biopsy punch (12mm

Acu-Punch, Acuderm Inc., Fort Lauderdale, FL, USA) was used to expunge tissue explants from the chorioamniotic membranes. The explants were treated with 500µL of 1x Dulbecco's Modified Eagle Medium (DMEM) (Corning, Manassas, VA, USA) containing 10% Fetal Bovine Serum (FBS) (Gibco, Life Technologies Corporation, Grand Island, NY, USA) and 1% penicillin/streptomycin (Gibco) either with or without Ultra-Pure HMGB1 (Catalog # REHM050, IBL International Corporation, Toronto, ON, Canada). Explants were placed in a falcon 24 well plate (Corning) and incubated for 24-hours in a humidified 5% CO_2 incubator.

ELISA

Mature IL1β and IL6 released from the chorioamniotic membrane explants into the culture media (n=6-13) was quantified using IL1β ELISA kit (R&D Systems, Inc. Minneapolis, MN, USA) and IL6 ELISA kit (R&D Systems, Inc.). The sensitivities of detection were <1pg/mL and <0.70pg/mL, respectively. Caspase-1 concentrations in the chorioamniotic membranes homogenized in their conditioning media (n=9) was determined using caspase-1 ELISA kit (Cloud Clone, Houston, TX, USA) with sensitivity of detection of <0.112 ng/ml. All ELISAs were run according to the manufacturers' protocols. Briefly, recombinant human standards and the samples were incubated in duplicate wells of the 96-well microplates pre-coated with immobilized monoclonal antibodies specific for target analytes. After washing the unbound substances, enzyme-conjugated anti-IL1β, anti-IL6 or anti-caspase-1 antibodies were added to the wells. After incubation, assay plates were washed again to remove the unbound antibodies, followed by the addition of a substrate solution, which produced color in proportion to the amount of bound target analytes. Finally, sulfuric acid solution was added to arrest the color development and the microplates were read using a programmable

spectrophotometer (SpectraMax M5 Multi-Mode Microplate Reader, Molecular Devices, Sunnyvale, CA, USA).

RT-PCR

TRIzol® (Life Technologies Corporation), Qiagen RNeasy® Kit (Qiagen, Valencia, CA, USA), RNase-Free DNase Sets (Qiagen), and QIAshredders (Qiagen) were used for total RNA extraction from the chorioamniotic membrane (n=5-8) on QIAcube (Qiagen). RNA concentration was determined with the NanoDrop® 1000 spectrophotometer (Thermo Scientific, Wilmington, DE, USA) and RNA integrity was assessed with the Bioanalyzer 2100 (Agilent Technologies, Wilmington, DE, USA).

Table 2: The list of primers used for RT-PCR in the HMGB1 study

Gene	Full Name	ID	Lot
NOD1	Nucleotide-Binding Oligomerization Domain-Containing Protein 1	hs00196075_m1	730289
NOD2	Nucleotide-Binding Oligomerization Domain-Containing Protein 2	hs00223394_m1	1130429
NLRP1	NLR Family, Pyrin Domain Containing 1	hs00249187_m1	696883
NLRP3	NLR Family, Pyrin Domain containing 3	hs00918082_m1	1204490
NLRC4	NLR family, CARD domain containing 4	hs00368367_m1	724373
AIM2	Absent in Melanoma 2	hs00915710_m1	1014056
CASP1	Caspase 1	hs00354836_m1	1035134
CASP4	Caspase 4	hs01031947_m1	1010522
IL1B	Interleukin 1, Beta	hs00174097_m1	815049
IL18	Interleukin 18	hs99999040_m1	666991
IL6	Interleukin 6	hs00985639_m1	941055
INFG	Interferon, Gamma	hs00989291_m1	970586
IL1A	Interleukin 1, Alpha	hs99999028_m1	937514
TNF	Tumor Necrosis Factor	hs00174128_m1	905231
TLR2	Toll-Like Receptor 2	hs00610101_m1	435401
TLR4	Toll-Like Receptor 4	hs00152939_m1	432491
AGER (RAGE)	Receptor for Advanced Glycation Endproducts	hs00153957_m1	897932
NFKB1	Nuclear Factor of Kappa Light Polypeptide Gene Enhancer in B-cells 1	hs00765730_m1	1208011
PTGS2	Prostaglandin-Endoperoxide Synthase 2	hs01573477_m1	816998
MMP9	Matrix Metallopeptidase 9	hs00234579_m1	439744
GAPDH	Glyceraldehyde 3-Phosphate Dehydrogenase	hs99999905_m1	1335169
ACTB	Actin, Beta	hs99999903_01	984416
RPLPO	Ribosomal Protein, Large, P0	hs99999902_m1	1347306
HMGB1	High Mobility Group Box 1	hs01590761_g1	1032400
S100A12	S100 Calcium Binding Protein A12	hs00194525_m1	866042
HSPA1A (HSP70)	Heat Shock 70kDa Protein 1A	hs00359163_s1	1310706
HMGB1	High Mobility Group Box 1	hs01923466_g1	946636

The abbreviations and the full names of genes are listed with assay IDs and Lot numbers for each primer.

The SuperScript® III First-Strand Synthesis System (Life Technologies

Corporations) and oligo(dT)20 primers (Life Technologies Corporation) was used to synthesize the cDNA. Gene expression profiling was performed on the BioMark™ System for high-throughput qRT-PCR (Fluidigm, San Francisco, CA, USA) with TaqMan® gene expression assays (Applied Biosystems, Life Technologies Corporation) listed in Table 2.

Immunoblotting

Chorioamniotic membrane explants homogenized in their conditioned medium (n=9 per group) were heated at 95°C for 5 minutes in NuPAGE® Sample Reducing Agent (Novex®, Life Technologies Corporation, Carlsbad, CA, USA) and NuPAGE® LDS Sample Buffer (Novex®, Life Technologies Corporation). NuPAGE® 4-12% Bis-Tris Gel (Catalog # IM-8042, Novex®, Life Technologies Corporation) was used to perform an SDS-PAGE of the samples and a protein ladder (BioRad Precision Plus Protein Dual Color Standards, Catalog# 161-0374) in Invitrogen Novex® Mini-Cell (Life Technologies Corporation) with NuPAGE® MES SDS Running Buffer (Novex®, Life Technologies Corporation). After electrophoresis, separated proteins were transferred onto nitrocellulose membranes (Bio-Rad, Hercules, CA, USA) using NuPAGE® Transfer Buffer (Novex®, Life Technologies Corporation) diluted in 20% methanol. Transfer was performed in a Bio-Rad Mini-Protean II Cell (Bio-Rad). Ponceau S solution (Sigma-Aldrich®, St. Louis, MO, USA) was used to visualize successful protein transfer. The membranes were blocked with StartingBlockTM T20 (TBS) Blocking Buffer (Thermo Scientific, Rockford, IL) for 30 minutes and probed with 1:500 mouse anti-CASP-1 monoclonal antibody (Catalog # MAB6215, R&D Systems) diluted in the StartingBlockTM T20 (TBS) Blocking Buffer overnight at 4°C. After washing with 1X TBS (Bio-Rad) containing 0.1% Tween-20 (BioRad), the membranes were incubated

with 1:5000 anti-mouse IgG HRP-linked secondary antibody (Catalog # 7076S, Cell Signaling, Boston, MA, USA). Chemiluminescence signals were detected with ChemiGlow West Reagents (Protein Simple, Santa Clara, CA, USA). Images were acquired was performed using the FUJIFILM LAS-4000 Imaging System (FUJIFILM North America Corporation, Valhalla, NY, USA) and semi-quantification was performed by ImageJ 1.44p (National Institute of Health, USA). Reference gene was probed for 1h at room temperature with a mouse anti-human GAPDH monoclonal antibody (Catalog # SC-32233, Santa Cruz Biotechnology, Inc.).

Zymography

Chorioamniotic membrane explants homogenized in their conditioned medium (n=9 per group) were mixed at 1:1 with a Tris-Glycine SDS Sample Buffer (2x) (Novex®, Life Technologies Corporation, Carlsbad, CA, USA) and loaded into Novex® 10% Zymogram (Gelatin) Gel (Catalog # EC6175, Novex®, Life Technologies Corporation) with a protein ladder (BioRad Precision Plus Protein Dual Color Standards, Catalog# 161-0374). SDS-PAGE was performed in an Invitrogen Novex® Mini-Cell (Life Technologies Corporation) with Novex® Tris-Glycine SDS Running Buffer (Novex®, Life Technologies Corporation). After electrophoresis, gels were removed and incubated for 30 minutes in Novex® Zymograph Renaturing buffer (Novex®, Life Technologies Corporation), followed by an additional 30-minute incubation in Novex® Zymograph Developing Buffer (Novex®, Life Technologies Corporation), both with a gentle agitation. Gels were then placed in a freshly made developing buffer and incubated overnight at 37°C. After overnight incubation, gels were washed 3x in ddH_2O with a gentle agitation, for 5 minutes each. Deionized water was removed and gels were stained for four hours with SimplyBlue™ SafeStain (Invitrogen, Life Technologies

Corporation). Once staining was complete, gels were washed 2x for 1 hour in ddH_2O. Images were taken using Alpha Innotech FluorChem™ SP (ProteinSimple, San Jose, CA, USA) and semi-quantified by ImageJ 1.44p (National Institute of Health, USA).

Trichromic staining

Chorioamniotic membrane explants embedded into paraffin blocks were cut into five-µm-thick sections, placed onto salinized slides, deparaffinized with xylene, and hydrated with ethanol and water. The staining was performed on the Dako AutostainerPlus (Dako, Carpinteria, CA, USA) using Masson's Trichrome Stain Kit (American MasterTech, Lodi, CA, USA) as per the manufacturer's protocol. Briefly, sections were incubated overnight in Bouin solution at room temperature, rinsed, and stained with Weigert's hematoxylin for 5 minutes. The slides were then rinsed again in water and stained with Biebrich Scarlet-Acid Fuchsin Solution for 15 minutes, rinsed a third time, and incubated with phosphomolybdic/phosphotungstic acid for 15 min. Final staining with Aniline Blue Stain for 10 minutes was followed by another rinse and incubation in 1% acetic acid for 5 minutes. The sections were then dehydrated in a series of alcohol baths, cleared with Xylene, and cover slipped. The images were taken using the Pannoramic MIDI Digital Slide Scanner (PerkinElmer, Inc., Waltham, MA, USA) at 40X magnification.

Statistical analyses

Statistical analyses were performed using SPSS, Version 21.0 (IBM Corporation, Armonk, NY, USA), GraphPad Prism 6 Software (GraphPad Software, Inc., La Jolla, CA, USA), and R open-source software environment. For gene expression data, Ct values over technical replicates were averaged and gene expressions relative to reference (*BACT*, *GAPDH*, *RPLPO*) were quantified by subtracting target gene Ct

values from mean reference gene Ct values within the same sample. A Shapiro–Wilk test was performed to determine whether data were normally distributed and all normally distributed data were analyzed by the paired Student's t-test. Data that did not follow normal distribution were analyzed either by Wilcoxon signed-rank test for matched samples or by Mann-Whitney U test for unmatched samples. A value of $p<0.05$ was considered statistically significant.

Results

In vitro incubation with HMGB1 causes secretion of mature IL1β and IL6 by the chorioamniotic membranes

We first determined the concentration of HMGB1 that caused the release of pro-inflammatory cytokines by the chorioamniotic membranes *in vitro*.

It has been demonstrated that 10 and 50ng/mL HMGB1 can induce the release of pro-inflammatory cytokines such as IL6 and IL8 from the chorioamniotic membranes (61). A previous study showed that amniotic fluid concentrations of HMGB1 were lowest in women with PTL with intact membranes and no intra-amniotic infection/inflammation (median 0.98ng/mL) and highest in women with PTL with PPROM and intra-amniotic infection/inflammation (median 7.3ng/mL) (56). We used membrane explants from women who delivered at term without labor to test HMGB1 concentrations ranging from 0-1000 ng/mL and then measure released mature IL1β (Figure 2A) and IL6 (Figure 2B). We found that concentrations in the ng/mL range were not effectively inducing cytokine secretion from the chorioamniotic membrane tissue explants. However, a higher concentration of 25μg/mL significantly increased secretion of mature IL1β (Figure 2C) and IL6 (Figure 2D) from the chorioamniotic membrane explants *in vitro*. We found that 50μg/mL of HMGB1 increased IL1β secretion even

further (Figure 2C) and chose to use this concentration for the subsequent experiments. Therefore, these data show that incubation with a concentration of 50µg/mL of HMGB1 is capable of inducing sterile inflammation of the chorioamniotic membranes observed as secretion of mature IL1β and IL6 from the chorioamniotic membrane explants.

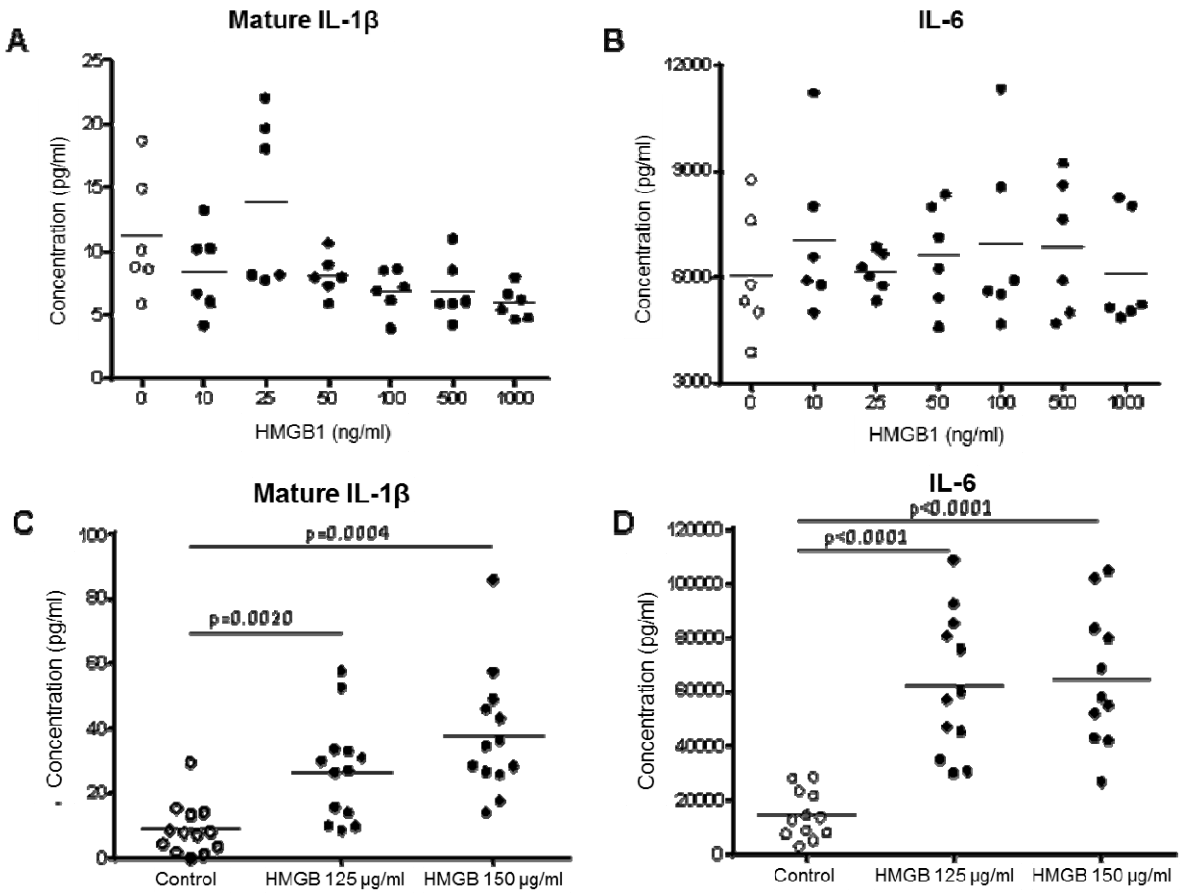

Figure 2: HMGB1 induces release of IL-1β and IL-6 from the chorioamniotic membranes. The chorioamniotic membranes treated with low doses (0-1000ng/mL) of HMGB1 (A and B) did not release pro-inflammatory cytokines. Higher concentrations (25µg/mL and 50µg/mL) of HMGB1 (C and D) significantly enhanced release of mature IL-1β and IL-6.

HMGB1 induces expression of pro-inflammatory cytokines in the chorioamniotic membranes

We used RT-PCR to confirm that secretion of IL1β and IL6 from the chorioamniotic membrane explants in response to HMGB1 treatment is also accompanied by the increased gene expression of *IL1B* and *IL6*. To further assess the

extent of sterile inflammation induced by HMGB1, we explored whether HMGB1 treatment was upregulating expression of other known pro-inflammatory cytokines *TNF*, *IL1A*, *IL18*, and *IFNG*. We also evaluated the expression of *NFKB1*, a master transcription factor of inflammation known to promote labor (62-65).

We found that all of these genes were significantly upregulated in response to HMGB1 (Figure 3) with an exception of *IL18*. *IL18* expression also tended to increase; however, this tendency did not reach significance (data not shown). Therefore, we concluded that the sterile inflammation induced by HMGB1 involves upregulation of multiple pro-inflammatory genes in the chorioamniotic membranes.

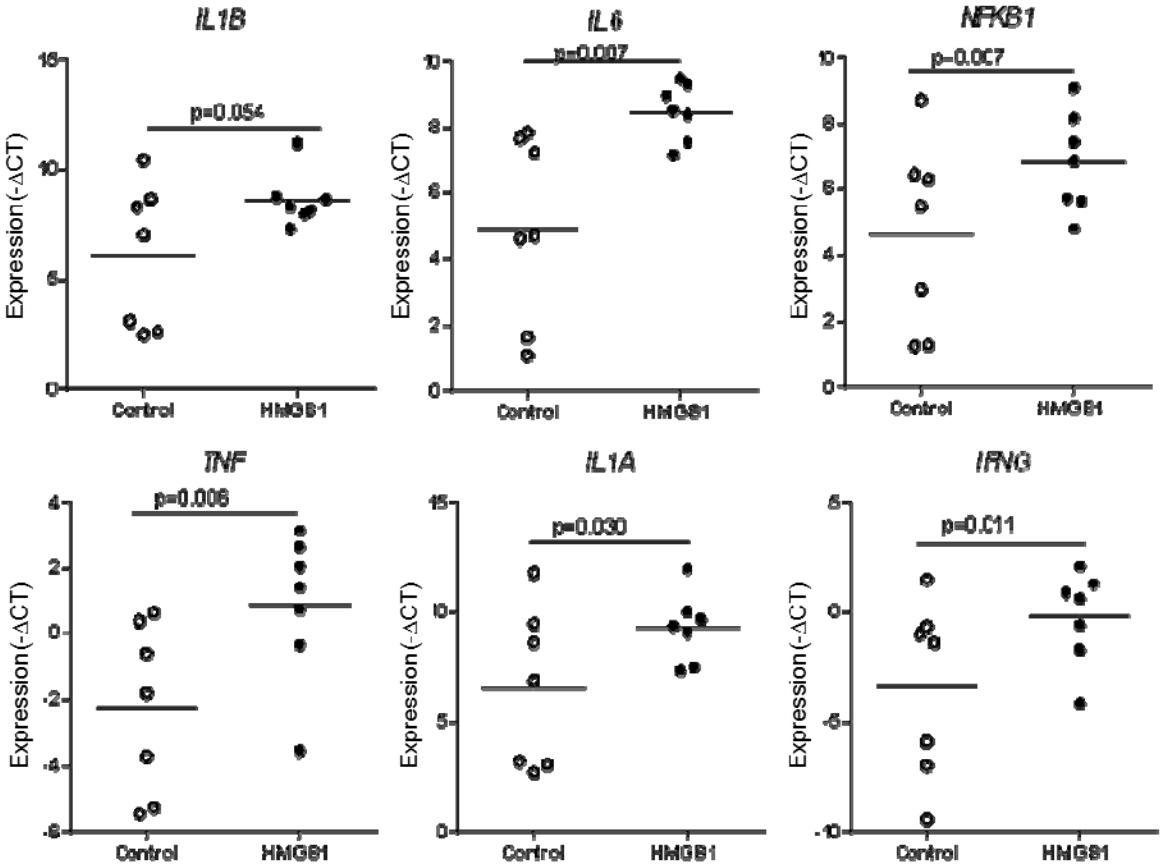

Figure 3: HMGB1 up-regulates expression of multiple pro-inflammatory cytokines in the chorioamniotic membranes. Expression of the pro-inflammatory transcription factor *NFKB1* and its downstream targets *IL1B*, *IL6*, *TNF*, *IL1A*, and *IFNG* was assessed in the chorioamniotic membranes treated with HMGB1 (50μg/mL).

HMGB1 upregulates the expression of inflammasome components and NOD proteins in the chorioamniotic membranes

Mature IL1β is a resulting product of inflammasome activation (38). Therefore, we next aimed to investigate whether HMGB1 stimulates release of mature IL1β by activating the inflammasome pathway. We recently demonstrated that expression of the inflammasome component NLRP3 (NOD-like receptor family, pyrin domain containing protein 3) is increased in the chorioamniotic membranes during spontaneous term labor compared with term delivery without labor (40). In the same study, we also found that expression of NOD1 (nucleotide-binding oligomerization domain-containing proteins 1), a NOD protein that directly activates nuclear factor kappa B (NF-κB) to induce expression of pro-IL1β (66-69), is elevated in term labor. Therefore, we hypothesized that HMGB1 may upregulate NLRP3, NOD1, and/or other inflammasome components and NOD proteins.

We used RT-PCR to measure the expression of *NOD1, NOD2, NLRP1, NLRP3, AIM2,* and *NLRC4* in the chorioamniotic membrane explants treated with HMGB1. We found that inflammasome components *NLRP1, NLRP3,* and *AIM2* were significantly upregulated, while *NLRC4* had a tendency to increase, after treatment with HMGB1 (Figure 4). We also found that that both NOD proteins – *NOD1* and *NOD2* – were upregulated by HMGB1 (Figure 4). Therefore, we concluded that HMGB1 is capable of upregulating the expression of specific inflammasome components and NOD proteins in the chorioamniotic membranes.

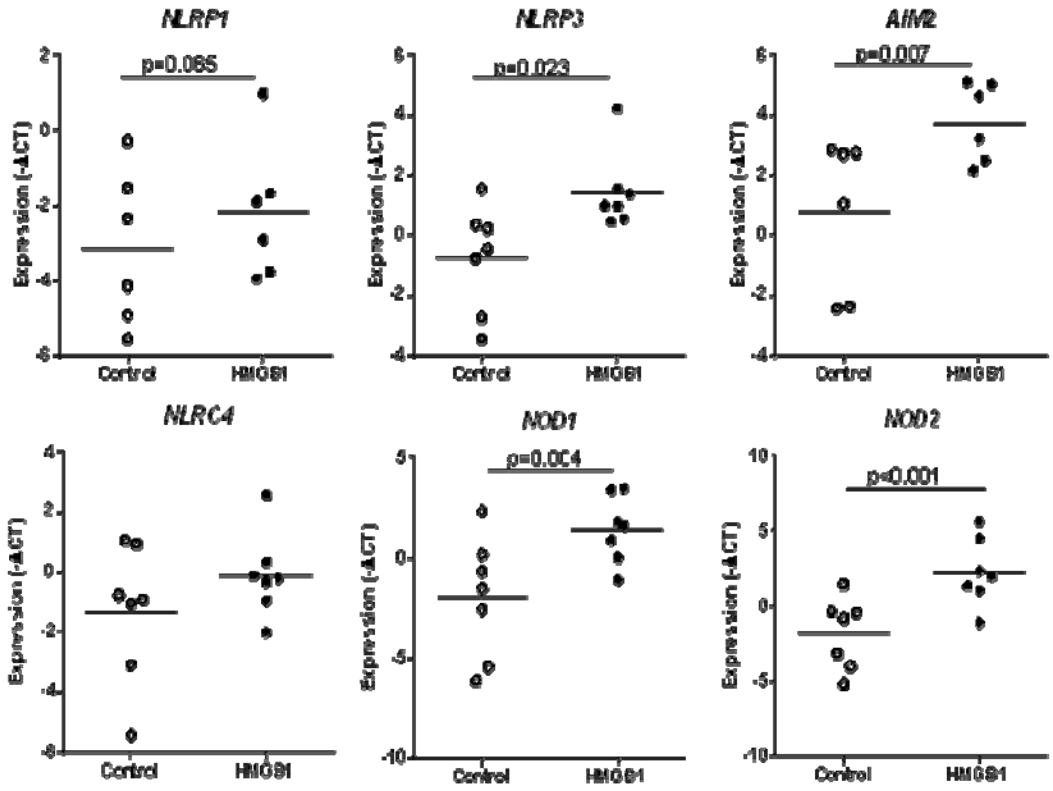

Figure 4: HMGB1 induces expression of the inflammasome components and NOD proteins in the chorioamniotic membranes. Expression of the inflammasome components *NLRP1*, *NLRP3*, and *AIM2*, as well as NOD proteins *NOD1* was assessed in the chorioamniotic membranes treated with HMGB1 (50μg/mL).

HMGB1 increases concentration and promotes activation of caspase-1

Inflammasomes activate inflammatory caspases, most notably caspase-1 (38, 70-72). Caspase-1 is an important enzyme for the IL1 cytokine family, as it is responsible for cleaving pro-IL1β, pro-IL18, and pro-IL33 into their mature active forms (73-76).

First, we examined the expression of *CASP1* in the chorioamniotic membrane explants to see whether HMGB1 upregulates caspase-1 at the mRNA level. We found that *CASP1* expression tended to increase following HMGB1 treatment, yet this tendency did not reach statistical significance (Figure 5A). We then evaluated the protein concentration of caspase-1 and found that HMGB1 treatment caused a

significant increase in total caspase-1 concentration in the chorioamniotic membranes (Figure 5B). Pro-caspase-1 must be cleaved into two non-identical subunits, p10 and p20, to become an active enzyme (75, 77). Therefore, we semi-quantified pro- and active forms of caspase-1 using Western blot. We found that both the immature pro-caspase-1 and the active caspase-1-p20 were significantly increased after treatment with HMGB1 (Figure 5C). We concluded that HMGB1 increases concentration and promotes activation of caspase-1.

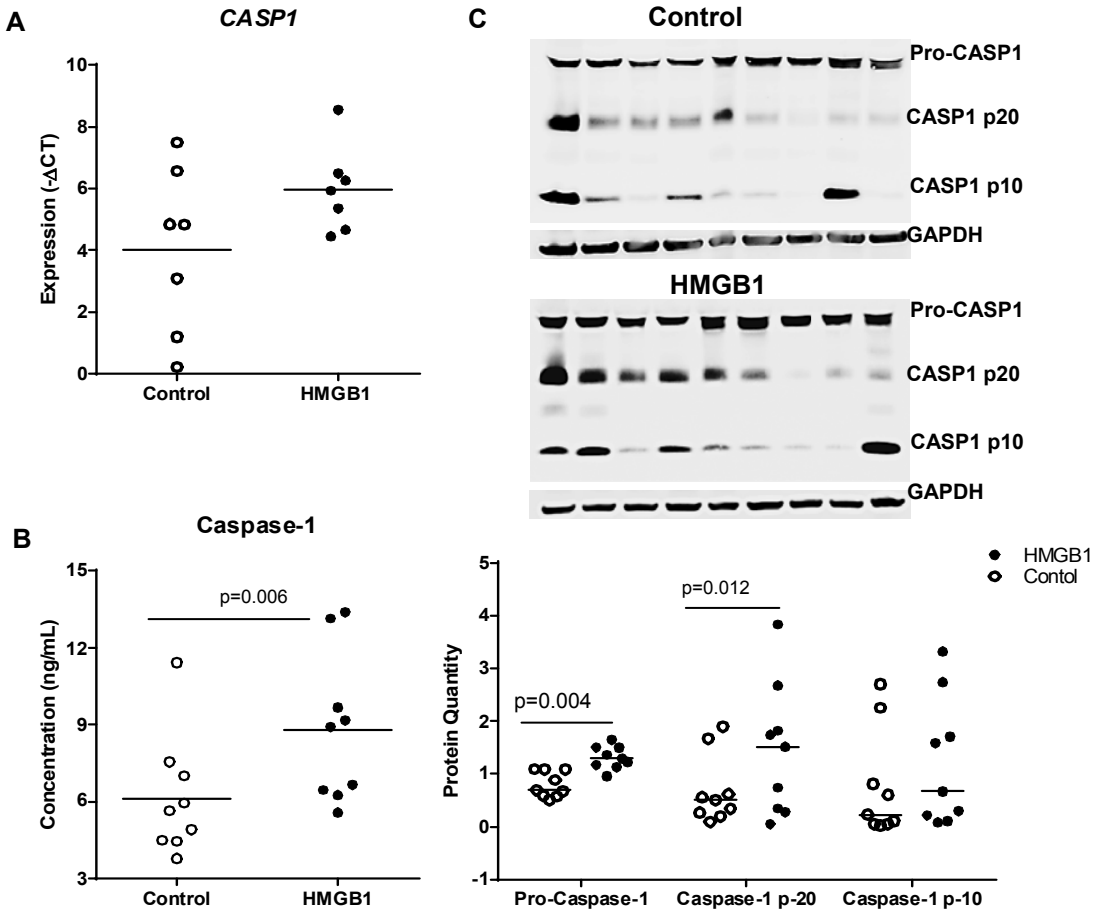

Figure 5: HMGB1 increases concentration and promotes activation of caspase-1 in the chorioamniotic membranes. Expression of *CASP1* gene (A), concentration of total Caspase-1 protein (B), and accumulation of active forms of Caspase-1 (p-20 and p-10) (C) were assayed in the chorioamniotic membranes treated with HMGB1 (50μg/mL).

HMGB1 upregulates the expression of its own receptors in chorioamniotic membranes

HMGB1 has been previously shown to interact with RAGE as well as TLR2 and TLR4 (47, 48). HMGB1 may act through positive feedback, increasing the expression of its own receptors during inflammation (78). We wanted to examine the expression of these receptors in the chorioamniotic membranes to see whether receptor expression correlated with HMGB1 treatment. We found that *RAGE* and *TLR2* were significantly upregulated in explants after culturing with HMGB1; additionally, *TLR4* showed a tendency to increase as well (Figure 6). We concluded that HMGB1 is capable of upregulating the expression of its own receptors *in vitro*.

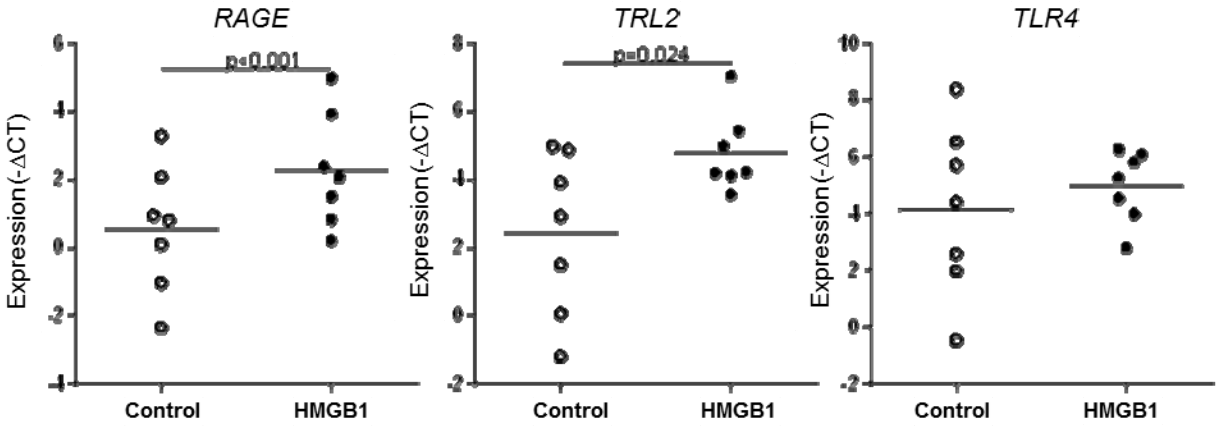

Figure 6: HMGB1 upregulates the expression of its own receptors in the chorioamniotic membranes. Expression of particle recognition receptors known to bind HMGB1 – *RAGE*, *TLR2*, and *TLR4* was assayed in the chorioamniotic membranes treated with HMGB1 (50μg/mL).

HMGB1 upregulates activity of MMP9 in the chorioamniotic membranes

Matrix metalloproteinase 9 (MMP9) is an enzyme that functions primarily to break down the extracellular matrix (ECM) and is implicated in the process of labor (13, 79-81). Active MMP9 has previously been shown to be increased in spontaneous rupture of membranes, term and preterm parturition, and microbial invasion (13, 82, 83), as well

as PPROM (84). *MMP9* expression can be stimulated by IL1β in the myometrium and chorioamniotic membranes (85, 86). We aimed to determine whether HMGB1 could upregulate the expression and activity of MMP9 *in vitro*. We found that *MMP9* gene expression is significantly increased in the membrane explants cultured with HMGB1 (Figure 7A). In addition to increased expression, the enzymatic activity of MMP9 was significantly elevated following HMGB1 treatment (Figure 7B).

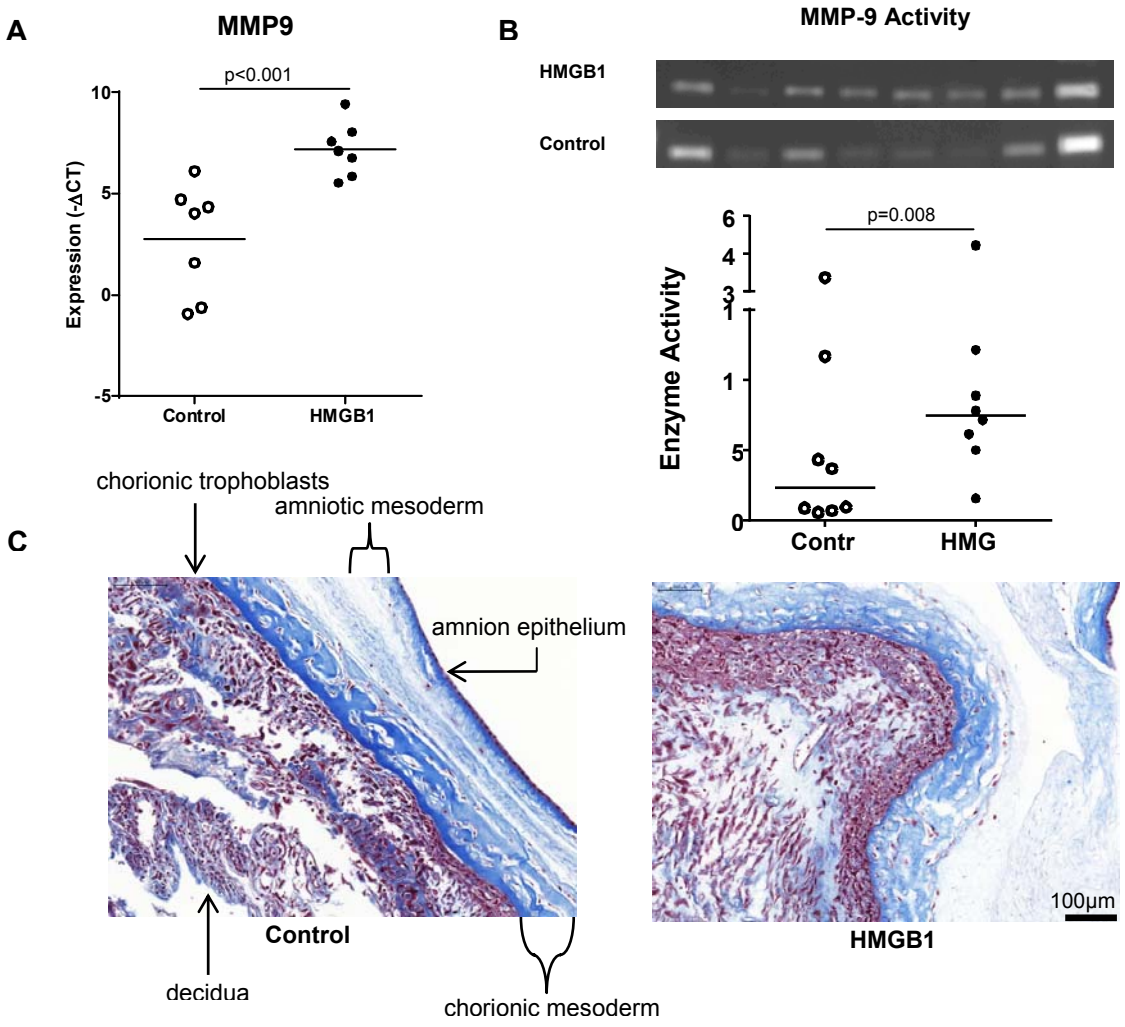

Figure 7: HMGB1 upregulates expression and activity of MMP9 in the chorioamniotic membranes. Expression (A), and activity of MMP9 (B) was assayed in the chorioamniotic membranes treated with HMGB1 (50μg/mL) by RT-PCR and zymography, respectively. The collagen reorganization was examined by the trichrome stain (C).

This was further demonstrated by the trichrome staining which showed decreased collagen content (blue) in the chorioamniotic membranes treated with HMGB1 (Figure 7C). Therefore, we showed that HMGB1 upregulates the expression and activity of *MMP9* in the chorioamniotic membranes.

Discussion

HMGB1 induces sterile inflammation of the chorioamniotic membranes

The study herein affirms that HMGB1 is capable of inducing sterile inflammation of the chorioamniotic membranes by increasing concentration and/or expression of multiple pro-inflammatory cytokines including IL1β, IL6, TNF, IL1α, and IFNγ (Figures 2 & 3) and pro-inflammatory PRRs Nod1 and Nod2 (Figure 4). This inflammatory cascade may be amplified by positive-feedback via up-regulation of HMGB1 receptors (RAGE and TLR2) by HMGB1 itself (Figure 6).

Pathogen Associated Molecular Patterns (PAMPs) present during microbial infection have been shown to act, in part, by promoting release of DAMPs from the infected cells, including HMGB1 (87, 88). Interestingly, the evidence suggests that HMGB1 also participates in mediating infection-induced inflammation at the maternal-fetal interface. For instance, chorioamniotic membranes stimulated with LPS have been shown to release HMGB1 *in vitro* (61) and intraamniotic administration of LPS significantly increases HMGB1 concentration in the chorioamniotic membranes in the sheep model of preterm birth (89). Additionally, co-expression of HMGB1 and its receptor RAGE was observed in sites of brain and liver tissue injury of mouse embryos in murine model of LPS-induce preterm birth (90). Therefore, HMGB1-induced signaling is a possible treatment target for both infection- and non-infection-associated preterm birth.

The induction of sterile inflammation by HMGB1 occurs via the inflammasome pathway

We found that the mechanism by which HMGB1 increases release of IL1β from the chorioamniotic membranes includes up-regulation of inflammasome components. Inflammasome activation requires two steps: 1) priming via NF-κB-dependent transcriptional up-regulation of multiple pro-inflammatory targets including pro-IL1β and inflammasome components; and 2) assembly of the inflammasome components including pro-capsapse-1, ASC adaptor protein, and specific PRRs, into a functional complex capable of inducing auto-catalytic cleavage of pro-caspase-1 into its mature/activated form (91-94). Activated caspase-1 then cleaves pro-IL1β, pro-IL18, and newly described pro-IL33, into their secreted forms (75-77, 95-105). The data presented herein suggests that HMGB1 promotes both steps of the inflammasome activation. The priming by HMGB1 is clearly demonstrated by the increased mRNA levels of *IL1B*, *NLRP1*, *NLRP3*, and *AIM2* (Figures 3 & 4). Although assembly of the inflammasome complex was not assessed by direct methods such as co-immunoprecipitation, Fluorescence Resonance Energy Transfer (FRET), or oligomerization assays, the increased production of active form of caspase-1-p20 (Figure 5) and elevated levels of released IL-1β (Figure 2) strongly suggest inflammasome assembly. Further studies are needed to establish the direct link between HMGB1 and assembly of the inflammasome complex.

HMGB1-induced sterile inflammation promotes remodeling of the chorioamniotic membranes

The data herein demonstrates that HMGB1 promotes inflammasome activation and IL-1β production at the maternal-fetal interface. Inflammasome activation is associated with enhanced production of labor-promoting eicosanoids (106) and

activation of MMP9 (107). Inflammasome-derived IL-1β induces labor by up-regulating the expression of cyclooxygenase-2/ prostaglandin synthase 2 (*COX2*/ *PTGS2*) (65) and promoting synthesis of prostaglandin E2 (108-110), as well as by activating the matrix remodeling enzymes such as MMP9 (111). Therefore, it is not surprising that systemic administration of IL-1β precipitates preterm birth in mice (45, 112) and monkeys (113-120). Recently we demonstrated that intraamniotic injections of HMGB1 also induce preterm birth (121). Our current results demonstrate that *in vitro* stimulation with HMGB1 causes up-regulation of MMP9 expression, increased MMP9 activity, and collagen remodeling of the chorioamniotic membranes (Figure 7), which may contribute to membrane rupture. However, we did not observe significant up-regulation of *COX2* with HMGB1 treatment (data not shown). Further studies are required to determine the exact mechanism by which HMGB1-induced sterile inflammation promotes labor.

CHAPTER 3 - S100A12 INDUCES STERILE INFLAMMATION OF THE CHORIOAMNIOTIC MEMBRANES

Introduction

S100 proteins are calcium triggers or sensory proteins that, upon calcium dependent activation, regulate the function and/or subcellular distribution of certain target proteins and peptides (122-124). S100 proteins are sensed as alarmins when they are released extracellularly (125), exerting pro-inflammatory effects on various cell types in the paracrine and autocrine manner (126). S100A12, along with S100A8 and S100A9, belong to a S100 protein subfamily termed calgranulins or myeloid-related proteins, whose members are linked to innate immune functions by their predominant expression in cells of myeloid origin (127, 128). S100A12 is known to be expressed in granulocytes (129), monocytes (130), and select epithelial cells (131). Although S100A12 is capable of binding multiple PRRs (132), the receptor for advanced glycation endproducts (RAGE) is the best studied specific PRR targeted by S100A12 (132, 133). RAGE is expressed at relatively low levels in homeostasis, but in situations characterized by enhanced cellular activation or stress, the expression of RAGE receptor is upregulated (123, 134). Human S100A12 is markedly amplified in inflammatory compartments i.e. synovial fluid of inflamed joints (135), and elevated serum levels of S100A12 are found in patients suffering from various inflammatory, neurodegenerative, metabolic, and neoplastic disorder (136-141).

In pregnancy, amniotic fluid concentration of S100A12 is elevated in women with intra-amniotic infection and correlates with the degree of inflammation and severity of histologic chorioamnionitis (140). S100A12 is also elevated in maternal serum, amniotic fluid, and infant fecal matter in preeclampsia (142), neonatal sepsis (143), and intestinal

distress in very-low-birth-weight infants (144), respectively. Furthermore, detection of elevated S100A12 in the amniotic fluid among four biomarkers termed as “MR score” was proposed to be a quick and accurate predictor of preterm birth (145). Based on these association studies, we aimed to determine whether S100A12 is indeed capable of inducing sterile inflammation of the human chorioamniotic membranes and causes preterm birth in mice. IL-1β was chosen as a marker of sterile inflammation because its systemic administration induces PTB (146). Biologically active form of IL-1β is produced by cleavage of pro-IL-1β by caspase-1, a protease that itself requires proteolytic processing by inflammasomes for activation. We have previously demonstrated that the increased release of mature IL-1β from the chorioamniotic membranes obtained from the women who underwent term labor (as opposed to the women who delivered at term without labor) is associated with increased concentration of both active caspase-1 and NLRP3 inflammasome in the membrane tissue extracts (40).

We therefore hypothesized that S100A12 induces sterile inflammation of the chorioamniotic membranes by up-regulating inflammasome components, which leads to activation of caspase-1 and subsequent maturation of IL-1β. The aims of this study were: 1) to determine whether S100A12 induces release of mature IL-1β from the chorioamniotic membranes; 2) to assess whether S10012A12 increases expression of the inflammasome components; 3) to evaluate the levels of total and mature casapase-1 following S100A12 treatment; 4) to discern the expression of pro-inflammatory and pro-labor genes in the chorioamniotic membranes treated with S100A12; and 5) to characterize the effects of S100A12 on gestation length and neonatal complications.

Materials and Methods

Study population

The chorioamniotic membranes were obtained from women who underwent term delivery without labor as described in Chapter 2. The demographical characteristics of the patients are summarized in Table 3.

In vitro S100A12 treatment

The chorioamniotic membrane explants (n=21) were cultured as described in Chapter 2. For S100A12 treatment, the media was supplemented with 5μg/mL of S100A12 (Catalog no. 11143-HNAE-50, Lot no. LCL06NO0926, Life Technologies Corporation). This concentration was chosen based on previous *in vitro* experiments (147-150).

ELISA/ RT-PCR/ Immunoblotting/ Trichromic staining

ELISA, RT-PCR, and immunoblotting experiments were performed as described in Chapter 2.

Animals and husbandry

C57BL/6 mice were purchased from The Jackson Laboratory (Bar Harbor, ME, USA) and acclimated for at least two weeks. Breeding took place in the animal facilities at Wayne State University under specific pathogen-free conditions on a 12-h light, 12-h dark circadian cycle. Pregnant dams were obtained by placing one or two females (8-12 weeks old) with a proven fertile male and checked daily between 0800 and 0900 hours for a vaginal plug which resulted from mating during the periovulatory period (2200-0200 hours). The morning of detection of a vaginal plug was considered the 0 day of gestation and 0.5 days post coitum (dpc). Plugged females were removed from the mating cage and housed individually with food and water *ad libitum*. Protocol for

animal handling and care was approved by the Institutional Animal Care and Use Committee (IACUC) of Wayne State University (Detroit, MI, USA).

Table 3: Demographic characteristics of the patients whose samples were used for the S100A12 study.

Race: African-American Caucasian	 19 (90.5%) 2 (9.5%)
Maternal age (years)	29 (20-40)
Maternal weight (kg)	189 (102-304)
Maternal body mass index (kg/m^2)	32.7 (20.4-50.6)
Gestational age at delivery (weeks)	38.9 (37-41.9)
Newborn weight (grams)	3190 (1775-3820)
C-section	21 (100%)
Acute chorioamnionitis	3 (14%)

Age, body mass index, gestational age at delivery, and newborn weight are shown as mean (min-max). Race, Primiparity, C-section, and absence of chorioamnionitis are shown as percent (positive/total).

In vivo S100A12 injections

C57BL/6 plugged females were monitored by weight to confirm pregnancy. Pregnant dams were injected intraperitoneally at 16.5 dpc with 5µg/mL S100A12 (n=8) dissolved in a vehicle of 1X sterile PBS. Additional pregnant dams (n=8) were injected with just the vehicle as a negative control. Following injections, pregnant mice were recorded by video camera until delivery. Gestational length, duration of active labor, and the rate of stillbirth were determined based on the video recordings. Gestational length was defined as the time between detection of the vaginal plug and the appearance of the first pup in the cage. The duration of active labor was defined as the time between the appearance of the first pup and the appearance of the last pup of the litter. The rate of stillbirth was defined as the proportion of pups that were born dead out of the total number of pups. The surviving pups were weighed at weeks 1, 2, and 3 postpartum and their survival rate was recorded.

Statistical analyses

Statistical analyses were performed using SPSS, Version 21.0 (IBM Corporation, Armonk, NY, USA), GraphPad Prism 6 Software (GraphPad Software, Inc., La Jolla, CA, USA), and R open-source software environment. A Shapiro–Wilk test was performed to determine whether the data was normally distributed. The normally distributed data were analyzed by the paired Student's t-test, while those data that did not follow normal distribution were analyzed by Wilcoxon signed-rank test. Neonatal mortality was analyzed by Logistic Regression. A value of $p<0.05$ was considered statistically significant.

Results

S100A12 induces release of mature IL-1β from the chorioamniotic membranes in vitro

We first aimed to determine whether S100A12 is capable of inducing sterile inflammation of the chorioamniotic membranes. Indeed, release of mature active form of IL-1β, a marker of sterile inflammation, was drastically elevated ($p<0.0001$) in those membranes that were treated with S100A12 *in vitro* (Figure 8).

Additionally, a four-fold increase ($p=0.0009$) was observed in the expression of *IL1B* gene in the chorioamniotic membranes after S100A12 treatment (Figure 8). This suggested that S100A12 regulates IL-1β on two levels – maturation of pro-IL-1β precursor protein and enhancement of *IL1B* gene transcription.

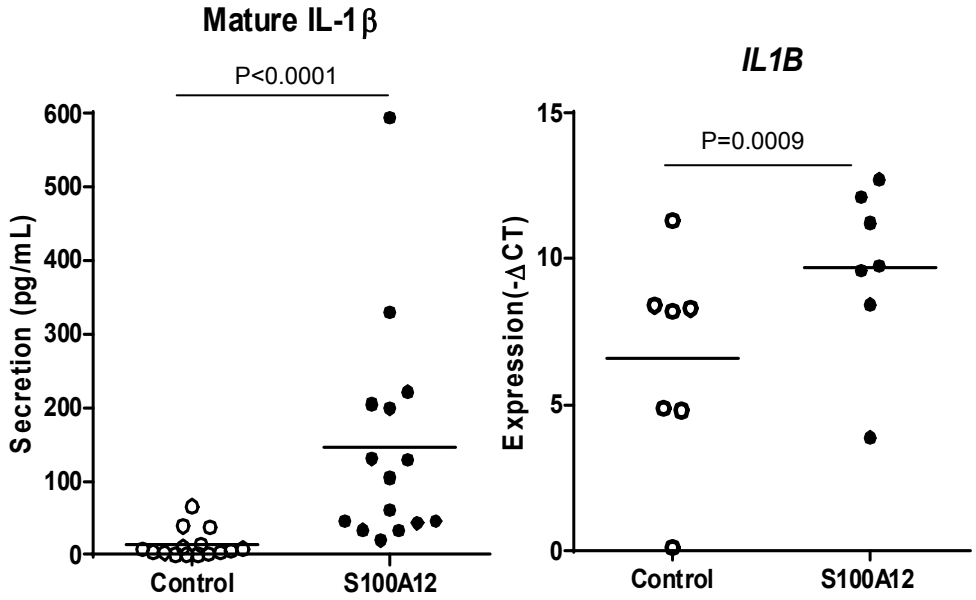

Figure 8: S100A12 induces IL-1β secretion from the chorioamniotic membranes. The chorioamniotic membrane explants were treated with S100A12 (5μg/mL), after which ELISA and RT-PCR assays were performed to determine the secretion of mature IL-1β and the expression of *IL1B*, respectively.

S100A12 increases expression of inflammasome components

Proteolytic processing pro-IL-1β precursor protein into active IL-1β is performed by a cysteine-aspartic acid protease caspase-1 that must be activated by inflammasomes.

We assessed expression of the inflammasome components *NLRP1*, *NLRP3*, *AIM2*, and *NLRC4* in the chorioamniotic membranes treated with S100A12 to determine whether S100A12 stimulates maturation of IL-1β by up-regulation of inflammasomes. Chorioamniotic membrane explants cultured with S100A12 exhibited significant increase in *NLRP3* expression (p=0.046) and tended to up-regulate *NLRP1* (p=0.06) (Figure 9). Thus, S100A12 activates transcription of the specific inflammasome components in the chorioamniotic membranes.

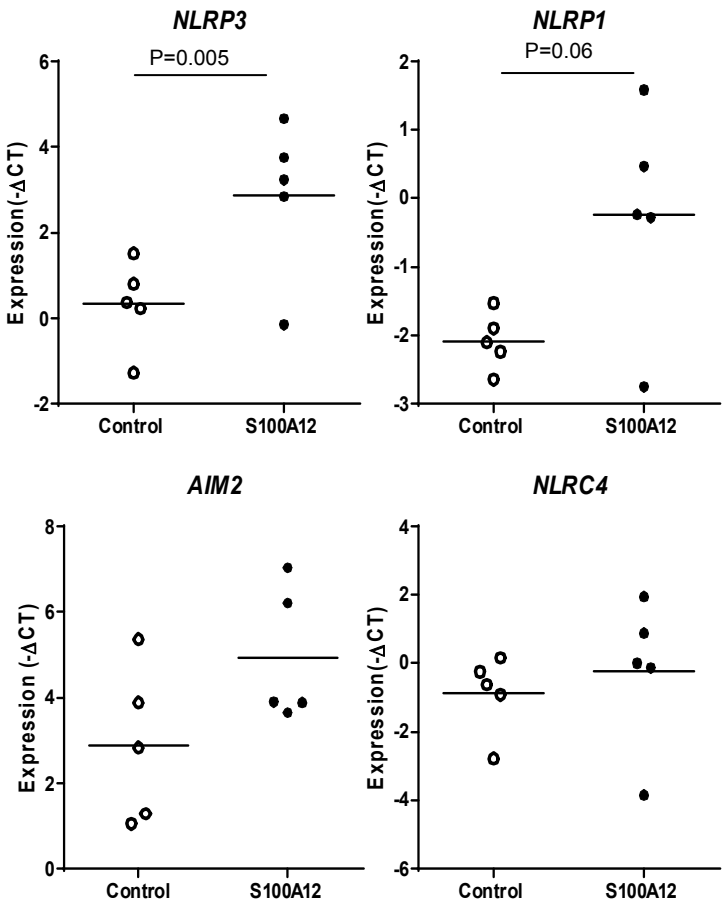

Figure 9: S100A12 upregulates expression of the inflammasome components in the chorioamniotic membranes. The chorioamniotic membranes treated with S100A12 (5µg/mL) were subjected to the RT-PCR assay to analyze expression of the known inflammasome components *NLRP3*, *NLRP1*, *AIM2*, and *NLRC4*.

S100A12 activates caspase-1

In order to evaluate the effect of S100A12 on caspase-1, we first quantified the concentration of total caspase-1 in the chorioamniotic membrane explants cultured with S100A12. Although caspase-1 concentration tended to increase with S100A12 treatment, this tendency was not statistically significant (Figure 10A). Similarly, expression of *CASP1* gene was not significantly affected by S100A12 treatment (Figure 10B). Western blot analysis was performed to differentiate between pro- (p50) and mature (p20 and p10) forms of caspase-1. Caspase-1-p20 was significantly elevated in the chorioamniotic membranes treated with S100A12 (p=0.0154) (Figure 10C). These results demonstrate that S100A12 promotes activation of caspase-1 in the chorioamniotic membranes.

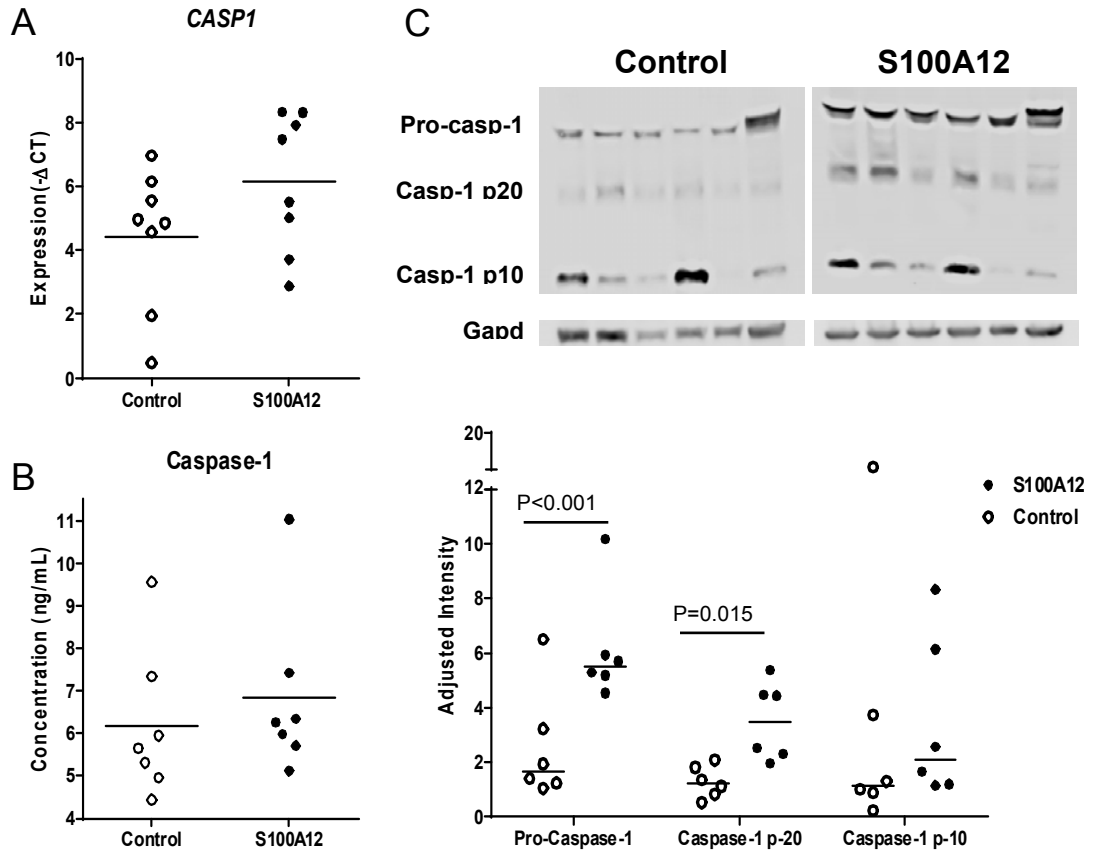

Figure 10: S100A12 activates caspase-1 in the chorioamniotic membranes. Caspase-1 expression in the chorioamniotic membranes treated with S100A12 (5μg/mL) was determined on the mRNA level by RT-PCR (A) and on the protein level by ELISA (B) and Western blot (C).

Augmented secretion of IL-1β from the chorioamniotic membrane explants cultured with S100A12 occurs concurrently with increased expression of the inflammasome subunits and accelerated maturation of caspase-1. Therefore, S100A12 up-regulates expression of inflammasomes, which may cause the demonstrated activation of caspase-1 and the subsequent release of mature IL-1β.

S100A12 induces NF-κB signaling in the chorioamniotic membranes

Although maturation of IL-1β in the chorioamniotic membranes treated with S100A12 may occur via the inflammasome-dependent activation of caspase-1, increased expression of *IL1B* gene (Figure 8) suggests additional effect of S100A12 on transcription.

NF-κB is a transcription fact known to regulate transcription of *IL1B* (151) as well as a multitude of other pro-inflammatory mediators, including cytokines, chemokines, immunoreceptors, proteins involved in antigen presentation, and so on (152). NOD1 and NOD2 are intracellular PRRs that induce nuclear translocation of NF-κB for initiation of transcription (153). We found that S100A12 increases expression of both *NOD1* (p=0.009) and *NOD2* (p=0.0009) in the chorioamniotic membranes. Expression of *NFKB1* gene itself was significantly up-regulated by S100A12 (p=0.001), as was the expression of two prototypical NFκB targets *TNF* (p=0.014) and *IL6* (p=0.0009). Expression of several other pro-inflammatory genes that were tested tended to increase with S100A12 treatment as well, although this tendency did not reach significance (Figure 11). All together, these data indicate that S100A12 is capable of inducing NF-κB-dependent transcriptional activation in the chorioamniotic membranes.

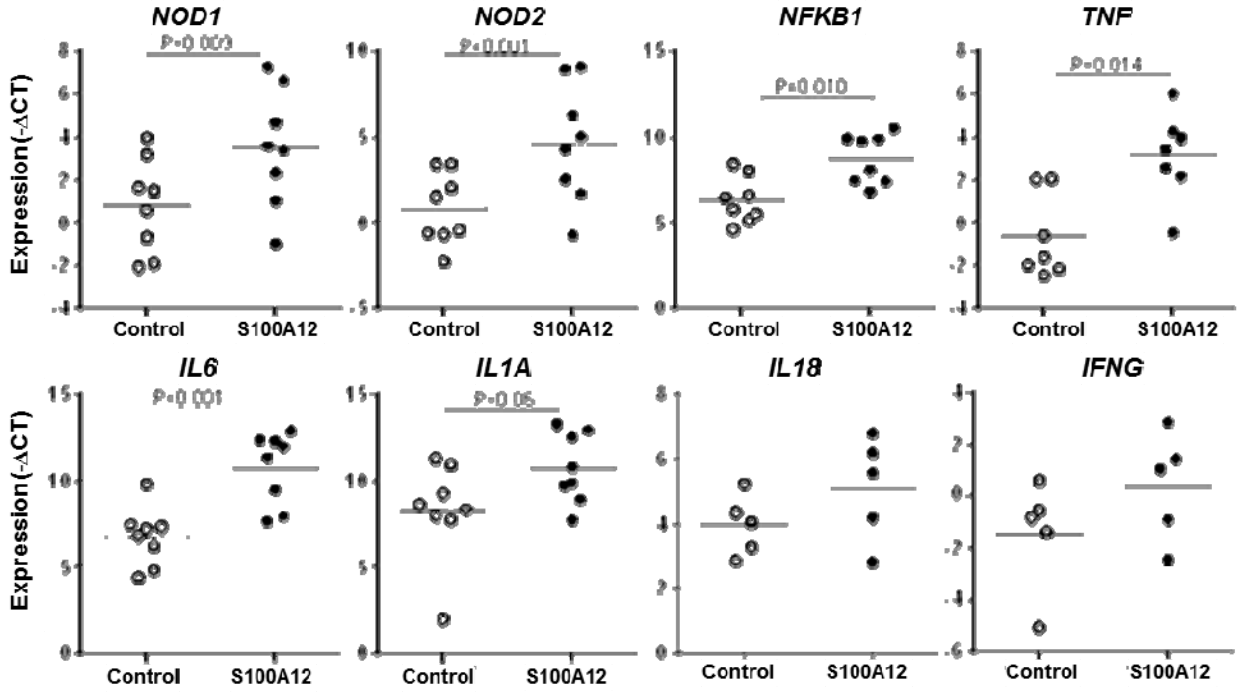

Figure 11: S100A12 induces NF-κB signaling in the chorioamniotic membranes. The chorioamniotic membranes treated with S100A12 (5μg/ml) were subjected to RT-PCR assay to determine the expression of NOD proteins (*NOD1* and *NOD2*) as well as of the pro-inflammatory transcription factor *NFKB1* and its targets *TNF*, *IL6*, and *IL1A*, *IL18*, and *IFNG*.

Propagation of inflammation often requires positive feedback loop, as seen most strikingly in cytokine storm. We assessed whether S100A12 treatment enhances sensitivity of the chorioamniotic membrane to S100A12 itself. Indeed, S100A12 increased expression of its own receptor, *RAGE* (p=0.005) (Figure 12). Interestingly, expression of another putative S100A12 receptor *TLR4* (132) was not effected by S100 treatment, while expression of *TLR2* (p=0.026) was (Figure 12). Considering that transcription of both *RAGE* (154) and *TLR2* (155) is stimulated by NF-κB, it is possible that S100A12-induced NF-κB signaling leads to up-regulation of these PRRs, which, in turn, increases cellular sensitivity to various DAMPs, including S100A12 itself.

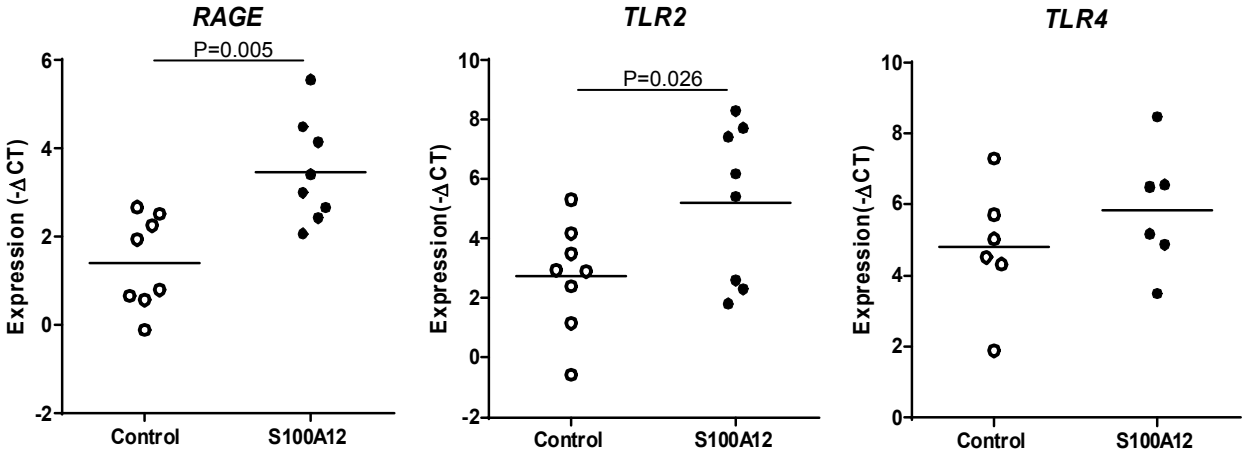

Figure 12: S100A12 increases expression of its own receptors in the chorioamniotic membranes. Expression of the PRRs known to interact with S100A12 (*RAGE*, *TLR2*, and *TLR4*) was determined by RT-PCR using the chorioamniotic membrane explants treated with S100A12 (5μg/ml).

S100A12 initiates pro-labor signaling in the chorioamniotic membranes

Labor is characterized by the influx of immune cells and the release of pro-inflammatory mediators at the maternal-fetal interface. Since treatment of the chorioamniotic membranes with S100A12 induces sterile inflammation of the chorioamniotic membranes, we evaluated whether this inflammation leads to up-regulation of pro-labor markers. Treatment with S100A12 caused up-regulation of

prostaglandin-endoperoxide synthase 2 (PTGS2), a key enzyme in the biosynthesis of labor-inducing prostaglandins (Figure 13A). S100A12 also increased expression of matrix metallopeptidase 9 (MMP9), the extracellular matrix degradation enzyme that mediates rupture of the chorioamniotic membranes among other remodeling processes of labor (Figure 13A). When stained with Masson trichrome stain, the collagen fibers in the chorioamniotic membrane explants treated with S100A12 appeared less organized and more degraded (Figure 13B), which is also indicative of pro-labor state.

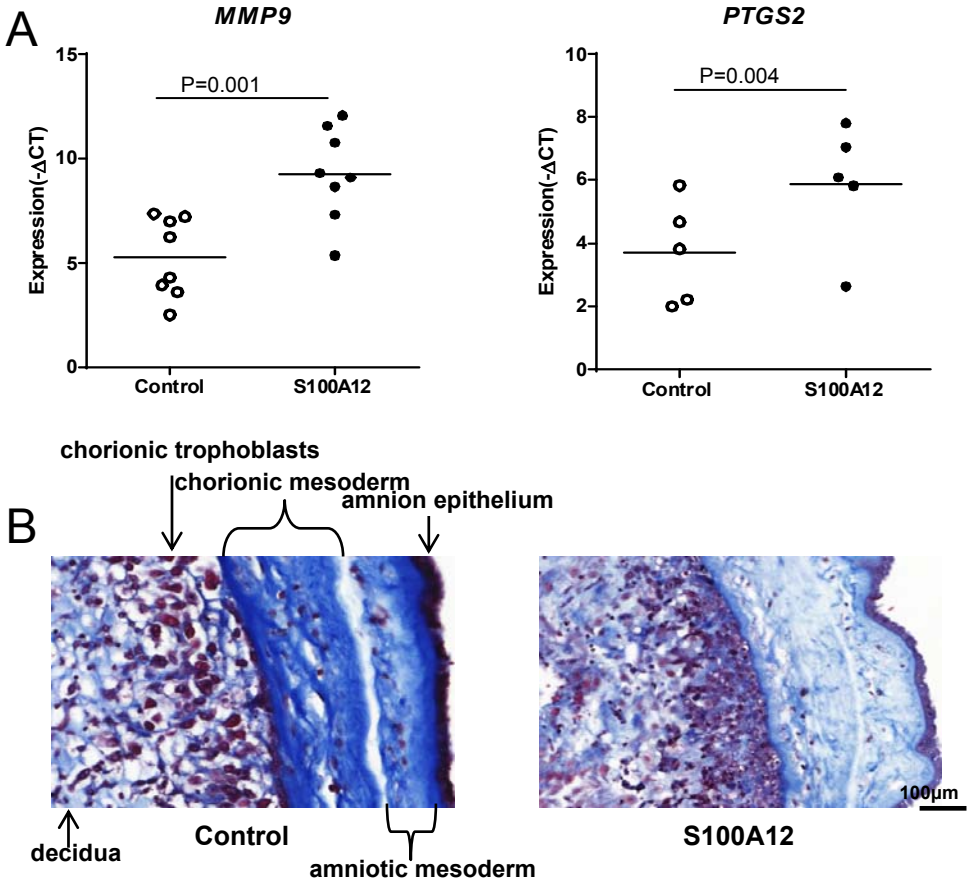

Figure 13: S100A12 increases expression of MMP9 and PTGS2 in the chorioamniotic membranes. The chorioamniotic membranes treated with S100A12 (5μg/mL) were subjected to RT-PCR assay to determine expression of MMP9 and PTGS2 (A) as well as to Trichromic Staining to visualize MMP-dependent collagen rearrangement (B).

S100A12 causes neonatal complications in vivo

Based on the pro-labor effects of S100A12 on the chorioamniotic membrane explant *in vitro*, we designed a murine model to determine whether S100A12 is capable of inducing labor *in vivo*. In this model, pregnant dams were intraperitoneally injected either with S100A12 or with PBS as a negative control at late gestation (16.5 dpc). The S100A12 injections did not precipitate preterm delivery (data not shown). However, the cohort of mice injected with S100A12 exhibited significantly increased neonatal mortality ($p<0.001$) (Figure 14). The pups that survived weighed significantly less three weeks after birth than the pups from mothers injected with PBS ($p<0.001$). Therefore, intraperitoneal injections of S100A12 at 16.5 dpc do not induce preterm birth in mice, but cause serious neonatal complications.

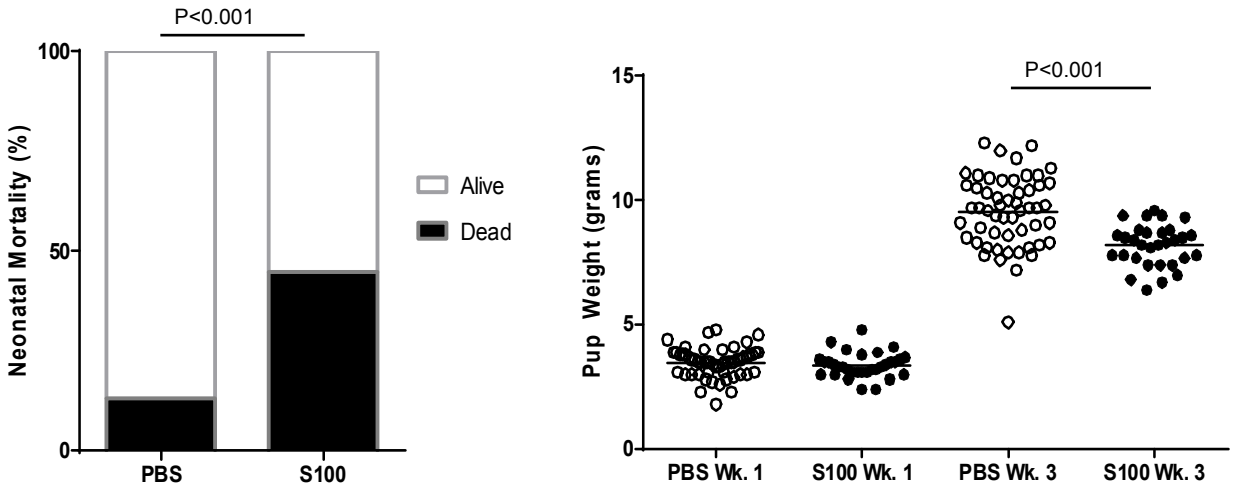

Figure 14: S100A12 confers adverse neonatal effects *in vivo*. Neonatal mortality was observed following labor and pup weight were recorded at week 3 post-delivery in the mice that were intraperitoneally injected with S100A12 (5µg/ml).

Discussion

Major findings

The major findings of this study are: 1) S100A12 is capable of inducing sterile inflammation of the chorioamniotic membranes confirmed by increased secretion and/or

expression of pro-inflammatory cytokines IL-1β, IL-1α, TNF, and IL-6, pro-inflammatory transcription factor NF-κB, and pro-inflammatory NOD proteins NOD1 and NOD2; 2) S100A12 significantly up-regulates expression of the inflammasome component NLRP3 and tends to up-regulate NLRP1; 3). The up-regulation of inflammasome components occurs together with elevated expression of pro- and active (p20) forms of inflammasome-dependent caspase-1; 4) S100A12 up-regulates expression of its own PRRs RAGE and TLR2, suggesting positive feedback regulation; 5) Chorioamniotic membranes treated with S100A12 exhibit increased expression of MMP9 and PTGS2 and decreased collagen integrity; 6) The neonates born to mothers who were intraperitoneally injected with S100A12 in late gestation exhibit higher rate of mortality and reduced weights three week after delivery.

S100A12 induces inflammasome-associated sterile inflammation of the chorioamniotic membranes

Our findings confirm that S100A12 is capable if inducing sterile inflammation of the chorioamniotic membranes via up-regulation of pro-inflammatory transcription factor NF-κB and its down-stream targets including IL-1β, IL-1α, TNF, and IL-6, as well as NOD proteins NOD1 and NOD2 (Figure 11). Interestingly, S100A12-induced sterile inflammation seems to involve up-regulation of the NLRP3 inflammasome (Figure 9) and corresponding maturation of caspase-1 (Figure 10). This is in concert with our previous findings that demonstrate up-regulation of NLRP3 in term spontaneous labor when compared to term delivery without labor (40) and in preterm labor with chorioamnionitis when compared to preterm labor without chorioamnionitis (unpublished data). NLRP3 is a NOD-like receptor capable of responding to a multitude of chemically and structurally divergent stimuli including, but not limited to, nucleic acids such as fetal

DNA, crystals such as uric acid, extracellular adenosine triphosphate (ATP), calcium levels, and ultraviolet radiation (156). Thus, it is not surprising that both HMGB1 and S100A12 (Figure 4 & 9, respectively) are capable of up-regulating NLRP3.

S100A12 promotes remodeling of the chorioamniotic membranes in vitro and neonatal complications in vivo

Activation of the NF-κB pathway is known to occur in labor and is central to many of pro-labor processes (63), including prostaglandin synthesis. The promoter of human PTGS2 contains two NF-κB response elements (157), which have been demonstrated to be bound by NF-κB in the myometrial cells stimulated by IL-1β (158). Our results herein show that S100A12 actives NF-κB signaling (Figure 11) and up-regulates expression of *PTGS2* in the chorioamniotic membranes (Figure 13). Additionally, we found that S100A12 also up-regulates expression of MMP9 and promotes collagen rearrangement (Figure 13). Collagen remodeling contributes to the rupture of chorioamniotic membranes, which is one of the components of final pathway of labor (Figure 1). Thus, S200A12 may establish pro-labor environment at the maternal-fetal interface by promoting both the synthesis of prostaglandins and the membrane remodeling. However, intraperitoneal injections of S100A12 did not precipitate preterm birth in mice (data not shown). It was recently found that inducing sterile intraamniotic inflammation by intraamniotic injections of HMGB1 resulted in increased rate of murine preterm birth, while intraperitoneal injections of much higher doses of this alarmin did not affect the rate of preterm delivery (121). Therefore, it is possible that S100A12 needs to be injected intraamniotically in order to induce preterm labor in mice. Nevertheless, our data herein shows that intraperitoneal injections of S100A12 confer adverse effects on the offspring by increasing the rate of neonatal mortality and by

decreasing the weight of surviving pups (Figure 14), suggesting the mechanism by which sterile inflammation at the maternal-fetal interface can lead to fetal/ neonatal injury. Further studies are needed to assess the physiological relevance of S100A12 in women who undergo premature labor.

CHAPTER 4 - MONOSODIUM URATE INDUCES STERILE INFLAMMATION AT THE MATERNAL-FETAL INTERFACE

Introduction

Uric acid or urate is the final product of purine metabolism that, due to its limited solubility in bodily fluids, forms triclinic monosodium urate (MSU) crystals when present at high concentration by bonding to one sodium and one water molecule (159). Accumulation of MSU crystals is a well-known etiology of a form of arthritis known as gout and is also associated with the metabolic syndrome (160). In pregnancy, increased uric acid is associated with gestational hypertension and preeclampsia (161-164). Maternal hyperuricemia in pregnant women is also significantly associated with preterm and small-for-gestational-age delivery (165), while amniotic fluid urate concentrations are inversely proportional to infant birth weight (166), and serum uric acid levels are elevated in adolescents born prematurely when compared to those born at term (167).

High risk pregnancies are characterized by increased levels of both IL-1β and several alarmins, such as HMGB1 and MSU, in gestational tissues as well as systemically (168). We hypothesize that alarmins, including MSU, promote secretion of mature IL-1β by inflammasome activation. MSU is a known activator of the NLRP3 inflammasome in T cells (169), macrophages (170, 171), dendritic cells (172), and other immune and non-immune cell types (173-175). Dr. Vikki M. Abrahams' group has demonstrated that human trophoblasts, or specialized cells of placenta, respond to uric acid with inflammasome-dependent IL-1β production (176). More recently, Dr. Sylvie Girard's lab exhibited preliminary findings at the Society for Reproductive Investigations 63rd Annual Scientific Meeting suggesting that uric acid induces fetal growth restriction

in a rat model of non-infectious inflammation during pregnancy. We aimed to determine whether MSU is capable of inducing sterile inflammation at the maternal-fetal interface and whether it confers any negative perinatal outcome.

Materials and Methods

Study population

The chorioamniotic membranes were obtained from women who underwent term delivery without labor as described in Chapter 2. The demographical characteristics of the patients are summarized in Table 4.

Table 4: Demographic characteristics of the patients whose samples were used for the MSU study.

Age (years)	26.6 (22-38)
Body mass index (kg/m2)	29.1 (22.5-40.6)
Gestational age at delivery (weeks)	39.1 (38.1-39.9)
Newborn weight (g)	3279 (2260-4060)
Race African-American Caucasian	 94% (16/17) 6% (1/17)
Primiparity	6% (1/17)
C-section	100% (17/17)
Absence of chorioamnionitis	100% (17/17)

Age, body mass index, gestational age at delivery, and newborn weight are shown as mean (min-max). Race, Primiparity, C-section, and absence of chorioamnionitis are shown as percent (positive/total).

In vitro MSU treatment

The chorioamniotic membrane explants were cultured as described in Chapter 2. For MSU treatment, the media was supplemented with 50µg/mL of MSU (Catalog no. Catalog # tlrl-msu, InvivoGen, San Diego, California, USA). This concentration was chosen based on the previous dose-response experiments and the MSU/ uric acid concentrations used by other research groups (176-179). Additionally, previous studies showed that MSU concentrations below 400µg/mL do not affect cell viability measured

after 24 hours, 48 hours, and 72 hours of treatment (177).

ELISA/ RT-PCR/ Immunoblotting/ Trichromic staining/ Zymogrpahy

ELISA, RT-PCR, immunoblotting, trichromic staining, and zymography experiments were performed as described in Chapter 2.

Animals and husbandry/ MSU intraperitoneal injections

Animal husbandry was performed as described in Chapter 3. S100A12 was injected intraperitoneally at 16.5dpc at a concentration of 50µg/ml.

Statistical analysis

Statistical analysis was performed as described in Chapter 3.

Results

MSU induces the release of mature IL-1β from the chorioamniotic membranes

To determine whether MSU is capable of inducing IL-1β-dependent sterile inflammation, we measured the expression of IL-1β both on mRNA and protein level. We found that, although MSU only tends to up-regulate *IL1B* gene expression, it

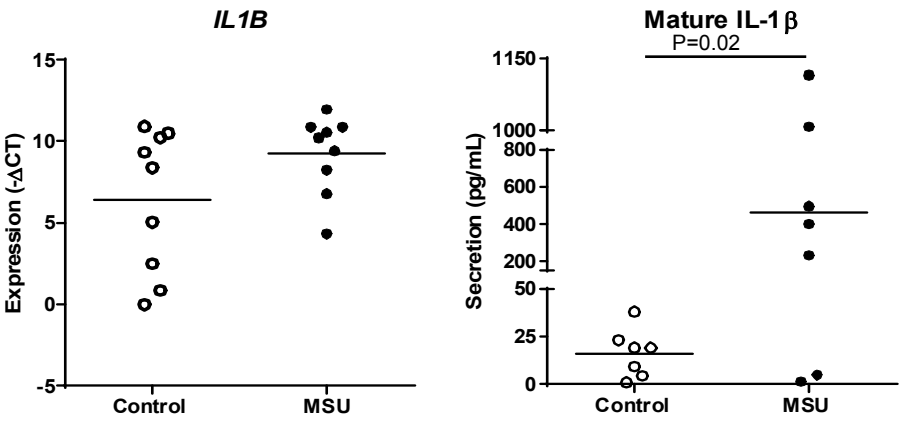

Figure 15: MSU induces the release of mature IL-1β from the chorioamniotic membranes. Expression of *IL1B* and release of mature IL-1β from the chorioamniotic membranes treated with MSU (50µg/mL) was determined by RT-PCR and ELISA, respectively.

significantly increases the release of mature IL-1β protein from the chorioamniotic membranes (Figure 15). Interestingly, a great variability in response was seen, with some cases exhibiting over 20-fold increase in IL-1β secretion, while others showing

only minor change. Such a great variability in response was not observed for other alarmins that we tested (Chapters 2, 3, & 5), which suggests that pro-inflammatory effect of MSU is more dependent on the tissue micro-environment.

MSU up-regulates the expression of inflammasome components in the chorioamniotic membranes

Because of release of mature IL-1β requires proteolytic processing by the inflammasome-dependent caspase-1, we next aimed to determine whether MSU affects expression of the inflammasome components NLRP1, NLRP3, AIM2, and NLRC4. We found that *NLRP1* (p=0.025) and *NLRP3* (p=0.045) genes were significantly up-regulated by the MSU treatment (Figure 16).

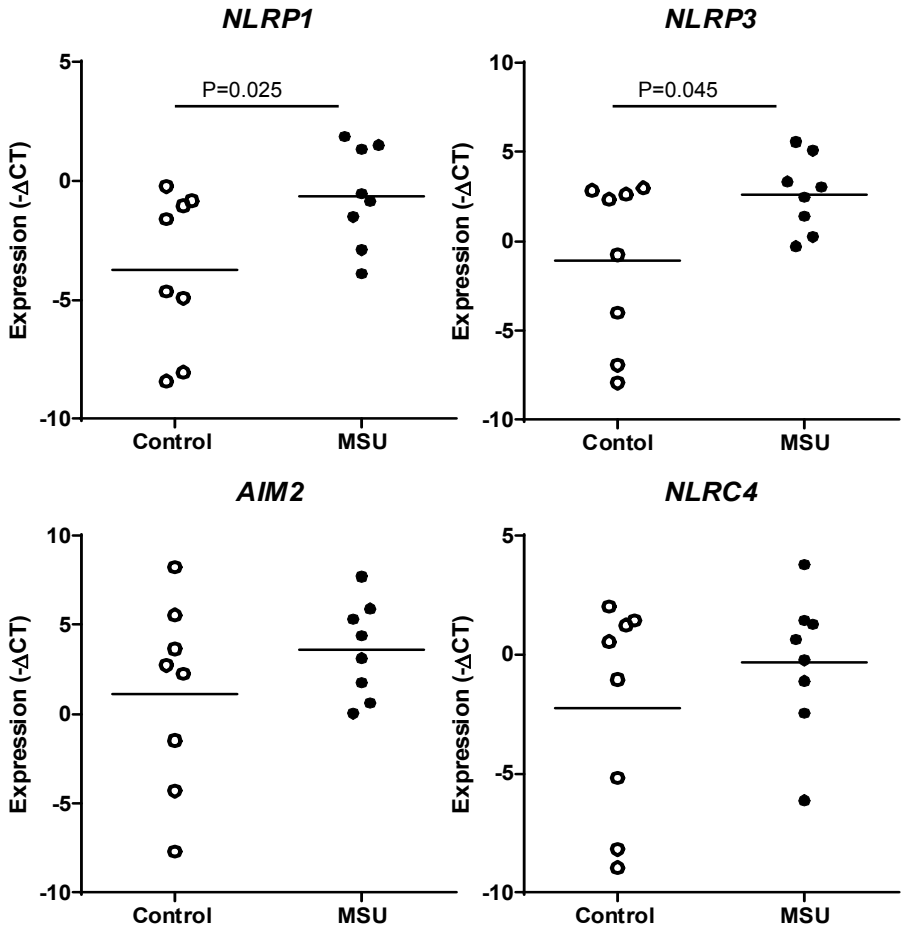

Figure 16: MSU induces the release of mature IL-1β from the chorioamniotic membranes. Expression of *IL1B* and release of mature IL-1β from the chorioamniotic membranes treated with MSU (50μg/mL) was determined by RT-PCR and ELISA, respectively.

MSU promotes activation of caspase-1 in the chorioamniotic membranes

The up-regulation of the inflammasome components NLRP1 and NLRP3 suggests that MSU is capable of activating caspase-1 in the chorioamniotic membranes. To test whether this is the case, we performed RT-PCR, ELISA, and Western blot to determine the levels of mRNA, total protein, and active forms of caspase-1, respectively.

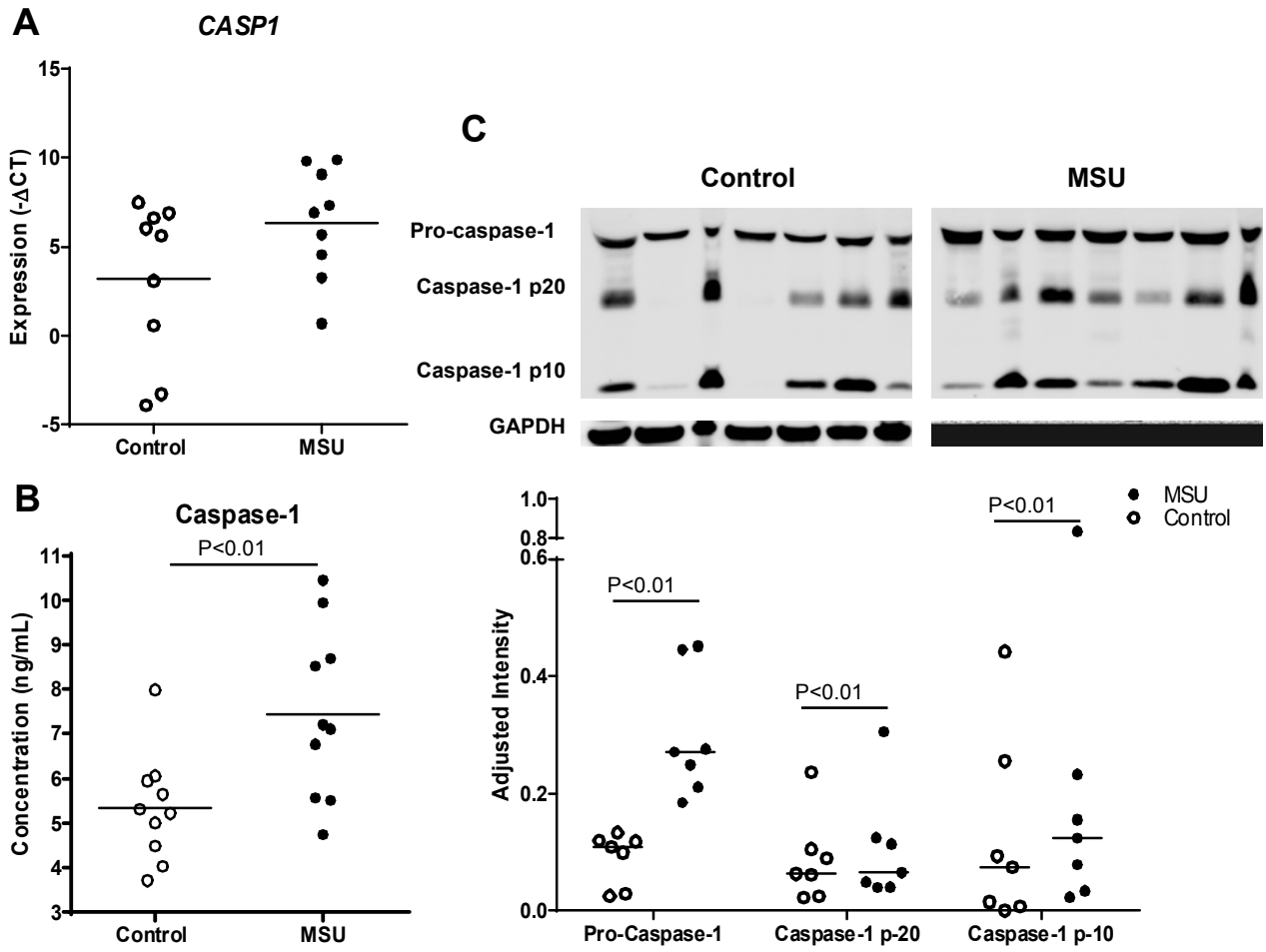

Figure 17: MSU increases concentration of active caspase-1 in the chorioamniotic membranes. Chorioamniotic membranes treated with MSU (50μg/mL) were subjected to RT-PCR to determine expression of the *CASP1* gene (A), to ELISA to evaluate the concentration of total caspase-1 protein (B) and to immunoblotting to detect mature forms (p-10 and p-20) of caspase-1 (C).

We found that MSU tends to increase *CASP1* gene expression (Figure 17A) and

significantly elevates the concentration of total caspase-1 protein ($p<0.01$) in the chorioamniotic membranes (Figure 17B). When we evaluated the mature forms of caspase-1, we found that both caspase-1 p-20 ($p<0.01$) and caspase-1 p10 ($p<0.01$) are significantly elevated after MSU treatment (Figure 17C). This suggests that MSU is capable of inducing inflammasome-regulated caspase-1 activation and subsequent IL-1β release from the chorioamniotic membranes.

MSU up-regulates expression of pro-inflammatory mediators IL6, IFNG, HMGB1, and TLR2

Next, we assayed the expression of multiple pro-inflammatory targets upon MSU treatment to determine the extent to which MSU propagates sterile inflammation and the molecular pathways involved. We found that, in addition to IL-1β, MSU promotes gene expression of two other pro-inflammatory cytokines: IL-6 ($p=0.07$) and IFNγ ($p=0.04$) (Figure 18). Interestingly, MSU also promotes expression of another alarmin – HMGB1 ($p=0.04$) and its particle recognition receptor TLR2 ($p=0.07$) (Figure 18). As discussed in Chapter 2, HMGB1 is a potent pro-inflammatory agent of its own. This suggests that MSU propagates inflammation, in part, by activating HMGB1-dependent pro-inflammatory response. Under physiological conditions of sterile inflammation due to tissue stress or injury, multiple alarmins are released simultaneously from the activated leukocytes by active secretion or from the dying somatic cells by passive release. Therefore, it is plausible that various alarmins work synergistically to promote the single outcome – activation of the immune system required for healing.

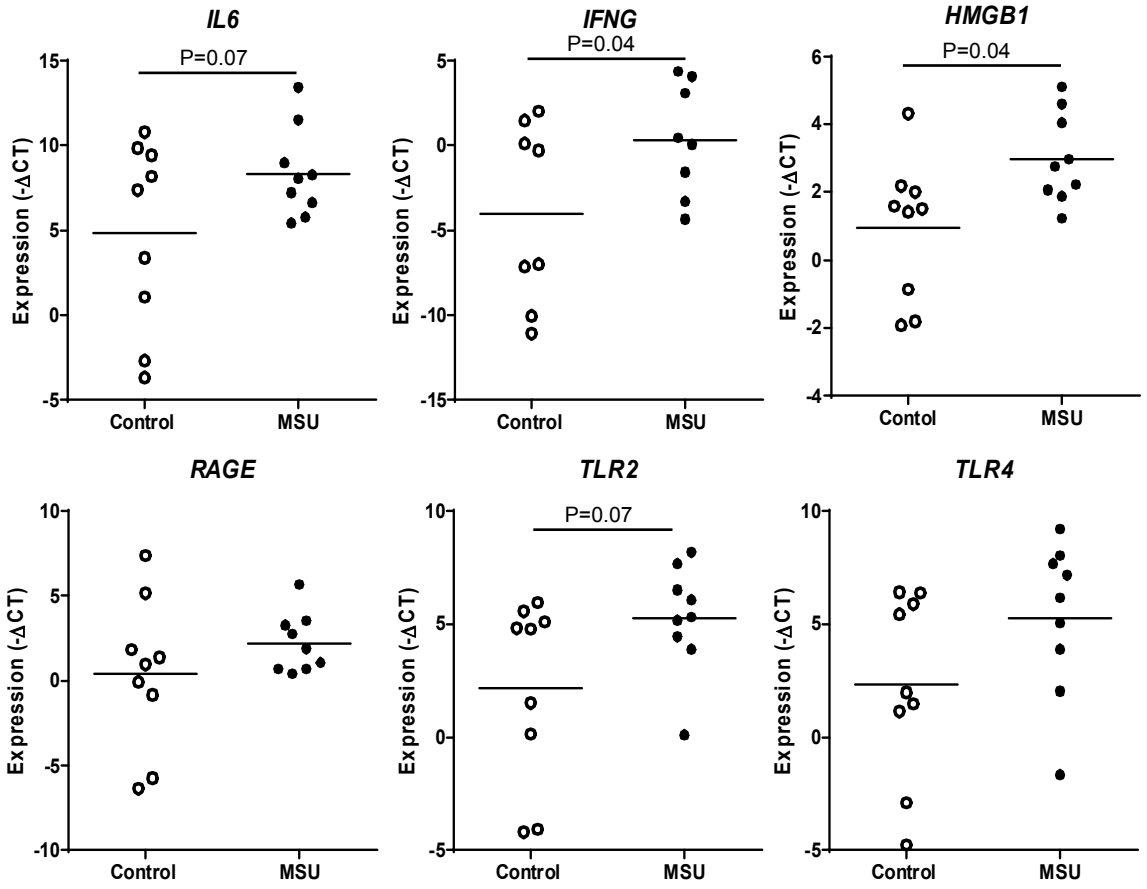

Figure 18: MSU up-regulates expression of pro-inflammatory mediators in the chorioamniotic membranes. Chorioamniotic membranes treated with MSU (50μg/mL) exhibited increased expression of *IL6*, *IFNG*, *HMGB1*, and *TLR2*.

MSU activates MMP2 and up-regulates expression of PTGS2

Next we aimed to determine whether MSU-induced inflammation leads to establishment of pro-labor microenvironment. We found that MSU significantly actives matrix-remodeling enzyme MMP2 (p=0.01) (Figure 19A) and collagen integrity tended to decrease as observed using the trichrome staining (Figure 19C). In addition, MSU upregulated expression of *PTGS2* (p=0.05) (Figure 19B), which is an important enzyme in prostaglandin biosynthesis. Therefore, MSU seems to promote remodeling of the chorioamniotic membranes and establishment of the pro-labor environment at the maternal-fetal interface.

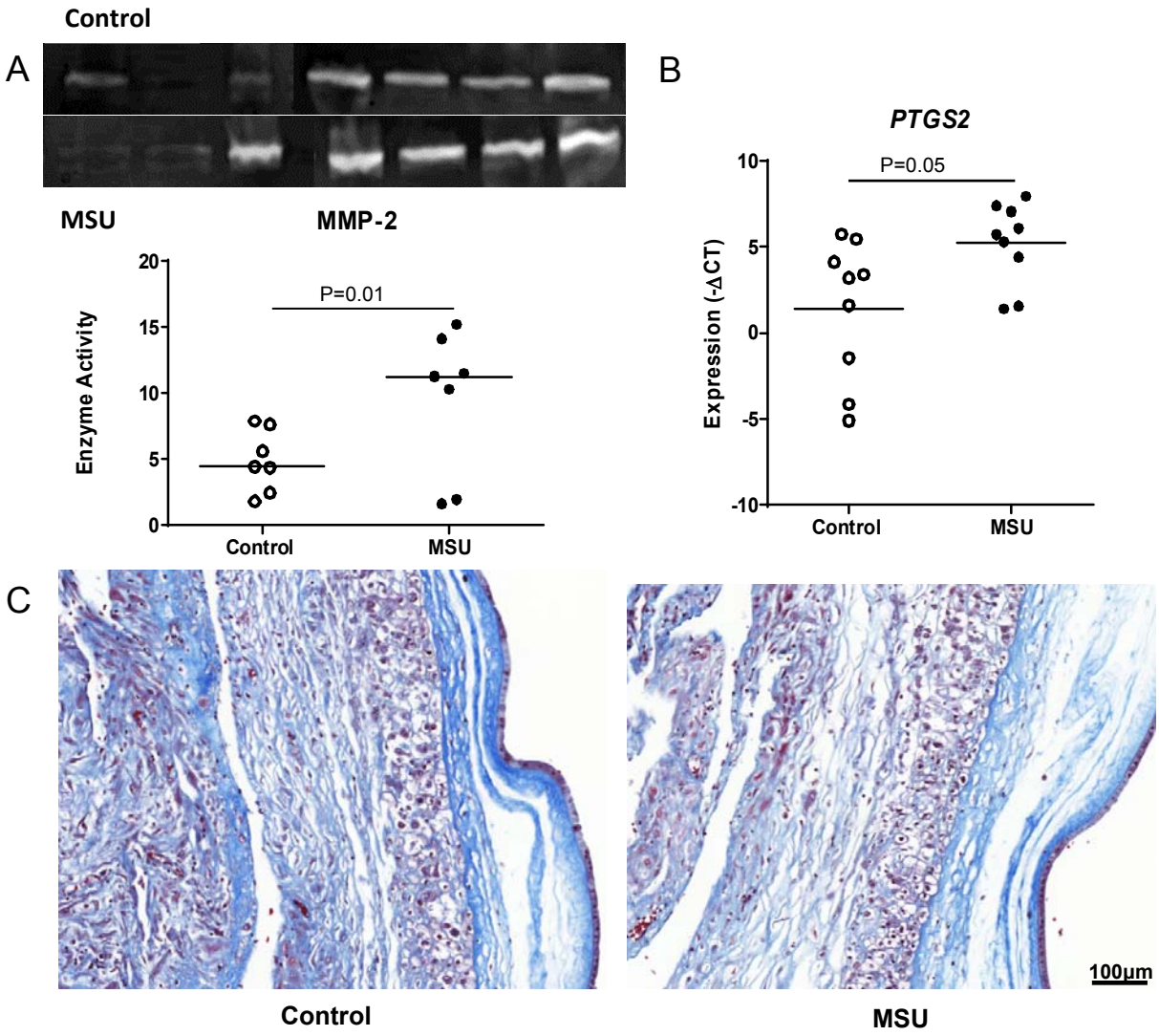

Figure 19: MSU activates MMP2 and up-regulates expression of *PTGS2*. Chorioamniotic membranes treated with MSU (50µg/mL) were subjected to zymography to determine MMP2 activity (A), to RT-PCR to assess *PTGS2* gene expression (B), and to trichrome staining to visualize collagen distribution (C).

Intraperitoneal HMGB1 injections do not cause adverse neonatal outcomes

Finally, we aimed to determine whether MSU injections can induce adverse perinatal outcome in a murine animal model. Based on our findings that neither HMGB1 nor S100A12 induces preterm birth when injected intraperitoneally, we hypothesized that intraperitoneal injections of MSU may not cause preterm labor but may have adverse effects on the neonates. However, we found that neither the rate of

neonatal mortality nor the weights of pups changed with the administration of MSU at 16.5dpc (Figure 20). Therefore, a single intraperitoneal injection of MSU at 16.5dpc does not cause adverse perinatal outcomes.

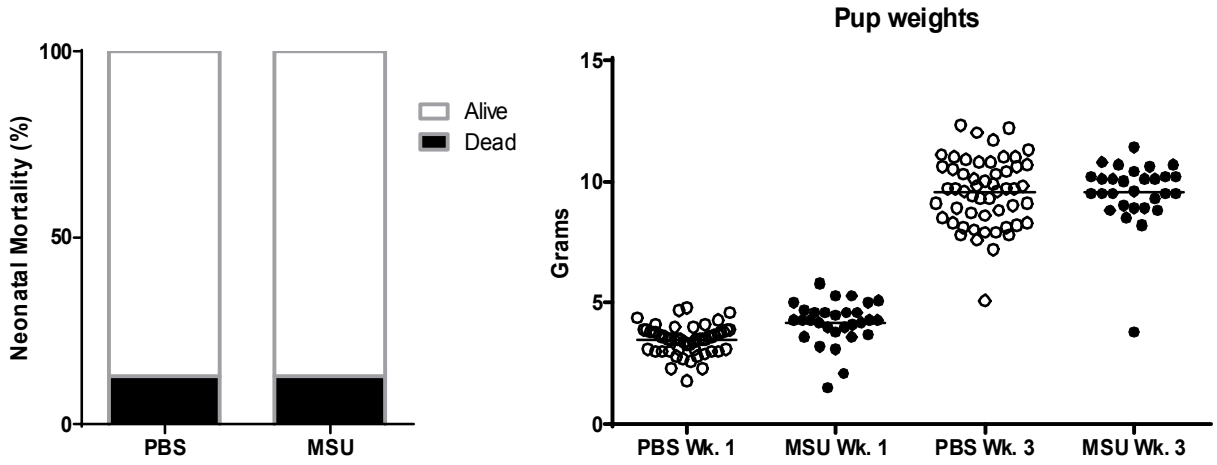

Figure 20: Intraperitoneal injection of MSU does not cause adverse neonatal outcomes. Pregnant dams were injected intraperitoneally with 100ug/mL of MSU at 16.5dpc. After delivery, the neonates were monitored for survival and weight gain.

Discussion

Major findings of the study

The major findings of this study are: 1) MSU promotes expression and/or secretion of pro-inflammatory cytokines including IL-1β, IL-6, and IFNγ in the chorioamniotic membranes; 2) MSU significantly up-regulates gene expression of the inflammasome components NLRP1 and NLRP3; 3) MSU increases concentration of pro- and active forms of caspase-1; 4) MSU promotes MMP2 activity and collagen remodeling of the chorioamniotic membranes and up-regulates *PTGS2* gene expression; 5) A single intraperitoneal injection of MSU at 16.5 dpc does not cause adverse perinatal outcomes in a mouse model.

MSU promotes sterile inflammation of the chorioamniotic membranes

We found that MSU is capable of inciting sterile inflammation of the

chorioamniotic membranes via up-regulation of pro-inflammatory cytokines, most notably IL-1β (Figure 15 & 18). The increased secretion of mature IL-1β coincided with up-regulation of two inflammasome components – NLRP1 and NLRP3 (Figure 16) and elevated concentration of inflammasome-activated caspase-1 (Figure 17). Interestingly, we showed that NLRP3 expression in the chorioamniotic membranes gets up-regulated *in vitro* by three alarmins tested by us: HMGB1 (Figure 4), S100A12 (Figure 9), and MSU (Figure 16). Preterm labor is a syndrome associated with multiple pathological processes (8) which eventually converge on the common final pathway of parturition (180). The NLRP3 inflammasome may respond to the various pathological signals at the maternal-fetal interface and initiate pro-inflammatory cascade that ultimately leads to labor. The sequential activation of the inflammasome and caspase-1 leading to release of IL-1β was proposed previously as a candidate pathway towards parturition when the amniotic fluid concentration of caspase-1 was found to be elevated in term labor and in preterm labor with intraamniotic infection/inflammation (41). Our current findings support this hypothesis and provide a mechanism by which multiple stimuli can incite the inflammasome-regulated IL-1β release.

MSU promotes pro-labor environment but fails to induce adverse perinatal outcomes

We hypothesized that sterile inflammation incited by MSU can promote preterm labor. We found that MSU-induced pro-inflammatory signaling indeed coincided with increased activity of extracellular matrix remodeling enzyme MMP2 as well as with collagen rearrangement and increased expression of prostaglandin synthase PTGS2 (Figure 19). However, these *in vitro* observations did not coincide with any adverse perinatal effects *in vivo* (Figure 20). This discrepancy may be due to insufficient *in vivo*

stimulation at the maternal-fetal interface, since a single 100mg/ml injection was performed intraperitoneally rather than intraamniotically. A rat model of non-infectious inflammation during pregnancy that involved consecutive injections of MSU crystals from gestation day 18 to 21 (250, 500, or 1000mg/kg/12hr) reportedly resulted in fetal growth restriction (Dr. Sylvie Girard's lab, data not published). Since urate is a normal product of purine metabolism and is normally found in the amniotic fluid, higher doses may be required to elicit pro-inflammatory response strong enough to induce preterm birth and/or other perinatal complications. Serial injections with higher concentration of MSU will have to be performed in order to better analyze the effect of this alarmin on gestation and fetal/neonatal health.

CHAPTER 5 - HEAT SHOCK PROTEIN 70 INDUCES STERILE INFLAMMATION AT THE MATERNAL-FETAL INTERFACE

Introduction

70-kDa heat shock proteins (HSP70s) are folding catalysts and molecular chaperones (181) that are thought to act as alarmins when released extracellularly (182, 183). HSP70 proteins are associated with numerous disorders characterized by pathological inflammation including inflammatory bowel disease (184), stroke (185), chronic kidney disease (186), cancer (187), and others (188-190). In pregnancy, elevated HSP70 levels in the amniotic fluid correlate with term labor and spontaneous preterm labor with premature rupture of membranes and intraamniotic infection/ inflammation (191). Increased HSP70 in the maternal and fetal circulations is also associated with preterm delivery (192). Finally, increased placental expression of HSP70 is associated with preterm birth and/or low birth weights (193).

However, anti-inflammatory effects of HSP70 have been reported as well (194-196). For instance, vaginal HSP70 protein expression in mid trimester pregnant women is associated with the downregulation of the pro-inflammatory immune response to abnormal vaginal flora (197). A paper by Eden et al. (198) even proposes to reclassify heat shock proteins as “DAMPERs” rather than DAMPs because of their tendency to dampen the inflammation. Recently, a hypothesis was proposed asserting that extracellular to intracellular HSP70 ratio determines pro- vs anti-inflammatory action of this protein (199). We aimed to ascertain whether HSP70 acts as an alarmin at the maternal-fetal interface. Based on our findings with other DAMPs (Chapters 2 through 4), we specifically hypothesized that HSP70 is capable of inducing inflammasome-dependent, caspase-1-mediated release of IL-1β as well as other pro-inflammatory

cytokines from the chorioamniotic membranes, which leads to perinatal complications in an animal model.

Materials and Methods

Study population

The chorioamniotic membranes were obtained from women who underwent term delivery without labor as described in Chapter 2. The demographical characteristics of the patients are summarized in Table 5.

Table 5: Demographic characteristics of the patients whose samples were used for the HSP70 study

Age (years)	28.5 (20-36)
Body mass index (kg/m2)	33 (20.4-50.6)
Gestational age at delivery (weeks)	39.1 (37-41.9)
Newborn weight (g)	3341 (2740-3820)
Race African-American Caucasian	 90.5% (19/21) 9.5% (2/21)
Primiparity	9.5% (2/21)
C-section	100% (23/23)
Absence of chorioamnionitis	95.2% (20/21)

Age, body mass index, gestational age at delivery, and newborn weight are shown as mean (min-max). Race, Primiparity, C-section, and absence of chorioamnionitis are shown as percent (positive/total).

In vitro HSP70 treatment

The chorioamniotic membrane explants were cultured as described in Chapter 2. For HSP70 treatment, the media was supplemented with 10µg/mL of full-length HSP70 (Catalog no. ab78434, Abcam). Injury-induced lysis of as little as a half a gram of tissue could cause extracellular release of 100µg/mL of HSP70 (200). The concentration that we chose for the *in vitro* treatment was lower or in line with the published studies from several research groups (200-204).

ELISA/ RT-PCR/ Immunoblotting/Trichromic staining/Statistical methods

ELISA, RT-PCR, immunoblotting, and trichromic staining experiments were

performed as described in Chapter 2. Statistical methods were described in Chapter 3.

Animals and husbandry/ HSP70 Intraperitoneal injections

Animal were handled and injected as described in Chapter 3. Concentration of 20µg/ml was used for the intraperitoneal injections.

Results

HSP70 induces the release of mature IL-1β from the chorioamniotic membranes

To determine whether HSP70 can exert pro-inflammatory effect on the chorioamniotic membranes, the membrane explants cultured with recombinant HSP70 were subjected to RT-PCR and ELISA to determine expression of *IL1B* gene and secretion of mature IL-1β protein, respectively. We found that, although HSP70 did not change expression of *IL1B*, it significantly up-regulated IL-1β protein secretion ($p<0.001$) (Figure 21). This finding supports the assertion that HSP70 is an alarmin that initiates pro-inflammatory signaling.

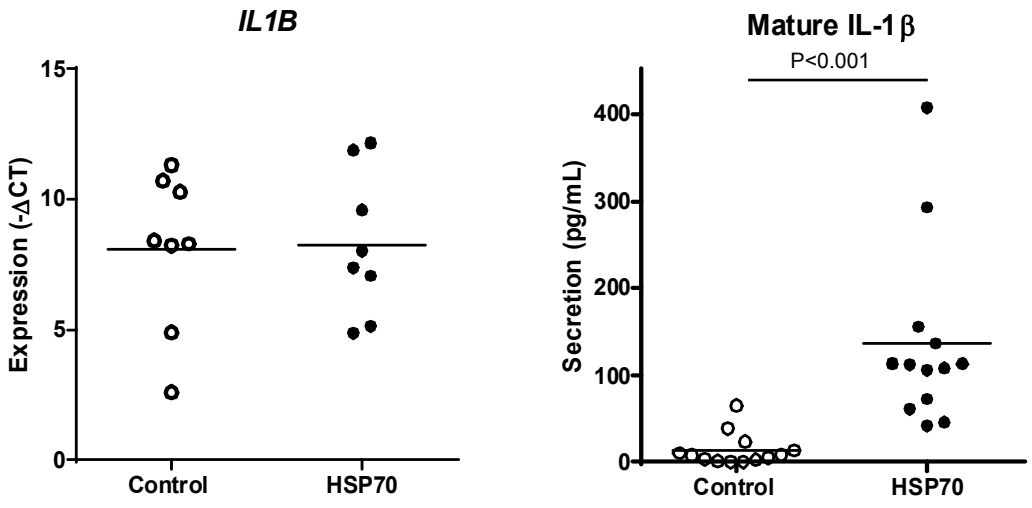

Figure 21: HSP70 induces release of mature IL-1β from the chorioamniotic membranes. Chorioamniotic membrane explants treated with HSP70 (10µg/mL) were subjected to RT-PCR to determine expression of *IL1B* and to ELISA to measure concentration of mature IL-1β released into the media.

HSP70 promotes activation of caspase-1

To determine whether the observed increase of IL-1β upon HSP70 treatment occurs via activation of the caspase-1 enzyme, we measured *CASP1* gene expression, concentration of total caspase-1 protein as well as pro- and active forms of caspase-1. We found that HSP70 does not significantly affect the gene expression of *CASP1* (Figure 22A) and the concentration of total caspase-1 protein (Figure 22B), yet it does promote activation of caspase-1 as confirmed by the increased immunoreactivity of caspase-1 p20 ($p<0.01$) after HSP70 treatment (Figure 22C). Thus, HSP70 promotes activation, but not transcription, of caspase-1.

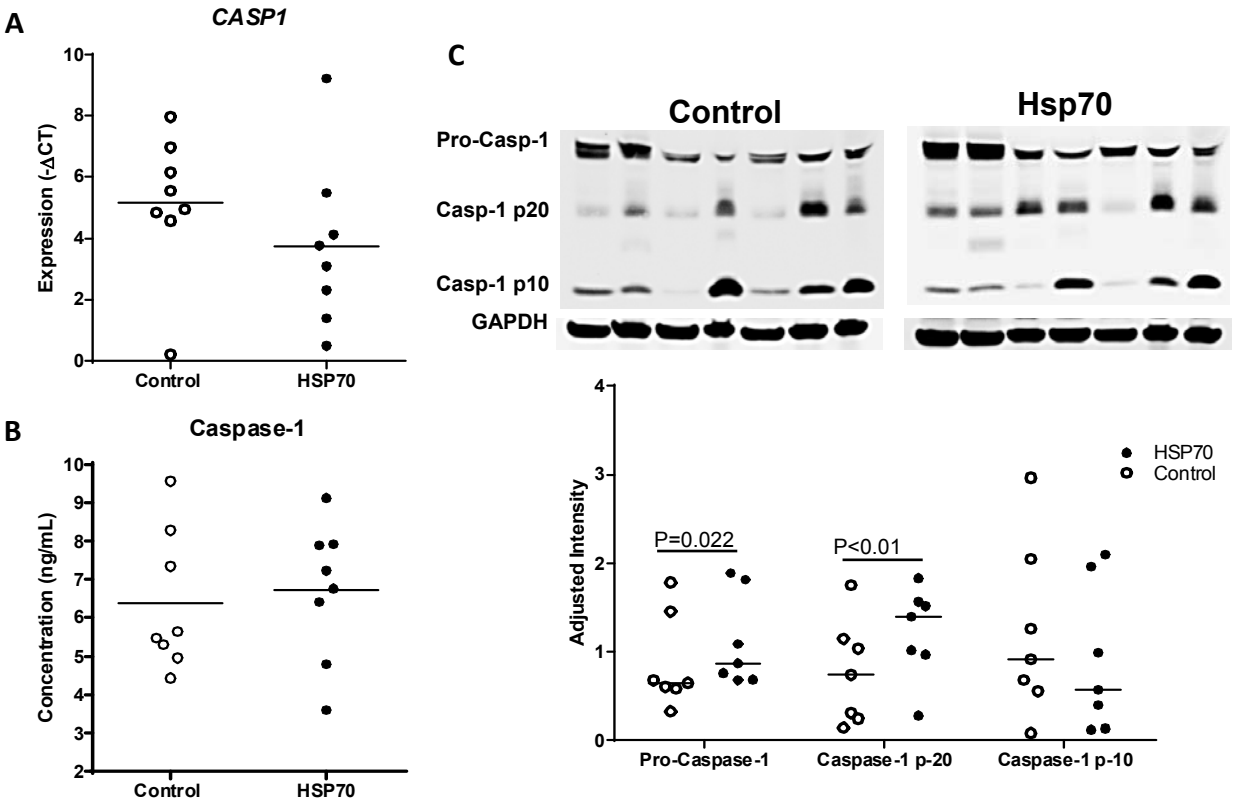

Figure 22: HSP70 promotes activation of caspase-1 in the chorioamniotic membranes. Chorioamniotic membranes treated with HSP70 (10μg/mL) were assayed for expression of *CASP1* gene by RT-PCR (A), concentration of total caspase-1 protein by ELISA (B), and the presence of active forms of caspase-1 by Western blot (C).

HSP70 does not induce expression of the major inflammasome components

Because inflammasome complexes are known to activate caspase-1, we next aimed to determine whether increased activity of caspase-1 after HSP70 treatment corresponds to up-regulation of the inflammasome components. We found that neither one of the four inflammasome components tested (*AIM2*, *NLRP1*, *NLRP3*, and *NLRC4*) was up-regulated in response to HSP70 (Figure 23). In fact, HSP70 tended to down-regulate these genes.

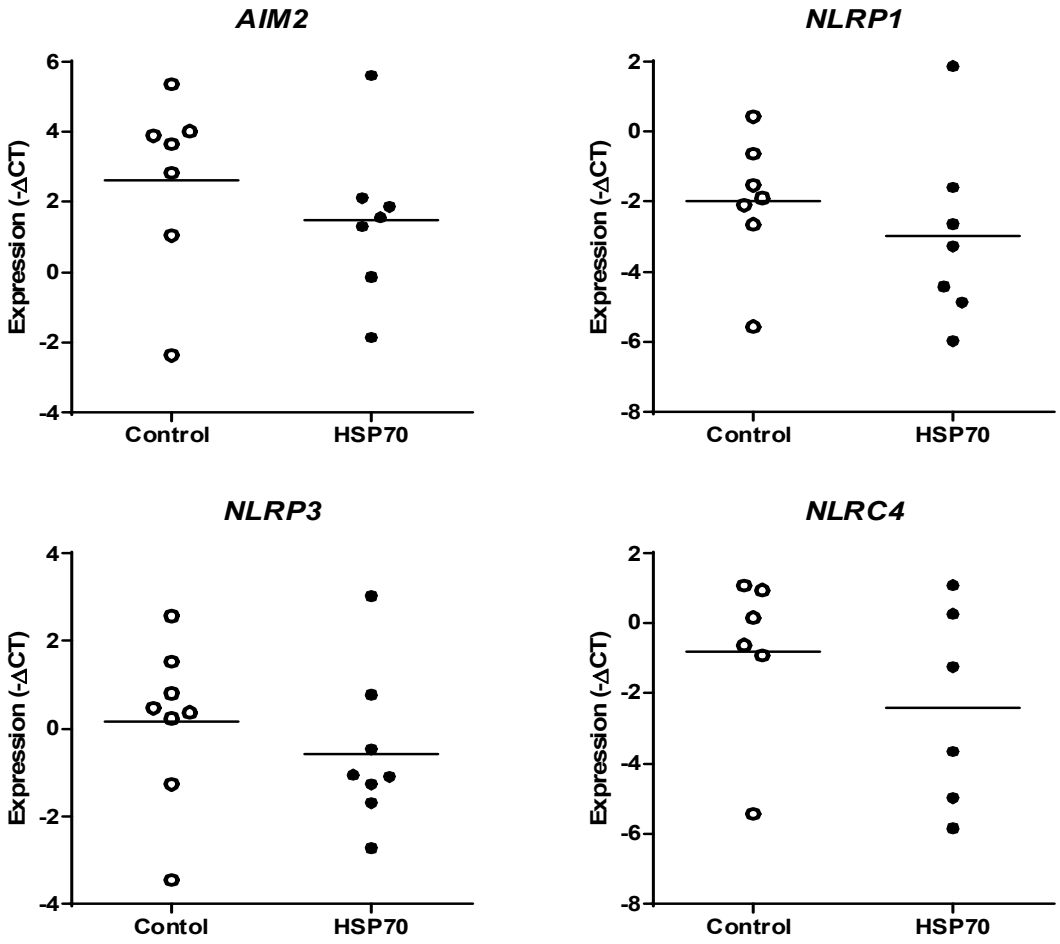

Figure 23: HSP70 does not induce expression of the major inflammasome components in the chorioamniotic membranes. Chorioamniotic membranes treated with HSP70 (10μg/mL) were assayed for expression of *AIM2*, *NLRP1*, *NLRP3*, and *NLRC4* by RT-PCR.

This surprising finding suggests that HSP70 either induces inflammasome assembly rather than the expression of inflammasome components or promotes activation of caspase-1 via inflammasome-independent signaling.

HSP70 increases expression of NOD2 and TNF

To further determine the extent of HSP70-induced sterile inflammation, we assayed the expression of the NOD proteins (*NOD1* and *NOD2*), the pro-inflammatory transcription factor (*NFKB1*), and its down-stream targets *TNF*, *IL6*, *IL1A*, *IFNG*, and *IL18*).

We found that HSP70 significantly up-regulated *TNF* (p=0.01) and tended to up-regulate *NOD2* (p=0.06) (Figure 24). Therefore, HSP70 does not seem to induce strong pro-inflammatory transcriptional response in the chorioamniotic membranes.

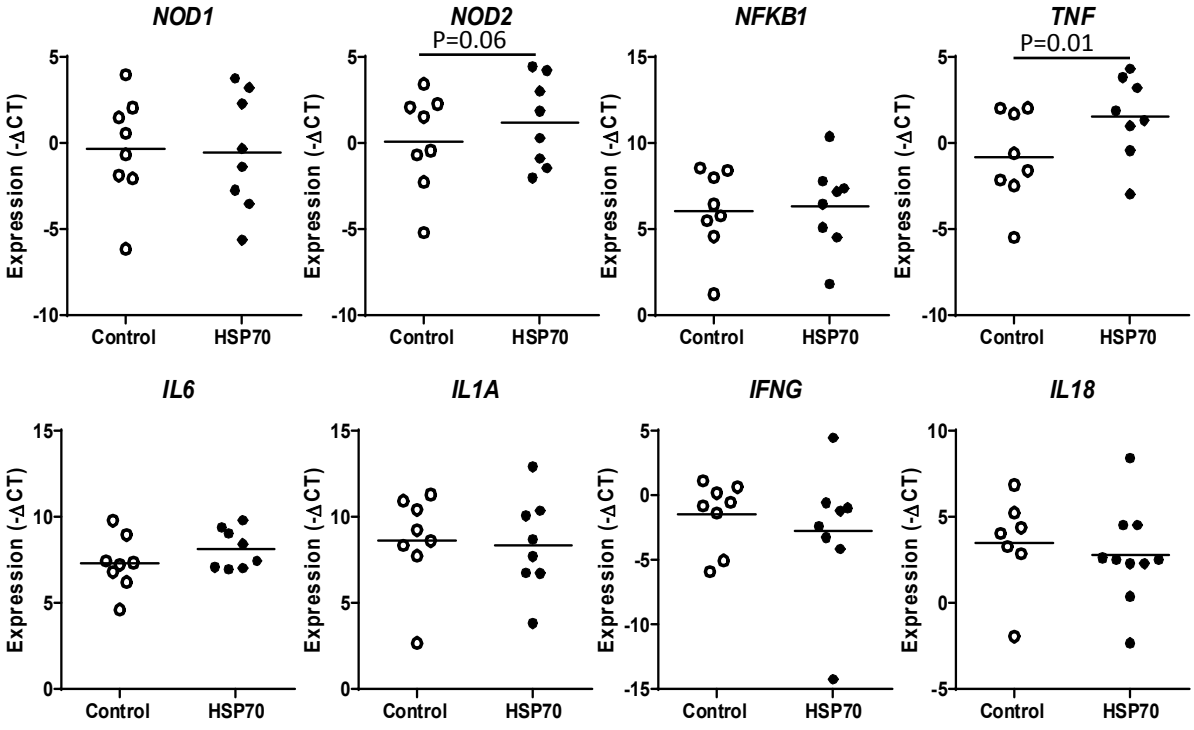

Figure 24: HSP70 increases expression of *NOD2* and *TNF* in the chorioamniotic membranes. The chorioamniotic membranes treated with HSP70 (10μg/mL) were subjected to RT-PCR to determine expression of *NOD2* and *TNF*, but not of *NOD1*, *NFKB1*, *IL6*, *IL1A*, *IFNG*, or *IL18*.

HSP70 up-regulates expression of MMP9 in the chorioamniotic membranes

Although HSP70 seemed to elicit weaker pro-inflammatory response compared to the other alarmins that we tested (Chapters 2 through 4), we aimed to determine whether HSP70-stimulated release of mature IL-1β is able to induce membrane remodeling and establish pro-labor environment in the chorioamniotic membranes.

We found that HSP70 significantly upregulated expression of *MMP9* (p=0.018), but not of *PTGS2* (Figure 25A). Trichromic staining suggested that HSP70 promotes collagen reorganization of the chorioamniotic membranes (Figure 25B).

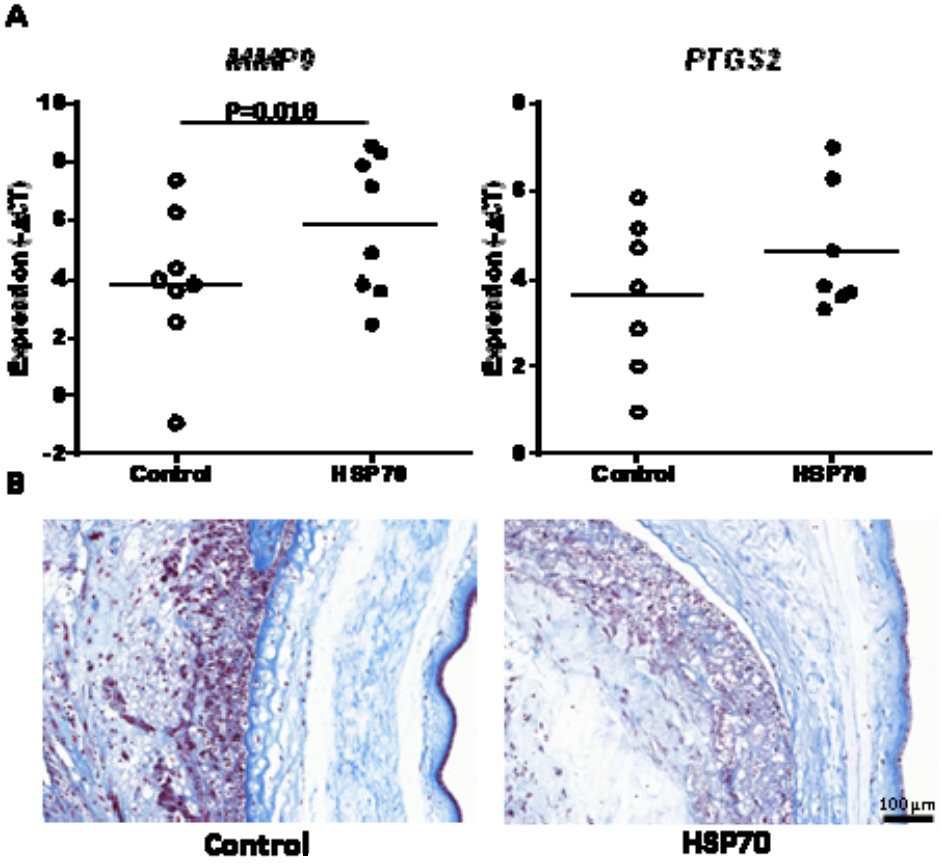

Figure 25: HSP70 up-regulates expression of MMP9 and remodels collagen composition of the chorioamniotic membranes. The chorioamniotic membranes treated with HSP70 (10µg/ml) exhibited increased expression of MMP9 (A) and collagen remodeling (B).

HSP70 increases neonatal mortality in vivo

Finally, to determine whether HSP70 has adverse perinatal effects, pregnant mice were administered HSP70 via intraperitoneal injection at 16.5dpc. Although, no preterm birth was observed (data not shown), the neonatal mortality rate significantly increased ($p<0.001$), while pup weights were not affected (Figure 26). Thus, intraperitoneal administration of HSP70 promotes neonatal mortality *in vivo*.

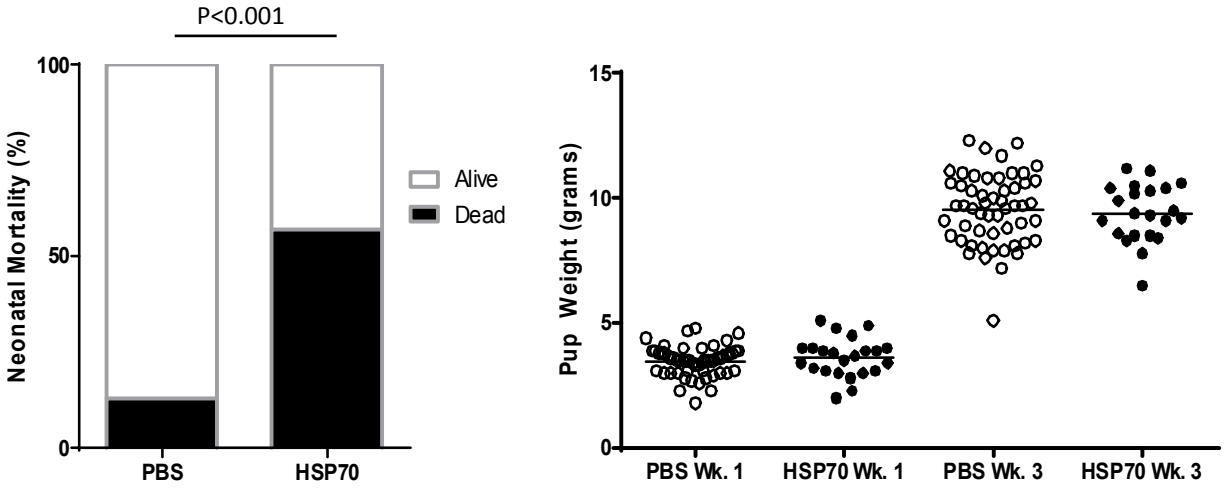

Figure 26: HSP70 increases neonatal mortality *in vivo*. Damps were injected intraperitoneally with HSP70 (20μg/mL) at 16.5dpc. After term delivery, neonatal mortality and pup weights were recorded.

Discussion

Major findings

The major findings of this study are: 1) HSP70 significantly increases secretion of mature IL-1β from the chorioamniotic membranes; 2) Although HSP70 does not up-regulate expression of the inflammasome components, it does promote activation of caspase-1; 3) HSP70 upregulates expression of the pro-inflammatory cytokine *TNF* and the matrix remodeling enzyme *MMP9*; 4) Intraperitoneal injection of HSP70 at 16.5dpc greatly increases the rate of neonatal mortality.

HSP70 promotes maturation of IL-1β by caspase-1

The findings herein show that HSP70 significantly increases the release of mature IL-1β from the chorioamniotic membranes (Figure 21) and simultaneously promotes activation of the IL-1β cleaving enzyme caspase-1 (Figure 22). However, HSP70 does not increase the expression of the inflammasome components that we tested (Figure 23). Inflammasome activation is a two-step process that requires both priming and assembly of the inflammasome complex (92, 93). The priming step involves NFκB-directed transcriptional up-regulation of the inflammasome components to a functional level (91-93). The second step is post-transcriptional and allows the assembly of the NLRP3 inflammasome complex (92, 93). Considering that treatment with HSP70 did not up-regulate expression of *NFκB* and its downstream targets, with an exception of *TNF* (Figure 24), it is possible that HSP70 acts at the second step of inflammasome activation by promoting assembly of the inflammasome complex. To test this possibility, additional experiments that assess the inflammasome assembly will have to be performed. It is also possible that HSP70 promotes secretion of IL-1β via inflammasome-independent pathway. Several such pathways have been described in the literature (105, 205-208) and inflammasome/caspase-1-independent processing of IL-1β is an area of active research. Further research is required to determine if and what inflammasome-independent pathways are involved in HSP70-stimulated secretion of IL-1β at the maternal-fetal interface.

CHAPTER 6 - INVARIANT NKT CELL ACTIVATION INDUCES LATE PRETERM BIRTH THAT IS ATTENUATED BY ROSIGLITAZONE

(This chapter contains previously published material. See Appendix C)

Introduction

Administration of such alarmins as IL1α (112) or HMGB1 (209) induces preterm labor/birth. In addition, IL33, a classic alarmin (102), is expressed in decidual tissues and up-regulated in acute chorioamnionitis (210), a placental lesion associated with preterm labor (211). Recently, it was demonstrated that IL33 is a potent activator of invariant (i)NKT cells (212, 213). Therefore, we hypothesized that activation of iNKT cells, immune cells that can be activated by alarmins in the context of sterile inflammation, could participate in the immune mechanisms that lead to non-infection-related preterm labor/birth.

iNKT-cell activation induces the initiation of signaling pathways (e.g., the NF-κB pathway) that lead to the production of Th1 and Th2 cytokines and chemokines (214-219) which, in turn, leads to a massive immune response mediated by innate and adaptive immune cells (220). Hence, we hypothesized that iNKT-cell activation via α-galactosylceramide (α-GalCer), a high affinity iNKT ligand (221, 222), would activate innate and adaptive immune cells at the maternal-fetal interface promoting pathological inflammation and leading to spontaneous preterm labor/birth. In addition, we proposed that suppression of this inflammatory response would prevent PTB induced by NKT-cell activation. In search of an anti-inflammatory drug to prevent PTB, we evaluated rosiglitazone, a selective peroxisome proliferator-activated receptor (PPAR)γ agonist (223). Rosiglitazone causes activation of the PPARγ pathway which, in turn, suppresses gene transcription by interfering with signal transduction pathways, such as

the NF-κB, STAT, and AP-1 pathways (224-226). PPARγ activation has been suggested as a therapeutic intervention for preventing PTB (227) since treatment with 15-deoxy-$\Delta^{12,14}$-prostaglandin J_2 compound, a PPARγ agonist (228, 229), delays endotoxin-induced PTB (230). However, whether PPARγ activation blunts the inflammatory response induced by iNKT-cell activation has not been investigated.

Using a murine model, our investigations demonstrate for the first time that administration of α-GalCer in the third trimester leads to late PTB, which is prevented following PPARγ activation by treatment with rosiglitazone. In addition, we describe that PPARγ activation regulates immune mechanisms locally, at the maternal-fetal interface, and systemically to attenuate α-GalCer-induced late PTB. Finally, we broaden the significance of our findings by demonstrating an increase of activated iNKT-like cells in decidual tissue from women who underwent spontaneous preterm labor/birth.

Materials and Methods

Animals

C57BL/6J (B6) mice were bred in the animal care facility at the C.S. Mott Center for Human Growth and Development at Wayne State University, Detroit, Michigan, USA, and housed under a circadian cycle (light: dark=12:12 h). Eight- to 12-week-old females were mated with male mice of proven fertility. Female mice were examined daily between 8:00 a.m. and 9:00 a.m. for the presence of a vaginal plug, which denoted 0.5 days *post-coitum* (dpc). Upon observation of vaginal plugs, female mice were then separated from the males and housed in other cages. The weight gain of two or more grams confirmed pregnancy at 12.5 dpc. Procedures were approved by the Institutional Animal Care and Use Committee (IACUC) at Wayne State University.

α-GalCer-induced late preterm birth model

Pregnant B6 mice were i.v. injected with 1μg, 2μg, 3μg, or 4μg of α-GalCer (KRN7000, Funakoshi Co., Ltd., Tokyo, Japan; n=3 each for 1μg, 3μg, or 4μg, and n=20 for 2μg) that had been dissolved in 50μl of 4% DMSO (Sigma-Aldrich Co., LLC, St. Louis, MO, USA) or with 50μl of 4% DMSO alone (referred to throughout the manuscript as DMSO) as a control (n=19) at 16.5 dpc (third trimester). Following injection, pregnant mice were monitored using a video camera with infrared light (Sony Corporation, China) until delivery. A second group of mice was i.v. injected with either 2μg of α-GalCer or DMSO at 10.5 dpc (n=5 each; second trimester), and inspection of resorption sites was performed at 14.5 dpc. A third group of mice was i.v. injected with 2μg of α-GalCer at 10.5 dpc (n=3) and monitored during delivery; photographs of the neonates at 1 day and 2 days after birth were taken using a camera (Sony).

Video monitoring, pup mortality and neonatal weight

Video monitoring allowed for determination of gestational age and rate of pup mortality. Gestational age was calculated from the presence of the vaginal plug (0.5 dpc) until the observation of the first pup in the cage bedding. The rate of pup mortality for each litter was defined as the proportion of born pups found dead among the total litter size. Late PTB was defined as delivery between 18.0 and 18.5 dpc. Neonatal survival and weight were recorded after one week postpartum.

In vivo imaging by ultrasound

On the morning of 16.5 dpc, pregnant B6 mice were anesthetized by inhalation of 2-3% isoflurane (Aerrane, Baxter Healthcare Corporation, Deerfield, IL, USA) and 1-2 L/min of oxygen in an induction chamber. Using Doppler ultrasound, the fetal heart rate and umbilical artery hemodynamic parameters were recorded (VisualSonics Inc.,

Toronto, ON, Canada). Following ultrasound, dams were placed under a heat lamp for recovery, which occurred 10-20 min after heating. On the same day at noon, dams were injected either with 2μg of α-GalCer or DMSO as described previously (n=3 each). On the afternoon of 17.5 dpc (just prior to late PTB in those mice injected with α-GalCer), a second ultrasound was performed, and the same hemodynamic parameters were evaluated.

Video monitoring by infrared thermography

Pregnant B6 mice were i.v injected with 2μg of α-GalCer at 16.5 dpc (n=3). Immediately after late preterm delivery, the body temperature of the newborns was monitored using a thermal infrared camera (FLIR e50, FLIR Systems, Inc., Wilsonville, OR, USA). Temperature readings were recorded at intervals of 15 and 30 sec, and also at intervals of 1, 2, 3.5, 5.5, and 8 min after birth. A newborn that maintained a constant body temperature was considered a viable pup, while a newborn that gradually decreased in body temperature to the level of room temperature was qualified as a dead pup; viable and dead pups were also confirmed by visual analysis.

Fetal and placental weights

Pregnant B6 mice were i.v. injected with 2μg of α-GalCer (n=8) or DMSO (n=6) at 16.5 dpc. Six hours after injection, dams were euthanized, and placental and fetal weights were recorded using a scale (DIA-20, American Weight Scales, Norcross, GA, USA).

Rosiglitazone treatment of α-GalCer-induced late PTB

Pregnant B6 mice were i.v. injected with 2μg of α-GalCer (n=14) at 16.5 dpc. After 2h, mice were s.c. injected with a 10mg/kg of body weight dose of rosiglitazone (Selleck Chemicals, Houston, TX, USA) diluted in 1:10 DMSO. Control pregnant mice

received only the dose of rosiglitazone at 16.5 dpc (n=10). Following injection, mice were monitored via video camera with infrared light until delivery (Figure 2A).

Tissue collection from pregnant mice

Pregnant B6 mice were i.v. and/or s.c. injected at 16.5 dpc with: 1) DMSO, 2) 2μg of α-GalCer, 3) 2μg of α-GalCer followed by rosiglitazone (10mg/kg of bodyweight) 2h after, or 4) rosiglitazone alone as a control. Mice were euthanized 6h after the injection with α-GalCer or DMSO, or 4h after treatment with rosiglitazone (n=6-10 mice per group). Decidual and myometrial tissues from one implantation site were collected as previously described (231) and placed in RNAlater Stabilization Solution (Life Technologies, Grand Island, NY, USA) according to the manufacturer's instructions. Decidual and myometrial tissues from the remaining implantation sites were collected, and leukocytes were immediately isolated. The spleen, uterine lymph nodes (ULN), and liver were also collected, and leukocyte suspensions were prepared.

Leukocyte isolation from murine tissues

Isolation of leukocytes from myometrial and decidual tissues was performed as previously described (231). Briefly, tissues were cut into small pieces using fine scissors and enzymatically digested with StemPro Cell Dissociation Reagent (Accutase, Life Technologies) for 35 min at 37°C. The spleen, ULN, and liver were gently dissociated using two glass slides in order to prepare a single leukocyte suspension. Leukocyte suspensions were filtered using a 100μm cell strainer (Fisher Scientific, Hanover Park, IL, USA), and washed with FACS buffer [0.1% bovine serum albumin (Sigma-Aldrich) and 0.05% sodium azide (Fisher Scientific Chemicals, Fair Lawn, NJ, USA) in 1X PBS (Fisher Scientific Bioreagents)] before immunophenotyping.

Immunophenotyping of murine leukocytes

Leukocyte suspensions from decidual and myometrial tissues and the liver were stained using the LIVE/DEAD Fixable Blue Dead Cell Stain Kit (Life Technologies) prior to incubation with extracellular mAbs. Leukocyte suspensions were then centrifuged, and cell pellets were incubated for 10 min with the CD16/CD32 mAb (FcγIII/II Receptor; BD Biosciences, San Jose, CA, USA), and subsequently incubated with specific fluorochrome-conjugated anti-mouse mAbs (Table 6) for 30 min. Leukocyte suspensions were lysed/fixed with Lyse/Fix Buffer (BD Biosciences) for extracellular staining, and the BD Cytofix/Cytoperm™ Fixation/Permeabilization Solution Kit (BD Biosciences) for intracellular staining. At least 50,000 events for the spleen, liver, and decidual cells, or 25,000 events for the ULN and myometrial cells, were acquired using the BD LSRFortessa flow cytometer (BD Biosciences) and the FACSDiva 8.0 software (BD Biosciences). Leukocyte subsets were gated within the viability gate. Immunophenotyping included identification of: 1) CD1d-restricted iNKT cells (CD1d Tetramer$^+$DX5$^+$NK1.1$^+$TCRβ$^+$ cells) and their activation status by expression of CD69, CD44, IFNγ, and IL4; 2) conventional T cells (CD3$^+$CD4$^+$ and CD3$^+$CD8$^+$ cells) and their activation status by expression of CD69, CD25, PD1, CD40L, and CTLA-4; 3) neutrophils (CD11b$^+$Ly6G$^+$ cells) and their activation status by expression of IFNγ; 4) macrophages (CD11b$^+$F4/80$^+$ cells) and their activation status by expression of Arg1, iNOS, IFNγ, and IL10; and 5) expression of IFNγ by mature DCs (CD11b$^+$CD11c$^+$DEC205$^+$ cells). Data were analyzed using the FACSDiva 8.0 software. The total number of specific leukocytes was determined using CountBright absolute counting beads (Molecular Probes, Eugene, OR, USA). The figures were prepared using the FlowJo Software version 10 (FlowJo, LLC, Ashland, OR, USA).

Table 6: List of antibodies used for Flow Cytometry analysis for the iNKT study

Antibody	Fluorochrome	Clone	Catalog #	Company
CD3ε	APC-Cy7 or PE-Cy5	145-2C11	557596/553065	BD Biosciences
CD4	APC or AF 700	RM4-5	553051/561025	BD Biosciences
CD8	PE-CF594 or PE-Cy5	53-6.7	562283/561094	BD Biosciences
CD25	PE-Cy7	PC61	552880	BD Biosciences
CD154/CD40L	APC	MR1	17-1541-82	eBioscience
CD279/PD-1	FITC	J43	11-9985-85	eBioscience
CD69	PE-CF594	H1.2F3	562455	BD Biosciences
CD152/CTLA-4	PE	UC10-4F10-11	561718	BD Biosciences
CD11b	PE-CF594	M1/70	562287	BD Biosciences
Ly6G	APC	1A8	560599	BD Biosciecnces
F4/80	APC-efluor 780	BM8	47-4801-82	eBioscience
iNOS	PE	CXNFT	12-5920-82	eBioscience
IL4	PE-Cy7	11B11	560699	BD Biosciences
IFNγ	V450	XMG1.2	560661	BD Biosciences
CD49b/DX5	APC	DX5	560628	BD Biosciences
NK1.1	AF 700	PK136	560515	BD Biosciences
TCR-β	PerCP-Cy 5.5	H57-597	560657	BD Biosciences
CD44	APC-Cy7	IM7	560568	BD Biosciences
CD11c	AF488	N418	53-0114-82	eBioscience
DEC205	PerCP-eFluor 710	205yekta	46-2051-82	eBioscience
IL-10	AF700	JES5-16E3	56-7101-82	eBioscience
CD16/CD32	N/A	2.4G2	553142	BD Biosciences
CD1d Tetramer loaded with α-Galcer	PE	N/A	N/A	NIH

Antibody name, the directly conjugated flourochrome, clone, catalog number, and company are listed.

Gene expression determination

RNA was extracted from decidual and myometrial tissues using TRIzol Reagent (Life Technologies), QIAshredders (Qiagen, Valencia, CA, USA), RNase-Free DNase Sets (Qiagen), and RNeasy Mini Kits (Qiagen). RNA concentrations and purity were assessed with the NanoDrop 1000 spectrophotometer (Thermo Scientific, Wilmington, DE, USA), and RNA integrity was evaluated with the Bioanalyzer 2100 (Agilent

Technologies, Wilmington, DE, USA). cDNA was synthesized using RT^2 First Strand Kits (Qiagen).

The RT² Profiler Mouse PPAR Targets PCR Array (Qiagen) and RT² Profiler Mouse Inflammatory Cytokines & Receptors PCR Array (Qiagen) were used for initial screening (n=4 samples per group) and performed by using RT² SYBR Green ROX qPCR Mastermix (Qiagen) on a 7500 Fast Real-Time PCR System (Applied Biosystems, Life Technologies Corporation, Foster City, CA, USA). Expression profiling of those genes selected based on the screening results was confirmed by qRT-PCR using a BioMark High-throughput qRT-PCR System (Fluidigm, San Francisco, CA, USA) and an ABI 7500 FAST Real-Time PCR System (Applied Biosystems) using TaqMan gene expression assays (Applied Biosystems) (n=6-8 mice per group; Table 7).

Table 7: List of primers used for RT-PCR in the iNKT study

Gene Name	Gene Symbol	Assay ID	Company
β-actin	*Actb*	Mm00607939_s1	Invitrogen/Applied Biosystems
Chemokine (C-C motif) ligand 1	*Ccl1*	Mm00441236_m1	Invitrogen/Applied Biosystems
Chemokine (C-C motif) ligand 12	*Ccl12*	Mm01617100_m1	Invitrogen/Applied Biosystems
Chemokine (C-C motif) ligand 2	*Ccl2*	Mm00441242_m1	Invitrogen/Applied Biosystems
Fatty acid binding protein 4	*Fabp4*	Mm00445878_m1	Invitrogen/Applied Biosystems
Long-chain fatty acid transport protein 4	*Fatp4*	Mm01327405_m1	Invitrogen/Applied Biosystems
Tumor necrosis factor α	*Tnf*	Mm00443258_m1	Invitrogen/Applied Biosystems

Gene name, gene symbol, assay ID, and company are listed.

Chemokine/cytokine serum concentrations

Pregnant B6 mice were injected at 16.5 dpc with: 1) DMSO, 2) 2μg of α-GalCer, 3) 2μg of α-GalCer followed by rosiglitazone (10mg/kg bodyweight) 2h after, or 4) rosiglitazone alone as a control. Mice were euthanized 6h or 24h after the injection with α-GalCer or DMSO (n=8-9 mice per group). Blood was recovered by cardiac puncture,

and serum samples were separated by centrifugation and stored at -20°C until analysis. The Milliplex MAP Mouse Cytokine/Chemokine Kit (MCYTOMAG-70K-PX32, EMD Millipore, Billerica, MA, USA) was used to measure the concentrations of G-CSF, GM-CSF, IFNγ, IL1α, IL1β, IL2, IL3, IL4, IL5, IL6, IL7, IL9, IL10, IL12p40, IL12p70, IL13, IL15, IL17, CCL11, CXCL10, CXCL1, LIF, CXCL5, CCL2, M-CSF, CXCL9, CCL3, CCL4, CXCL2, CCL5, and TNF-α in the serum samples according to the manufacturer's instructions. Plates were read using the Luminex 100 System (Luminex Corporation, Austin, TX, USA), and analyte concentrations were calculated using the xPONENT3.1 software (Luminex). The sensitivities of the assays were: 1.7pg/ml (G-CSF), 1.9pg/ml (GM-CSF), 1.1pg/ml (IFNγ), 10.3pg/ml (IL1α), 5.4pg/ml (IL1β), 1.0pg/ml (IL2), 1.0pg/ml (IL3), 0.4pg/ml (IL4), 1.0pg/ml (IL5), 1.1pg/ml (IL6), 1.4pg/ml (IL7), 17.3pg/ml (IL9), 2.0pg/ml (IL10), 3.9pg/ml (IL12p40), 4.8pg/ml (IL12p70), 7.8pg/ml (IL13), 7.4pg/ml (IL15), 0.5pg/ml (IL17), 1.8pg/ml (CCL11), 0.8pg/ml (CXCL10), 2.3pg/ml (CXCL1), 1.0pg/ml (LIF), 22.1pg/ml (CXCL5), 6.7pg/ml (CCL2), 3.5pg/ml (M-CSF), 2.4pg/ml (CXCL9), 7.7pg/ml (CCL3), 11.9pg/ml (CCL4), 30.6pg/ml (CXCL2), 2.7pg/ml (CCL5), 2.3pg/ml (TNF-α) and 0.3pg/ml (VEGF). Inter-assay and intra-assay coefficients of variation were below 15% and 4.9%, respectively.

Human samples

Chorioamniotic membrane and basal plate samples were collected within 30 min after delivery from the Bank of Biological Specimens of the Perinatology Research Branch, an intramural program of the *Eunice Kennedy Shriver* National Institute of Child Health and Human Development, National Institutes of Health, U. S. Department of Health and Human Services (NICHD/NIH/DHHS), Wayne State University, and The Detroit Medical Center (Detroit, MI, USA). The Institutional Review Boards approved

the collection and use of biological materials for research purposes. All participating women provided written informed consent. The study groups included women who delivered at term without labor (TNL), at term with labor (TIL), preterm without labor (PTNL), and preterm with labor (PTL). Demographic and clinical characteristics of these study groups are represented in Table 8. Patients with multiple births or with neonates having congenital or chromosomal abnormalities were excluded. Labor was defined by the presence of regular uterine contractions at a frequency of at least two contractions every 10 minutes with cervical changes resulting in delivery (232). In each case, several tissue sections of the chorioamniotic membranes, umbilical cord, and placental disc were evaluated for acute chorioamnionitis and chronic chorioamnionitis, according to published criteria (233, 234), by pathologists who had been blinded to the clinical outcome.

Table 8: Demographical characteristics of patients whose samples were used for the iNKT study

Demographic or clinical characteristic	TNL (*n*=7)	TIL (*n*=26)	PTNL (*n*=13)	PTL (*n*=14)	*P* value
Maternal age (years)*	28 (23-32)	23.5 (22-27)	25 (22-30)	22 (19.5-25)	NS
Race**					
African-American	7 (100%)	26 (100%)	11 (84.6%)	13 (92.9%)	NS
Caucasian	0 (0.0%)	0 (0.0%)	1 (7.7%)	1 (7.1%)	
Hispanic	0 (0.0%)	0 (0.0%)	0 (0.0%)	0 (0.0%)	
Other	0 (0.0%)	0 (0.0%)	1 (7.7%)	0 (0.0%)	
Maternal weight (kg)*	93 (68.8-98.7)	90.05 (71.1-106.0)	74.8 (62.6-102.7)	75.6 (56.7-88.2)	NS
Body mass index (kg/m²)*	31.2 (26.35-41.45)	33.9 (27.38-39.25)	32.8 (23-39.4)	28.35 (21.53-31.6)	NS
Primiparity**	0 (0%)	6 (23.08%)	3 (23.08%)	1 (7.14%)	NS
Gestational age at delivery (weeks)*	39 (38.5-39.5)	39.4 (38.2-39.9)	34.9 (32-36.1)	34.2 (31.2-35.3)	<0.0001
Birth weight (grams)*	3005 (2855-3073)	3240 (2906-3419)	1510 (1255-2375)	2148 (1674-2554)	<0.0001
Cesarean section**	100%	15.4%	100%	14.3%	<0.0001
Chronic	28.6%	30.8%	46.2%	21.4%	NS
Acute chorioamnionitis**	0%	34.6%	7.7%	42.8%	NS
Smoked during Pregnancy**					
Yes	1 (14.3%)	5 (19.2%)	2 (15.4%)	0 (0%)	NS
No	6 (85.7%)	21 (80.8%)	11 (84.6%)	14 (100%)	

(*Kruskal-Wallis test, **Chi-square test). Maternal age, race, maternal weight, body max index, Primiparity, gestational age at delivery, birth weight, Cesarean section, chronic chorioamnionitis, acute chorioamnionitis, smoking during pregnancy are listed as median (interquantile range) or n (%). Either Kruskal-Wallis test or Chi-square test were used to analyze the statistical differences between the study groups (TNL, TIL, PTNL, and PTL).

Decidual leukocyte isolation from human samples

Decidual leukocytes from human decidual tissue were isolated as previously described (235). Briefly, the decidua basalis was collected from the basal plate of the placenta, and the decidua parietalis was separated from the chorioamniotic membranes (Figure 8A). Decidual tissue was homogenized using a gentleMACS Dissociator (Miltenyi Biotec, San Diego, CA, USA) in StemPro Cell Dissociation Reagent. Homogenized tissues were incubated for 45 min at 37°C with gentle agitation. After incubation, tissues were washed in ice-cold 1X PBS (Life Technologies) and filtered through a 100μm cell strainer. Cell suspensions were collected and centrifuged at 300 x g for 10 min, and the cell pellet was suspended in FACS buffer. Mononuclear leukocytes were purified using a density gradient (Ficoll-Paque Plus; GE Healthcare Bio-Sciences AB, Sweden), following the manufacturer's instructions. Lastly, mononuclear cell suspensions were washed using FACS buffer before immunophenotyping.

Immunophenotyping of human decidual leukocytes

Mononuclear cell suspensions from decidual tissues were stained with BD Horizon Fixable Viability Stain 510 dye (BD Biosciences) prior to incubation with extracellular mAbs. Mononuclear cell suspensions were then washed with staining buffer (Cat No. 554656; BD Biosciences) and centrifuged. Cell pellets were incubated for 10 min with FcR Blocking Reagent (Cat No. 130-059-901; Miltenyi Biotec). Next, mononuclear cell suspensions were incubated with the following fluorochrome-conjugated anti-human mAbs: CD14-BUV395 (clone MφP9; BD Biosciences), CD15-BV605 (clone W6D3; BD Biosciences), CD3-BV650 (clone OKT3; BD Biosciences), CD19-BUV737 (clone SJ25C1; BD Biosciences), CD56-PE-Cy7 (clone NCAM16.2; BD

Biosciences), CD69-Alexa Fluor 700 (clone FN50; BD Biosciences) and Vα24Jα18TCR-PE (clone 6B11; eBioscience; San Diego, CA, USA) for 30 min at 4 ºC in the dark. Finally, mononuclear cell suspensions were washed and re-suspended in 0.5ml of staining buffer and acquired using the BD LSRFortessa flow cytometer and FACSDiva 6.0 software. Leukocyte subsets were gated within the viability gate, and activated iNKT-like cells were identified as CD15-CD14-CD19-$CD3^+CD56^+CD69^+$ or $CD3^+$Vα24Jα18TCR^+CD69^+ cells. The analysis was performed, and the figures generated using FlowJo Software version 10.

Immunofluorescence

Immediately after collection, the chorioamniotic membranes were frozen in Tissue-Plus O.C.T. Compound (Fisher HealthCare, Houston, TX, USA). Ten-µm-thick cryosections were cut, placed on Fisherbrand Superfrost Plus microscope slides (Thermo Scientific, Waltham, MA, USA), fixed with 4% paraformaldehyde (Electron Microscopy Sciences, Hatfield, PA, USA), and washed with 1X PBS. Non-specific antibody interaction was blocked using a Protein Blocker serum-free (Cat No. X0909; Dako North America, Carpinteria, CA, USA) for 30 min at room temperature. Slides were then incubated with the following anti-human mAbs: mouse CD69-FITC (LifeSpan BioSciences, Inc., Seattle, WA, USA), mouse CD56-APC (clone MEM-188, BioLegend, San Diego, CA, USA), and rabbit CD3 (Abcam, Cambridge, MA, USA) at 4˚C overnight. Following incubation, slides were washed with 1X PBS containing 0.1% Tween-20 (Sigma-Aldrich). Secondary goat anti-rabbit IgG-Alexa Fluor 594 (Invitrogen, Molecular Probes, Eugene, OR, USA) was added for CD3 detection, and slides were incubated for 1h at room temperature. Slides were washed and mounted with the ProLong Gold Antifade reagent with DAPI (Life Technologies). Immunofluorescence was visualized

using a Zeiss LSM 780 laser scanning confocal microscope (Carl Zeiss Microscopy GmbH, Jena, Germany) at the Microscopy, Imaging and Cytometry Resources Core at Wayne State University School of Medicine (http://micr.med.wayne.edu/). Immunofluorescence signals for APC, Alexa Fluor 594, and FITC were excited using a 633 nm HeNe laser, a 561 nm HeNe laser, and the 488 nm line of a Multiline Argon laser, respectively. The DAPI signal was excited using a 405 nm diode laser.

Statistical analysis

Observational mouse data were analyzed using IBM SPSS, version 19.0, and all other analyses were performed in R (http://www.R-project.org/). For the gestational age, rate of pup mortality, and ultrasound parameters, the statistical significance of group comparisons was assessed using Mann-Whitney U tests. For flow cytometry data, the statistical significance of group comparisons was assessed using Mann-Whitney U tests. For fetal, placental, and neonatal weights, the statistical significance of group comparisons was assessed using pooled variance t-tests after log transformation. For qRT-PCR arrays, negative ΔCt values determined using multiple reference genes (*Gusb*, *Hsp90ab1*, *Gapdh* and *Actb*) averaged within each sample to determine gene expression levels. A heat map was created for the group mean expression matrix (gene x group mean) with each gene expression level being first standardized. A hierarchical clustering tree of genes was constructed using 1-Pearson correlation as distance metric and average linkage, while treatment groups clustering was based on an Euclidean distance with Ward linkage. For Fluidigm qPCR assays, negative ΔCt values were calculated using *Actb* as a reference gene. For Fluidigm gene expression and cytokine concentrations, statistical tests of group differences were performed using linear models, and whenever data was left, right, or interval censored,

a survival regression model with Gaussian error was used instead. Human demographic data were analyzed using IBM SPSS, version 19, and comparisons among the groups were performed using Chi-square tests for proportions as well as Kruskal-Wallis tests for non-normally distributed continuous variables. For proportions of activated iNKT-like cells in human decidual tissues, statistical significance of group differences was assessed using Mann-Whitney U tests. A p-value of < 0.05 was used to determine statistical significance.

Results

α-GalCer administration in the third trimester induces late preterm birth

Intravenous administration of 2μg of α-GalCer during the third trimester caused 75±18.9% of births to be categorized as late preterm (birth occurring between 18.0 and 18.5 dpc; α-GalCer-induced late PTB), while DMSO (control) resulted in no late PTB (Figure 27A). Consequently, dams that were i.v. injected with 2μg of α-GalCer had shorter gestations than the DMSO control group (Figure 27B). A high proportion of preterm pups were found dead minutes after delivery (Figure 27C). Intravenous administration of 3μg or 4μg of α-GalCer induced very early PTB (birth occurring before 17.5 dpc with 100% pup mortality); however, 1μg of α-GalCer did not cause PTB (data not shown). These data demonstrate that α-GalCer administration in the third trimester induces late PTB and pup mortality.

α-GalCer administration in the third trimester causes neonatal death

Dams that were injected with α-GalCer delivered premature viable and non-viable pups. We then investigated whether these pups were dying in the uterus (fetal death) or after delivery (neonatal death). Abnormal umbilical artery velocimetry and fetal heart rate are associated with fetal compromise (236-239). Therefore, Doppler

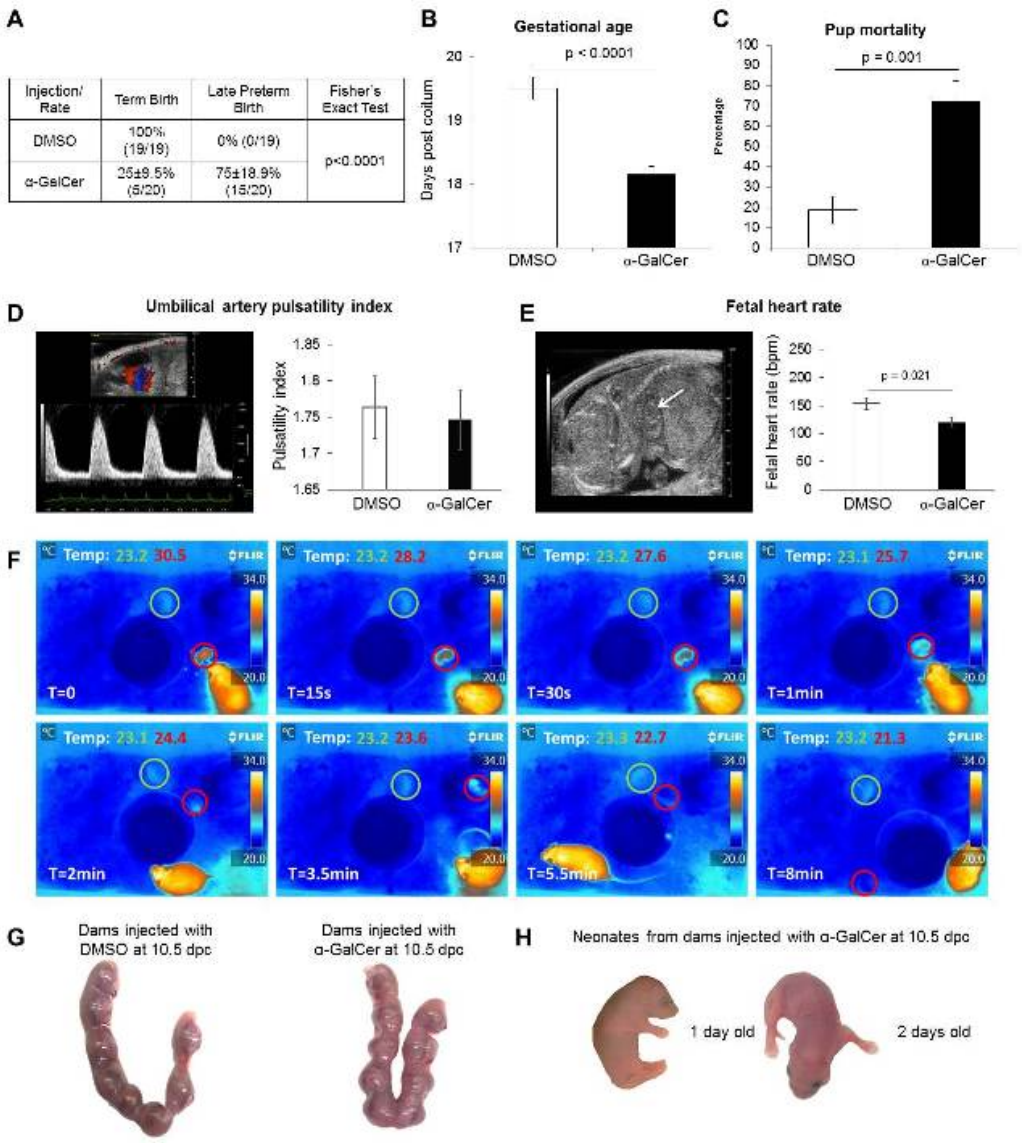

Figure 27: α-GalCer induces late PTB but not pregnancy loss. (A) The rate of term birth was defined as the percentage of dams delivering at 19.5 ± 0.5 dpc among all births. The rate of late PTB was defined as the percentage of dams delivering between 18.0 and 18.5 dpc among all births. Data are shown as percentage ± 95% confidence interval. (B) Gestational age was calculated from the presence of the vaginal plug (0.5 dpc) until the observation of the first pup in the cage bedding. (C) The rate of pup mortality for each litter was defined as the proportion of born pups found dead among the total litter size. Data in (A–C) are from individual dams (n = 19–20 each). (D and E) Doppler ultrasound was performed on fetuses just prior to α-GalCer–induced late PTB in dams injected with α-GalCer and in time-matched DMSO controls. Umbilical artery pulsatility index and fetal heart rate were recorded. Data are from three independent litters. (F) Immediately after α-GalCer–induced late PTB, the body temperature of the newborns was monitored using a thermal infrared camera. Temperature readings were recorded at 0, 15, and 30 s, as well as at 1, 2, 3.5, 5.5, and 8 min. Data are representative of individual dams (n = 3). (G) Uterine horns at 14.5 dpc from dams injected i.v. with DMSO or α-GalCer on 10.5 dpc. Data are representative of individual dams (n = 5 each). (H) Term neonates at 1 and 2 d old delivered from dams injected i.v. with α-GalCer on 10.5 dpc. Data are representative of individual dams (n = 3).

ultrasound was performed on 17.5 dpc, just prior to late PTB in those mice injected with α-GalCer. The umbilical artery pulsatility index did not differ between fetuses from dams injected with α-GalCer and DMSO (Figure 27D).

However, bradycardia, a reduction of the heart rate, occurred in fetuses from dams injected with α-GalCer when compared to the DMSO control (Figure 27E). These data demonstrated that, although pups do not die in the uterus, their health was compromised before birth. Administration of α-GalCer also reduced fetal and placental weights, but did not decrease the weight of one-week-old neonates (Figure 28A-C).

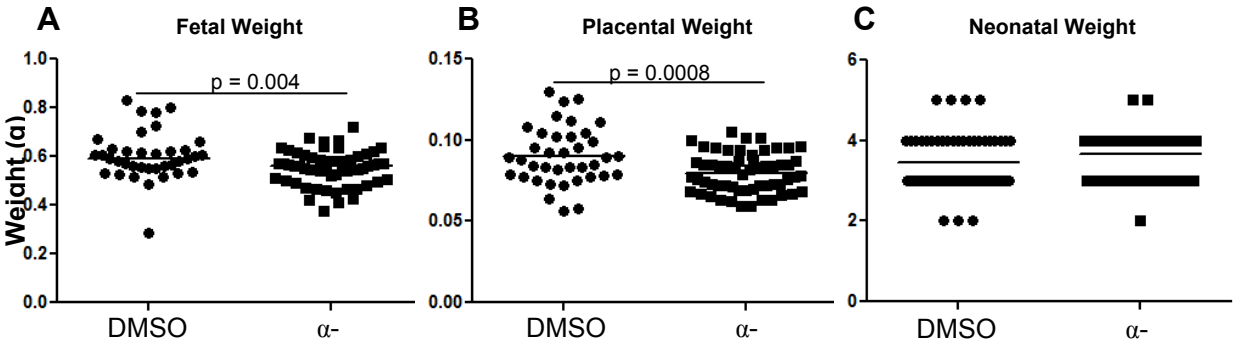

Figure 28: Fetal, placental, and neonatal weights with αGalCer treatment. (A&B) Fetuses and placentae from dams i.v. injected with 2μg of α-GalCer or DMSO were weighed 6 h post-injection. Data are pooled from 6-8 litters (n=38 for DMSO and n=58 for α-GalCer). (C) Neonates delivered by dams i.v. injected with 2μg of α-GalCer or DMSO were weighed at 1 week postpartum. Data are from independent neonates (n=57 for DMSO and n=46 for α-GalCer).

To further evaluate when the premature pups died, we placed dams injected with α-GalCer under video surveillance using infrared thermography. A high proportion of premature pups died within 10 min of delivery. In Figure 27F, representative frames demonstrate that the body temperature of a non-viable premature pup (red circle) reduced quickly from 30.5°C to 21.3°C. Conversely, a viable premature pup kept a constant temperature of 23.3°C to 23.1°C (green circle).

α-GalCer administration in the second trimester does not cause pregnancy loss

During mid-pregnancy, iNKT-cell activation by i.p. administration of α-GalCer

(100μg/kg of body weight, ~2.5μg) leads to pregnancy loss (240, 241). Herein, we demonstrated that i.v. administration of 2μg of α-GalCer in the second trimester did not cause pregnancy loss (Figure 27G). However, we could not rule out the possibility that this dose would cause PTB or have deleterious effects on neonates. Therefore, neonates from dams injected with α-GalCer at 10.5 dpc were observed up to one week post-partum. All delivered pups were viable and appeared healthy. Figure 27H shows viable term pups at 1 day and 2 days post-partum from dams injected with α-GalCer in the second trimester.

Rosiglitazone treatment reduces the rate of α-GalCer-induced late preterm birth

iNKT-cell activation can initiate the NF-κB pathway, leading to production of Th1 cytokines, such as IFNγ (216). We then hypothesized that activation of the PPARγ pathway by administration of rosiglitazone, which interferes with the NF-κB pathway (224, 225), would prevent α-GalCer-induced late PTB.

Dams that were injected with α-GalCer and subsequently treated with rosiglitazone had a 40% reduction in the rate of late PTB in comparison to dams injected with α-GalCer alone (35.7±25.1% *vs.* 75±18.9%; Figure 29B). Consequently, gestational age was greater in dams treated with rosiglitazone after α-GalCer injection than in dams injected with α-GalCer alone (Figure 29C). Importantly, dams that were treated with rosiglitazone after an injection of α-GalCer had a 30% reduction in pup mortality when compared to dams injected with α-GalCer alone (Figure 29D). These results demonstrate that treatment with rosiglitazone can prevent α-GalCer-induced late PTB and improve neonatal outcomes.

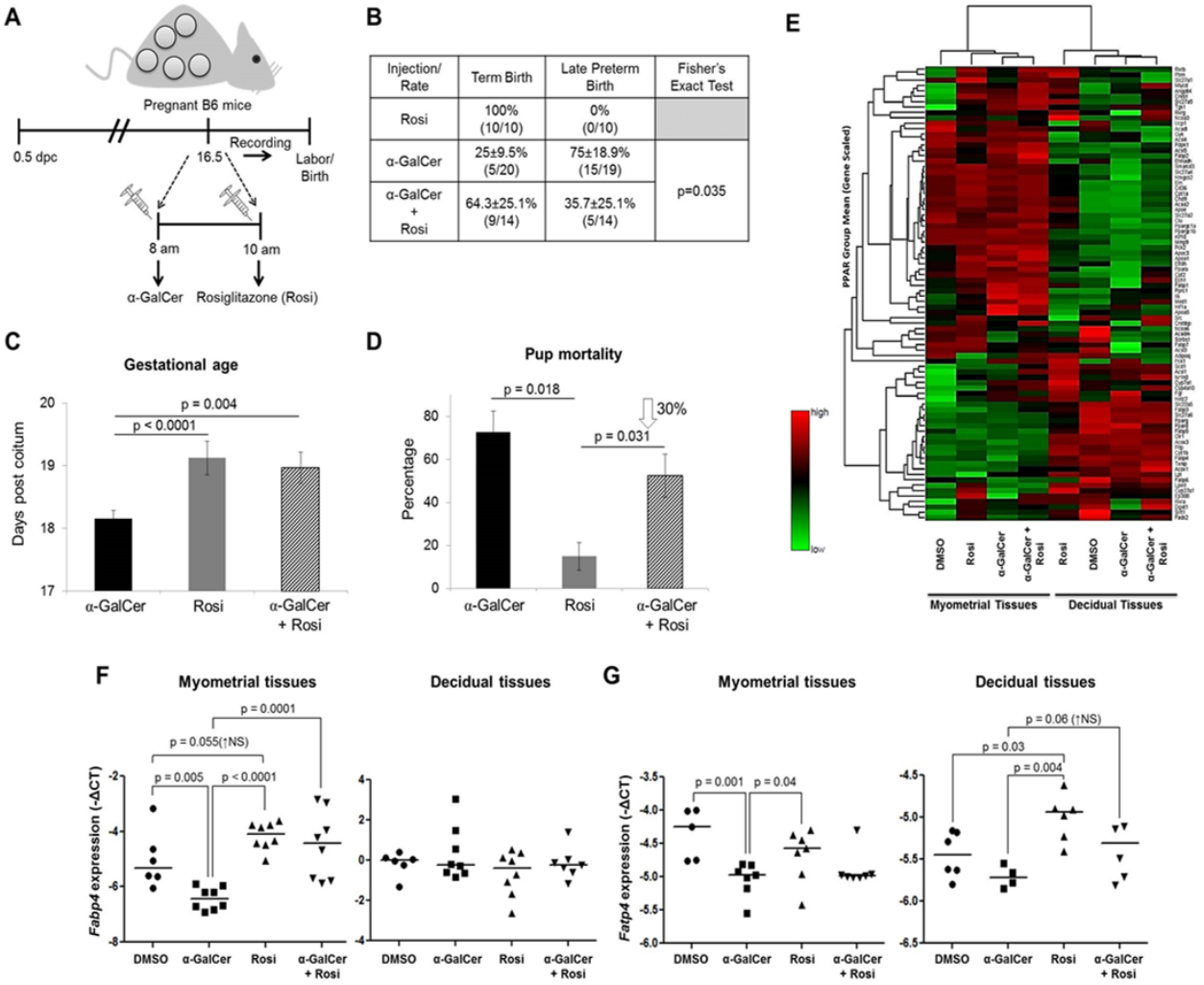

Injection/ Rate	Term Birth	Late Preterm Birth	Fisher's Exact Test
Rosi	100% (10/10)	0% (0/10)	
α-GalCer	25±9.5% (5/20)	75±18.9% (15/19)	p=0.035
α-GalCer + Rosi	64.3±25.1% (9/14)	35.7±25.1% (5/14)	

Figure 29: Rosiglitazone treatment reduces the rate of α-GalCer–induced late PTB by inducing PPARγ activation at the maternal–fetal interface. (A) On 16.5 dpc, pregnant mice were injected i.v. with α-GalCer and treated shortly after with rosiglitazone (Rosi; s.c.) and monitored via video camera (n = 14). Control mice were injected s.c. with rosiglitazone alone (n = 10). (B) The rate of term birth was defined as the percentage of dams delivering at 19.5 ± 0.5 dpc among all births. The rate of late PTB was defined as the percentage of dams delivering between 18.0 and 18.5 dpc among all births. Data are represented as percentage ± 95% confidence interval. (C) Gestational age was calculated from the presence of the vaginal plug (0.5 dpc) until the observation of the first pup in the cage bedding. (D) The rate of pup mortality for each litter was defined as the proportion of born pups found dead among the total litter size. (E) A heat map visualization of PPAR targets gene expression in myometrial and decidual tissues from dams injected with DMSO, α-GalCer, Rosi, or α-GalCer + Rosi. Data are from individual dams (n = 4 each). mRNA expression of Fabp4 (F) and Fatp4 (G) in myometrial and decidual tissues. Negative ΔCT values (F and G) were calculated using Actb as a reference gene. Data are from individual dams (n = 6–8 each).

α-GalCer inhibits PPARγ activation at the maternal-fetal interface that is restored by rosiglitazone

Since treatment with rosiglitazone reduced the rate of α-GalCer-induced late PTB, we investigated whether α-GalCer was inhibiting PPARγ genes at the maternal-fetal interface and whether this inhibition could be abrogated by rosiglitazone. Expression profiles of the PPAR pathway-related genes were different between myometrial and decidual tissues in all of the groups (Figure 29E). We specifically focused on PPARγ target genes. Adipocyte-specific fatty acid binding protein (Fabp4) and fatty acid transport protein 4 (Fatp4) are recognized as indicators of PPARγ activation (242, 243). Our array data showed that rosiglitazone up-regulated *Fabp4* in myometrial tissues and *Fatp4* and *Cyp410* in decidual tissues while α-GalCer down-regulated such genes; therefore, we validated the expression of *Fabp4* and *Fatp4* in these tissues. Administration of α-GalCer down-regulated expression of *Fabp4* in myometrial tissues; however, treatment with rosiglitazone resulted in up-regulation to basal levels (Figure 29F). Administration of α-GalCer down-regulated expression of *Fatp4* in myometrial tissues and tended to down-regulate expression of *Fatp4* in decidual tissues (Figure 29G). Treatment with rosiglitazone partially restored *Fatp4* expression in decidual tissues but not in myometrial tissues (Figure 29G). These results demonstrate that rosiglitazone prevents α-GalCer-induced late PTB by restoring PPARγ activation at the maternal-fetal interface.

α-GalCer induces an expansion of activated CD1d-restricted iNKT cells in decidual tissues that is blunted by rosiglitazone

Next, we investigated whether α-GalCer caused a systemic and local (maternal-fetal interface) expansion of iNKT cells and whether rosiglitazone reduced such

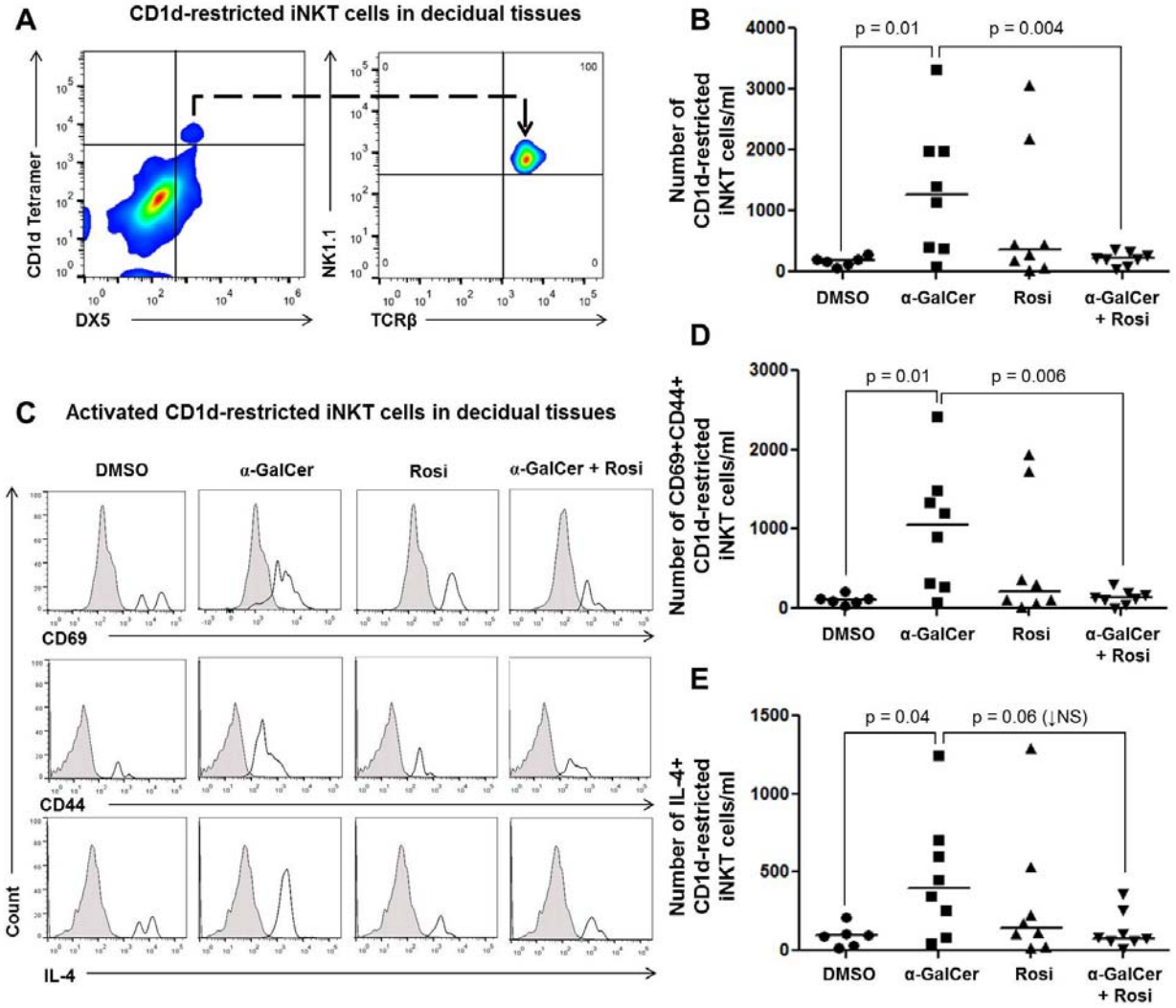

Figure 30: Administration of α-GalCer induces an expansion of activated CD1d-restricted iNKT cells in decidual tissues that is blunted by rosiglitazone. (A) Gating strategy used to identify CD1d-restricted iNKT cells (CD1d tetramer$^+$DX5$^+$NK1.1$^+$TCRβ$^+$ cells) in decidual tissues. (B) Number of CD1d-restricted iNKT cells in decidual tissues from mice injected with DMSO, α-GalCer, rosiglitazone (Rosi), or α-GalCer + Rosi. Data are from individual dams (n = 6–8 each). (C) Immunophenotyping of activation markers CD69, CD44, and IL-4 in CD1d-restricted iNKT cells in decidual tissues from mice injected with DMSO, α-GalCer, Rosi, or α-GalCer + Rosi. The shaded graph represents the autofluorescence control, and the open graph represents the fluorescence signal from CD1d-restricted iNKT cells. (D and E) Number of CD69$^+$CD44$^+$ and IL-4$^+$ CD1d-restricted iNKT cells in decidual tissues from mice injected with DMSO, α-GalCer, Rosi, or α-GalCer + Rosi. Data are from individual dams (n=6–8 each).

expansions. Because NKT-cell function and subsets are tissue- or organ-specific (244-246), we used a combination of markers including CD1d-Tetramer loaded with α-

GalCer, DX5, NK1.1, and TCRβ to identify iNKT cells (Figure 30A). Administration of α-GalCer caused an expansion of CD1d-restricted iNKT cells (CD1d Tetramer^{+}DX5^{+}TCRβ^{+}NK1.1^{+} cells) in decidual tissues; yet, this expansion was blunted by treatment with rosiglitazone (Figures 30B). In contrast, administration of α-GalCer did not significantly alter the number of CD1d-restricted iNKT cells in the liver (Figure 31A), myometrium (Figure 31B), spleen (Figure 31C), or ULN (Figure 31D).

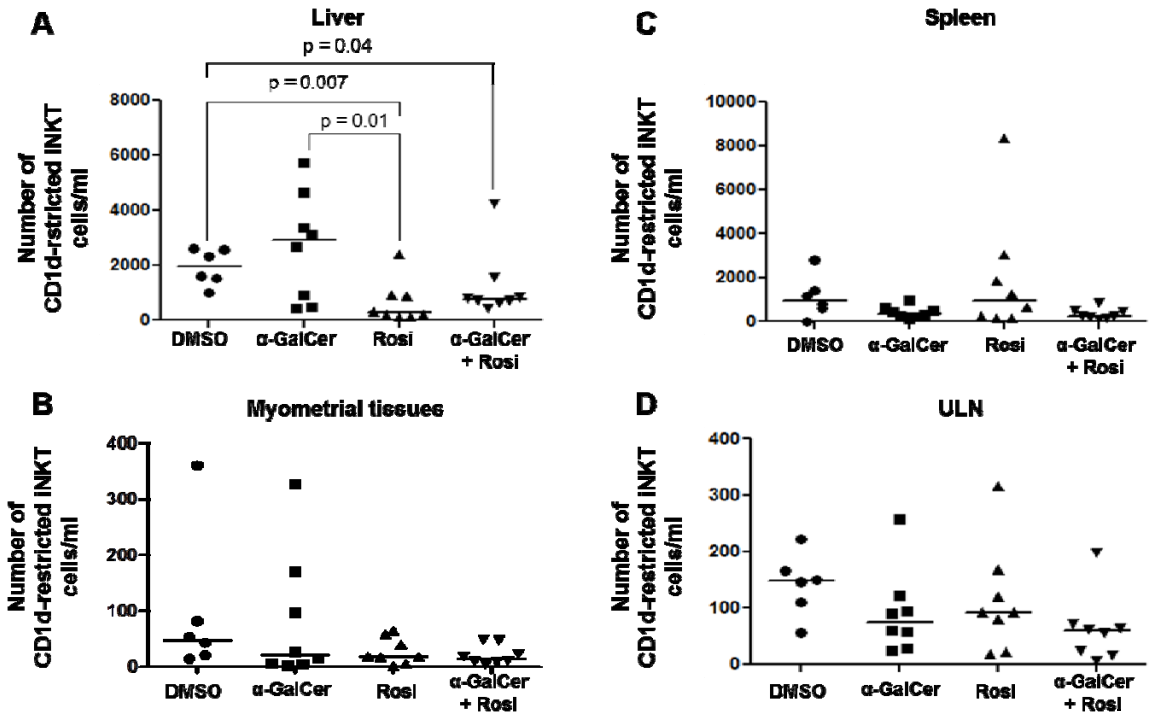

Figure 31: CD1d-restricted iNKT cells in the liver, myometrium, spleen, and lymph nodes. Number of CD1d-restricted iNKT cells in the liver (**A**), myometrium (**B**), Spleen (**C**), and uterine lymph nodes (**D**) from mice injected with DMSO, α-GalCer, rosiglitazone (Rosi), or α-GalCer + rosiglitazone. Data are representative of individual dams, n=6-8 each.

We also evaluated whether α-GalCer-expanded decidual iNKT cells were activated and, in such a case, whether rosiglitazone treatment reduced the number of these cells. Activated iNKT cells express CD69 and CD44, and release Th1 (e.g., IFNγ) and Th2 cytokines (e.g., IL4) (216, 218, 247).

Decidual CD1d-restricted iNKT cells expressed CD69, CD44, IL4 (Figure 30C),

and, to a lesser extent, IFNγ (Figure 32). Administration of α-GalCer increased the number of activated $CD69^+CD44^+$ and $IL4^+$CD1d-restricted iNKT cells in decidual tissues, both of which were reduced by treatment with rosiglitazone (Figure 30D&E). No significant effects were seen in $IFN\gamma^+$CD1d-restricted iNKT cells upon α-GalCer and/or rosiglitazone administration (Figure 32). Together, these data demonstrate that rosiglitazone prevents α-GalCer-induced late PTB by reducing activated CD1d-restricted iNKT cells at the maternal-fetal interface.

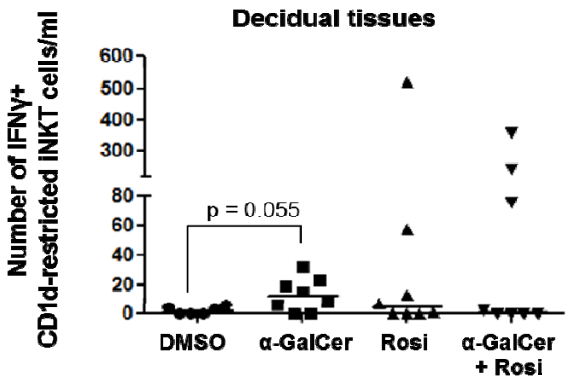

Figure 32: $IFN\gamma^+$ CD1d-restricted iNKT cells in decidual tissues. Number of $IFN\gamma^+$ CD1d-restricted iNKT cells in decidual tissues from mice injected with DMSO, α-GalCer, rosiglitazone (Rosi), or α-GalCer + rosiglitazone. Data are from individual dams, n=6-8 each.

α-GalCer induces activation of conventional $CD4^+$ T cells in myometrial tissues that is reduced by rosiglitazone

iNKT cells bridge the innate and adaptive limbs of the immune system; therefore, activation of iNKT cells triggers both innate and adaptive immune responses (248). Indeed, activation of CD1d-restricted iNKT cells by administration of α-GalCer in non-pregnant mice induces expression of CD69, an early activation marker, in T cells and B cells (249-252). We then investigated whether administration of α-GalCer in the third trimester induced T-cell activation in myometrial and decidual tissues, and whether this activation was reduced after treatment with rosiglitazone. Several markers of T-cell activation including CD25, CD40L, PD1, CD69, and CTLA-4 were determined in conventional $CD4^+$ and $CD8^+$ T cells. Administration of α-GalCer led to the activation of

conventional $CD4^+$ T cells demonstrated by the expression of CD25 and PD1 in myometrial tissues, which was reduced by treatment with rosiglitazone (Figures 33A-C).

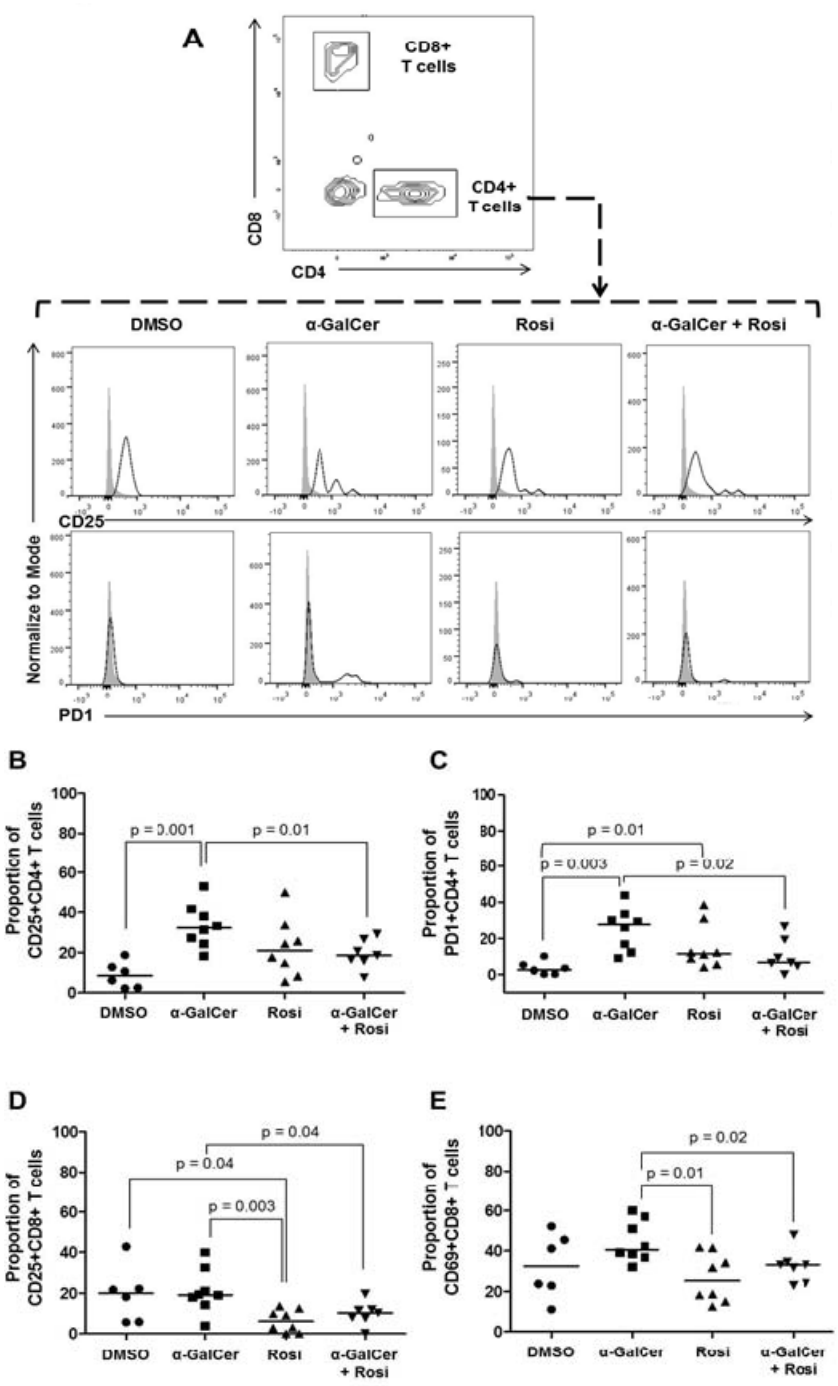

Figure 33: Administration of α-GalCer induces activation of $CD4^+$ T cells in myometrial tissues that is reduced by rosiglitazone. (A) Gating strategy used to identify activated $CD4^+$ T cells ($CD3^+CD4^+$ cells) in myometrial tissues. Immunophenotyping of activation markers CD25 and PD1 in $CD4^+$ T cells in myometrial tissues from mice injected with DMSO, α-GalCer, rosiglitazone (Rosi), or α-GalCer + Rosi. The shaded graphs represent the autofluorescence control, and the open graph represents the fluorescence signal from $CD4^+$ T cells. (B and C) Proportion of $CD25^+CD4^+$ T cells and $PD1^+CD4^+$ T cells in myometrial tissues from mice injected with DMSO, α-GalCer, Rosi, or α-GalCer + Rosi. Data are from individual dams (*n*=6–8 each). (D & E) Proportion of $CD25^+CD8^+$ T cells and $CD69^+CD8^+$ T cells in myometrial tissues from mice injected with DMSO, α-GalCer, Rosi, or α-GalCer + Rosi. Data are from individual dams (*n* = 6–8 each).

This treatment also reduced basal $CD8^+$ T cell activation in myometrial tissues (Figures 33D & E). No significant effects were seen in activated $CD4^+$ and $CD8^+$ T cells

upon α-GalCer administration in decidual tissues (Figure 34). These data demonstrate that rosiglitazone prevents α-GalCer-induced late PTB by reducing activated T cells in the myometrial tissues.

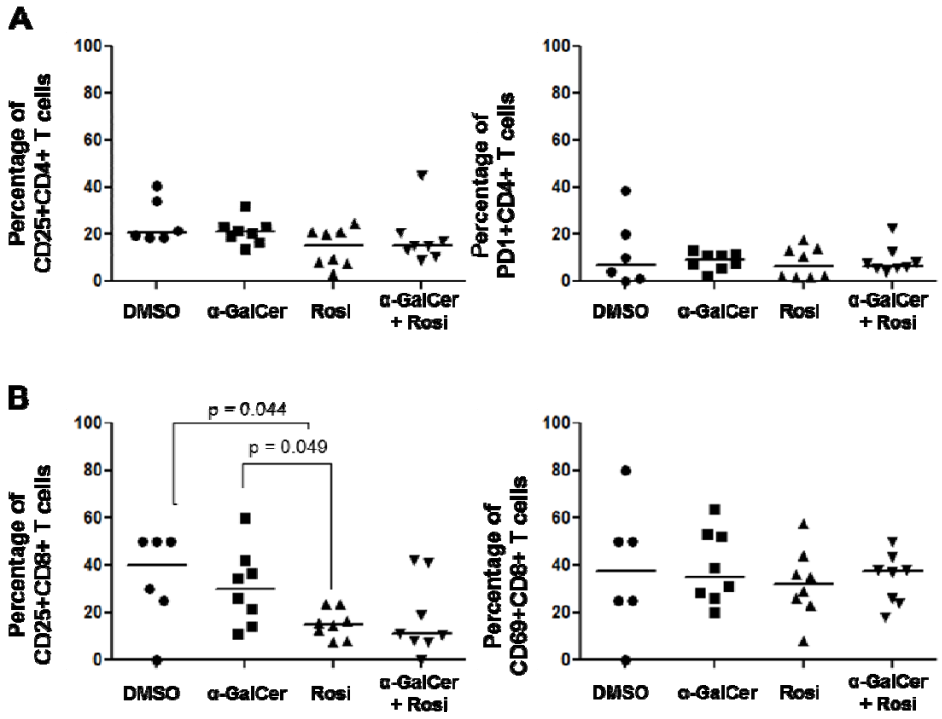

Figure 34: Activated CD4+ and CD8+ T cells in decidual tissues. (A) Proportion of CD25+CD4+ T cells and $PD1^{+}CD4^{+}$ T cells in decidual tissues from mice injected with DMSO, α-GalCer, rosiglitazone (Rosi), or α-GalCer + rosiglitazone. (B) Proportion of CD25+CD8+ T cells and CD69+CD8+ T cells in decidual tissues from mice injected with DMSO, α-GalCer, rosiglitazone, or α-GalCer + rosiglitazone. Data are from individual dams, n=6-8 each.

α-GalCer induces innate immune activation at the maternal-fetal interface that is attenuated by rosiglitazone

iNKT-cell activation also initiates innate immune responses mediated by macrophages and neutrophils (251, 253) as well as induces the full maturation of DCs manifested by the expression of MHC class II, IFNγ production, and APC function (254). First, we investigated whether administration of α-GalCer induces macrophage activation in myometrial and decidual tissues, and whether this activation was reduced after treatment with rosiglitazone. Macrophage activation is a complex process since it

depends on the nature of the stimulus and the microenvironment where these cells exhibit their function (255, 256).

The classical M1/M2 macrophage paradigm provides useful markers (Arg1, iNOS, IL10, and IFNγ) for macrophage activation (257-260); therefore, we evaluated the expression of these molecules in myometrial and decidual macrophages ($CD11b^+F4/80^+$ cells). Administration of α-GalCer increased the number of decidual

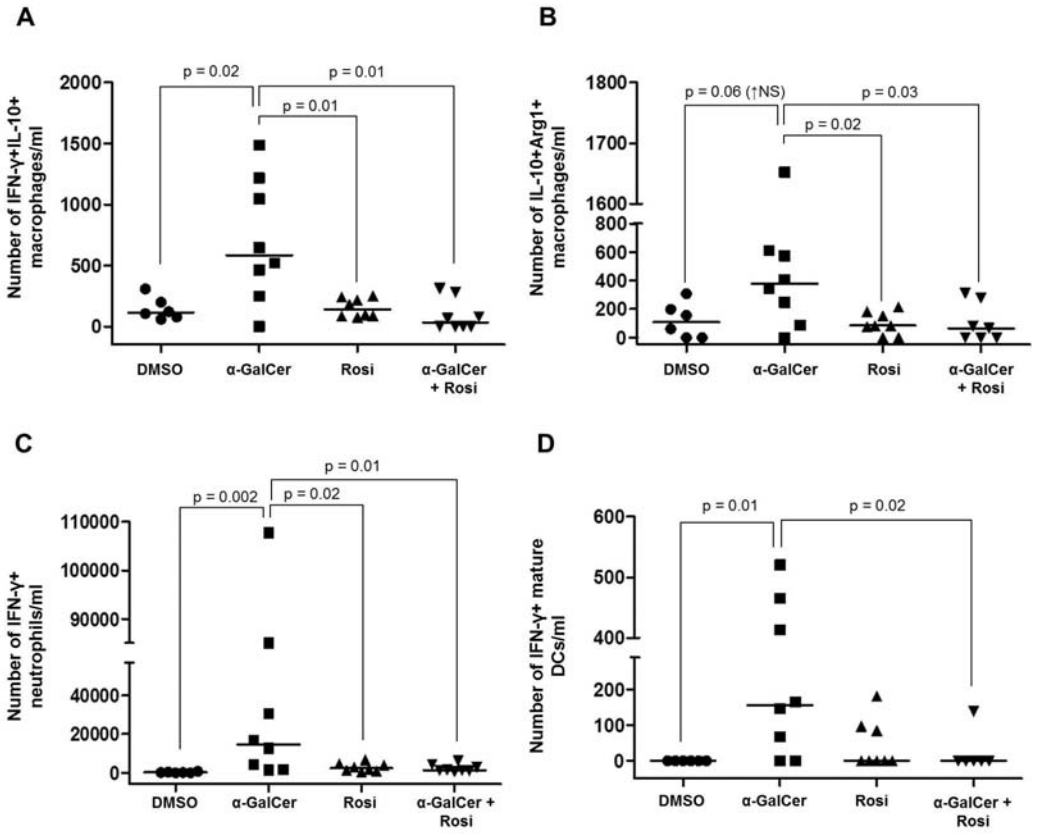

Figure 35: Administration of α-GalCer induces activation of innate immune cells at the maternal–fetal interface that is blunted by rosiglitazone. (A) Number of activated IFN-γ^+IL-10^+ macrophages in decidual tissues from mice injected with DMSO, α-GalCer, rosiglitazone (Rosi), or α-GalCer + Rosi. Data are from individual dams (n = 6–8 each). (B) Number of activated IL-10^+Arg1^+ macrophages in decidual tissues from mice injected with DMSO, α-GalCer, Rosi, or α-GalCer + Rosi. Data are from individual dams (n = 6–8 each). (C) Number of activated IFN-γ^+ neutrophils in decidual tissues from mice injected with DMSO, α-GalCer, Rosi, or α-GalCer + Rosi. Data are from individual dams (n = 6–8 each). (D) Number of IFN-γ^+ mature DCs in decidual tissue from mice injected with DMSO, α-GalCer, Rosi, or α-GalCer + Rosi. Data are from individual dams (n = 6–8 each).

macrophages that produce both IFNγ and IL10 (Figure 35A). Also, administration of α-GalCer increased the number of decidual macrophages that express both Arg1 and IL10; yet, this increase did not reach statistical significance (Figure 35B). In both cases, treatment with rosiglitazone reduced the number of activated macrophages (Figures 35A & B). Administration of α-GalCer did not have such effects on myometrial macrophages (data not shown).

Next, we investigated whether administration of α-GalCer induces neutrophil activation in myometrial and decidual tissues, and whether this activation was reduced after treatment with rosiglitazone. IFNγ expression is an indicator of neutrophil activation (261, 262). In the study herein, we demonstrated that administration of α-GalCer increased the expression of IFNγ by neutrophils in myometrial and decidual tissues, and this effect was reduced by treatment with rosiglitazone (Figures 35C & Figure 36).

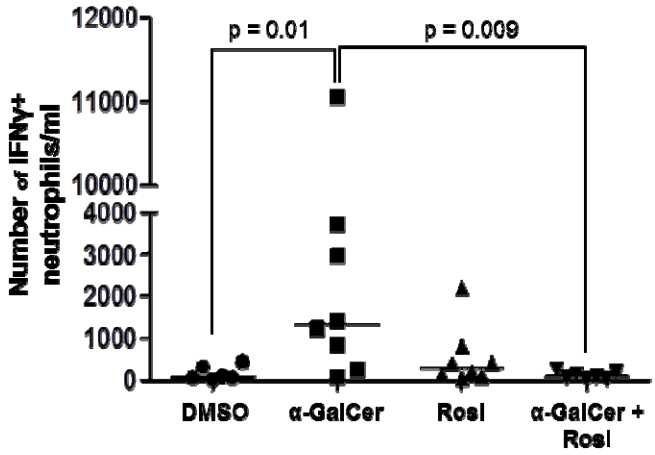

Figure 36: Number of IFNγ$^+$ neutrophils in myometrial tissues from mice injected with DMSO, α-GalCer, rosiglitazone (Rosi), or α-GalCer + rosiglitazone. Data are from individual dams, n=6-8 each.

Lastly, we investigated whether administration of α-GalCer in the third trimester induced DC maturation in decidual tissues, and whether this process was blocked by administration of rosiglitazone. Administration of α-GalCer increased the number of mature DCs ($CD11b^+CD11c^+DEC205^+$ cells; data not shown) and the number of $IFN\gamma^+$

mature DCs in decidual tissues (Figure 35D). Treatment with rosiglitazone did not reduce the number of mature DCs (data not shown); however, it reduced the number of IFNγ^{+} mature DCs in decidual tissues (Figure 35D). Taken together, these data demonstrate that rosiglitazone prevents α-GalCer-induced late PTB by attenuating innate immune activation at the maternal-fetal interface.

α-GalCer induces a pro-inflammatory microenvironment at the maternal-fetal interface that is partially attenuated by rosiglitazone

Whereas iNKT-cell activation induces the expression of inflammatory genes (214, 215), PPARγ activation suppresses their expression (224, 225). We next investigated whether α-GalCer up-regulated inflammatory genes at the maternal-fetal interface, and whether this up-regulation was suppressed by rosiglitazone. Expression profiles of inflammation-related genes were different between decidual and myometrial tissues (Figure 37A). As expected, several genes were up-regulated in both types of tissue upon administration of α-GalCer (α-GalCer *vs.* DMSO; Figure 37A). Some of these genes were down-regulated after treatment with rosiglitazone, mainly in decidual tissues (α-GalCer+Rosi *vs.* α-GalCer; Figure 37A). We selected some of the down-regulated genes after treatment with rosiglitazone and validated their expression. Administration of α-GalCer up-regulated the expression of *Ccl1*, *Ccl2*, *Ccl12,* and *Tnf* in decidual tissues; however, these genes were down-regulated after treatment with rosiglitazone (Figure 37B). Administration of α-GalCer also up-regulated expression of *Ccl2* and *Ccl12* in myometrial tissues; however, only *Ccl2* was significantly down-regulated after treatment with rosiglitazone (Figure 37C). These data demonstrate that rosiglitazone prevents α-GalCer-induced late PTB by partially reducing the pro-inflammatory milieu at the maternal-fetal interface.

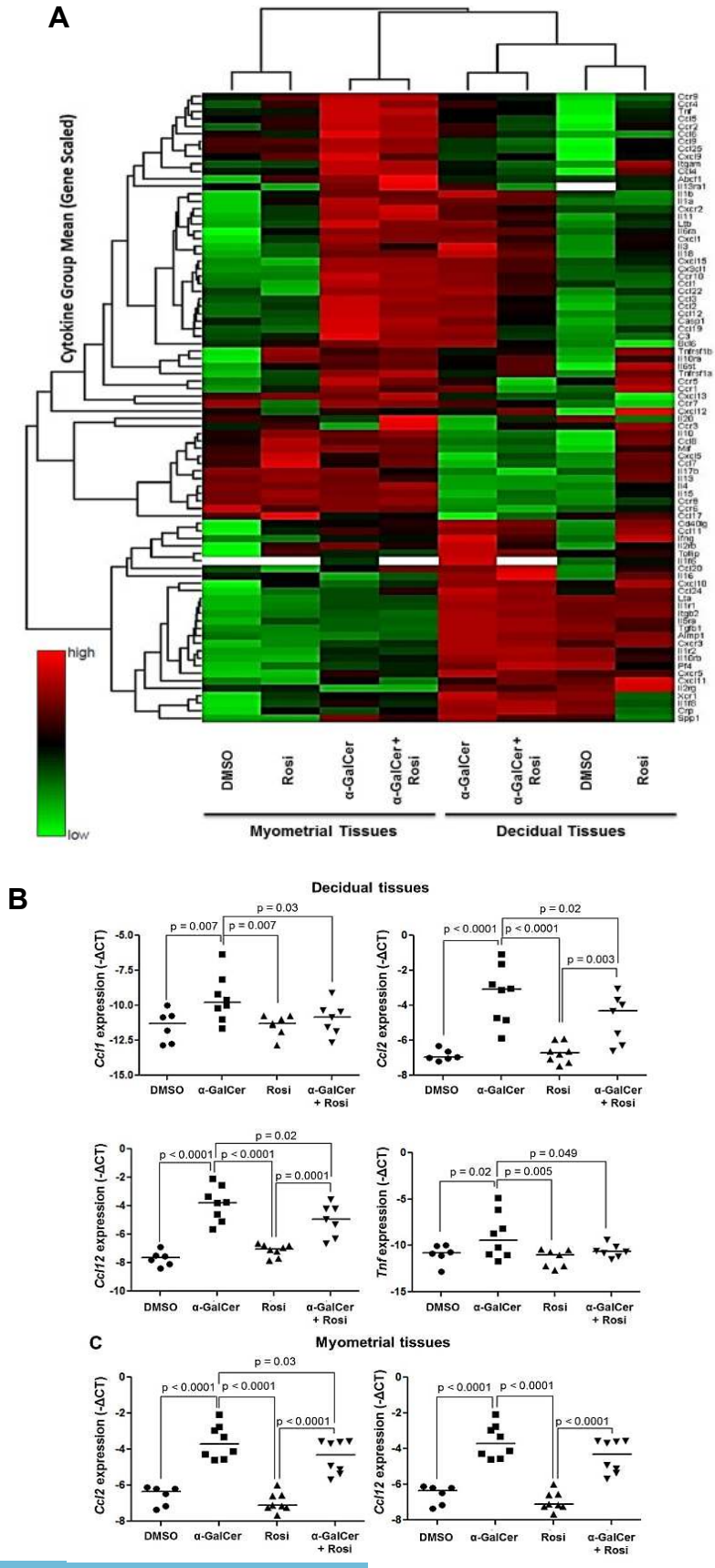

Figure 37: Administration of α-GalCer induces a pro-inflammatory microenvironment at the maternal–fetal interface that is partially attenuated by rosiglitazone. (A) A heat map visualization of cytokine and chemokine gene expression in myometrial and decidual tissues from dams injected with DMSO, α-GalCer, rosiglitazone (Rosi), or α-GalCer + Rosi. Data are from individual dams (n = 4 each). (B) mRNA expression of *Ccl1*, *Ccl2*, *Ccl12*, and Tnf in decidual tissues. Negative ΔCt values were calculated using *Actb* as a reference gene. Data are from individual dams (n=6–8 each). (C) mRNA expression of *Ccl2* and *Ccl12* in myometrial tissues. Negative ΔCt values (B and C) were calculated using *Actb* as a reference gene. Data are from individual dams (n = 6–8 each).

α-GalCer induces a maternal systemic pro-inflammatory response, yet rosiglitazone triggers a maternal systemic anti-inflammatory response

Next, we evaluated the effects of α-GalCer and rosiglitazone on cytokine serum concentration in maternal circulation at 6h or 24h (prior to α-GalCer-induced late PTB) post α-GalCer administration. Six hours post α-GalCer administration, the concentrations of all measured cytokines, except GMSCF, IL3, IL4, and IL7, were increased when compared to DMSO or rosiglitazone controls; however, none of these cytokines were reduced after treatment with rosiglitazone (data not shown). Twenty-four hours post α-GalCer administration, the pro-inflammatory cytokines —IFNγ,

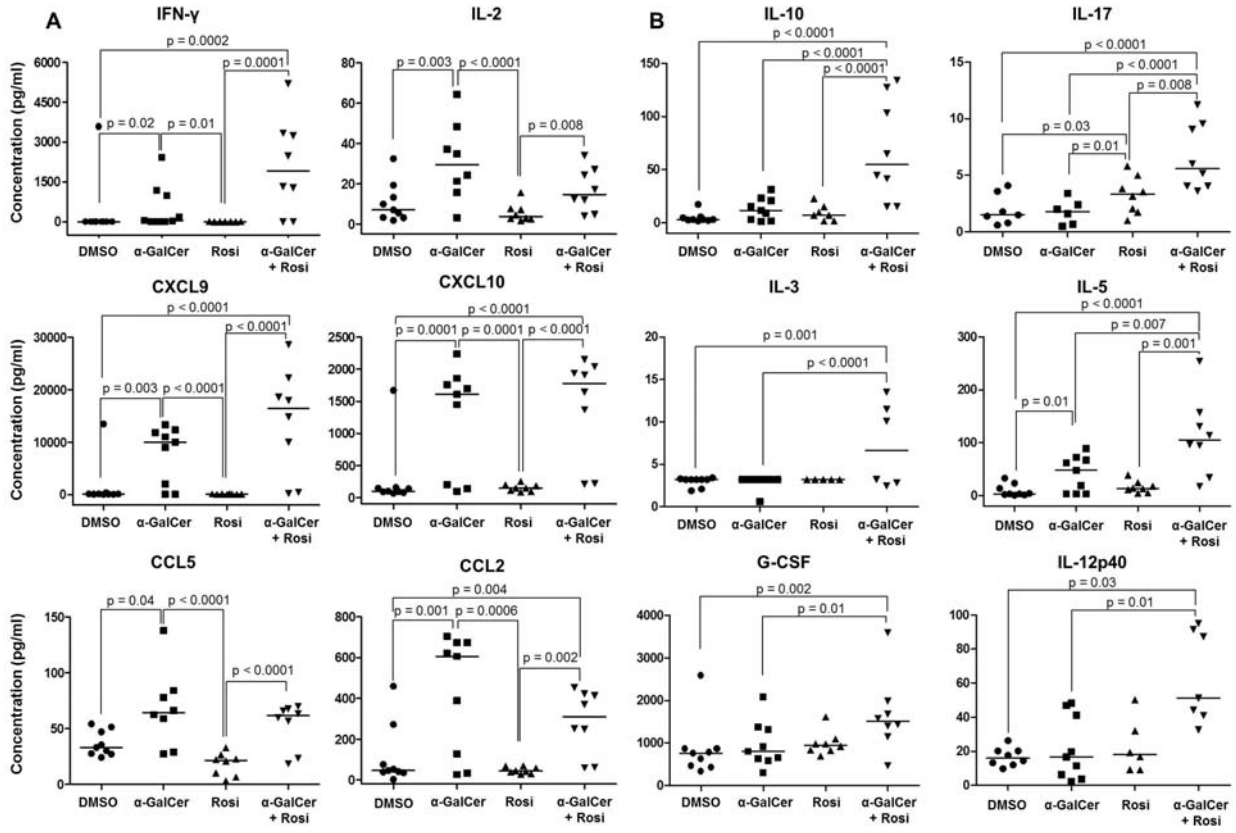

Figure 38: Administration of α-GalCer induces a maternal systemic proinflammatory response, yet rosiglitazone drives a maternal systemic anti-inflammatory response. Pregnant mice were injected with DMSO, α-GalCer, rosiglitazone (Rosi), or α-GalCer + Rosi. Serum concentrations of proinflammatory (A) and anti-inflammatory (B) cytokines/chemokines were determined 24 h after the initial injection. Data are from individual dams (n = 8–9 each).

IL2, CXCL9, CXCL10, CCL2, and CCL5 — were increased when compared to DMSO or rosiglitazone controls (Figure 38A).

Treatment with rosiglitazone did not reduce these high concentrations; indeed, it further increased the concentrations of IFNγ, CXCL9, CXCL10, and CCL2 (Figure 38A). Interestingly, dams injected with α-GalCer that were subsequently treated with rosiglitazone had increased concentrations of anti-inflammatory cytokines IL10, IL17, IL3, IL5, GSCF, and IL12p40 when compared to mice injected with only α-GalCer (Figure 37B). These data demonstrate that rosiglitazone prevents α-GalCer-induced late PTB by enhancing a maternal systemic anti-inflammatory response.

Spontaneous preterm labor/birth is associated with an increased proportion of activated iNKT-like cells in decidual tissues

Up to this point, our results demonstrated that activation of decidual iNKT cells leads to late PTB in mice; however, it was unknown whether these cells are increased during preterm labor/birth in humans. iNKT cells are present in first-trimester decidua (263); therefore, we hypothesized that preterm labor will be associated with an increase in the proportion of activated iNKT cells at the maternal-fetal interface. In humans, the maternal-fetal interface includes: 1) the decidua parietalis that lines the uterine cavity not covered by the placenta and is in juxtaposition to the chorion leave, and 2) the decidua basalis, located in the basal plate of the placenta where it is invaded by interstitial trophoblasts (Figure 39A). The gating strategy used to determine activated iNKT-like cells ($CD69^{+}CD56^{+}CD3^{+}$CD19-CD14-CD15- cells) in decidual tissues is shown in Figure 39B. In the decidua basalis and parietalis, activated iNKT-like cells were greater in women who underwent spontaneous term labor (TIL) or preterm labor (PTL) when compared to women who did not undergo labor at term (TNL) or preterm

(PTNL), respectively (Figure 39C). In the decidua basalis, activated iNKT-like cells were more abundant in PTL samples than in TIL samples (Figure 39C). Further immunophenotyping of decidual samples (TIL and PTL, n=4 each) revealed that activated iNKT cells ($CD3^+V\alpha24J\alpha18TCR^+CD69^+$ cells; Figure 39D) were present at proportions similar to previously identified activated iNKT-like cells ($CD3^+CD56^+CD69^+$ cells) (Figure 39B).

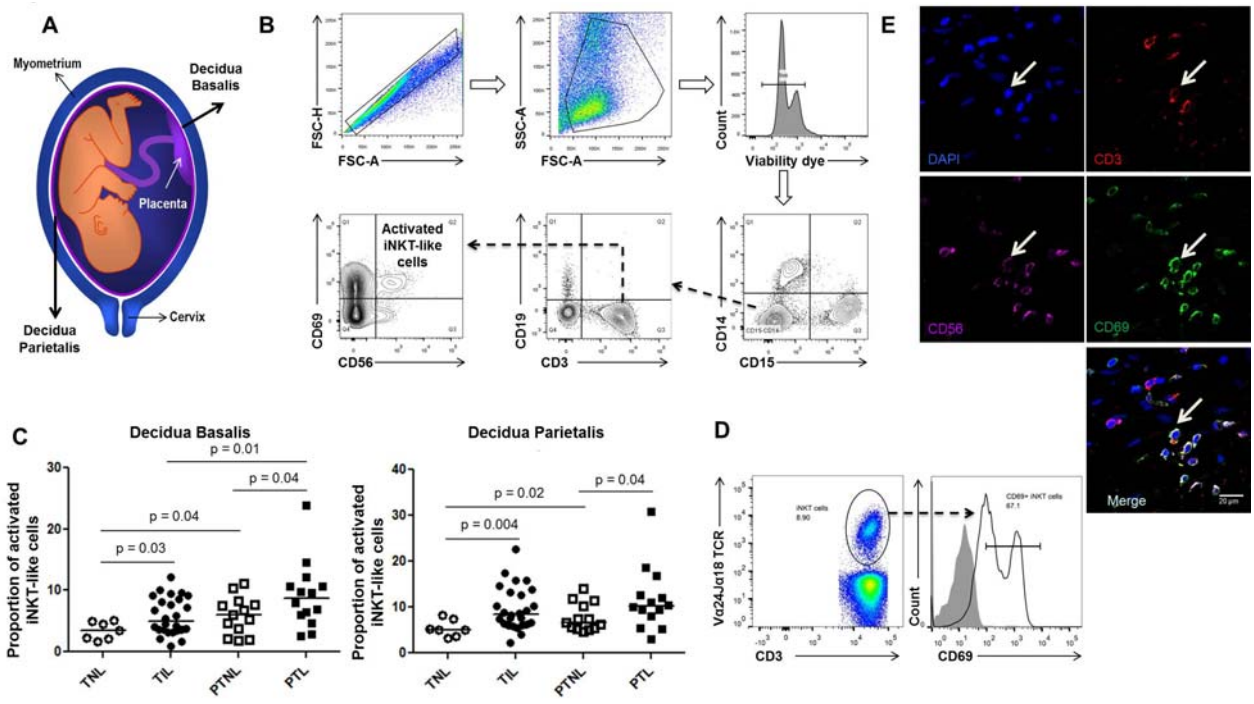

Figure 39: Spontaneous preterm labor/birth is associated with an increased proportion of activated iNKT-like cells in decidual tissues. (A) Schematic representation showing the decidua basalis and decidua parietalis. (B) Gating strategy used to identify activated iNKT-like cells ($CD69^+CD56^+CD3^+CD19^-CD14^-CD15^-$ cells) in human decidual tissue. (C) Activated iNKT-like cells in the decidual basalis or decidual parietalis from women who underwent spontaneous TIL or spontaneous PTL. Controls included samples from women who delivered at term (TNL) or preterm (PTNL) without labor. Data are from individual women: n = 7 for TNL, n = 26 for TIL, n = 13 for PTNL, and n = 14 for PTL. (D) Identification of $CD3^+V\alpha24J\alpha18TCR^+CD69^+$ cells in PTL decidual tissues. (E) Identification of activated iNKT-like cells in the decidua parietalis by confocal microscopy. Nuclei are blue (DAPI), $CD3^+$ cells are red (Alexa Fluor 594), $CD56^+$ cells are magenta (allophycocyanin), and $CD69^+$ cells are green (FITC). White arrows denote activated NKT cells. Scale bar, 20μm.

Since we did not use the iNKT marker, Vα24Jα18TCR, in our initial immunophenotyping, we cannot refer to these as iNKT cells and have instead termed

them iNKT-like cells. Localization of activated iNKT-like cells ($CD3^+CD56^+CD69^+DAPI^+$ cells; white arrows) in the decidua parietalis is shown in Figure 39E. This last set of data demonstrates that activated iNKT-like cells in human decidual tissues are linked to spontaneous preterm labor/birth.

Discussion

Sterile intra-amniotic inflammation is more frequent than microbial-associated intra-amniotic inflammation in patients with spontaneous preterm labor (21, 264). Sterile inflammation is initiated by alarmins (22) and such danger signals are potent activators of iNKT cells (212, 213); therefore, we hypothesized that these innate lymphocytes participate in the pathophysiology of sterile inflammation-related preterm labor/birth. Using a highly-affine iNKT-cell ligand, α-GalCer (222), we provided direct evidence that iNKT-cell activation is implicated in the mechanisms that lead to inflammation-induced preterm labor in the absence of infection. Indirect evidence for the role of iNKT cells in the pathophysiology of inflammation-induced preterm labor was based on two facts: (1) iNKT-cell null mice (*Ja18*$^{-/-}$ mice) are more resistant to endotoxin-induced PTB than wild type mice (265), and (2) adoptive transfer of decidual iNKT cells into iNKT-cell null mice injected with an endotoxin rapidly induces the onset of PTB (266). However, endotoxins are not iNKT-cell ligands and can only indirectly activate autoreactive iNKT cells through TLR signaling and the release of IL12 by APCs (217, 220, 267). Therefore, indirect activation of iNKT cells by an endotoxin resembles Gram-negative bacteria-related preterm labor, and direct activation via an iNKT-cell ligand could explain sterile inflammation-related preterm labor.

Administration of α-GalCer in the second trimester did not result in pregnancy loss. This finding is not surprising since the mechanisms that lead to pregnancy loss

differ from those implicated in preterm labor/birth. For example, during the second trimester, pregnancy maintenance depends on regulatory T cells (Tregs), as their depletion causes pregnancy loss (268, 269). In the third trimester, however, depletion of Tregs does not cause preterm labor/birth (270). These data led us to suggest that during the third trimester, Treg-independent regulatory mechanisms such as iNKT-cell quiescence may be responsible for pregnancy maintenance. Further studies are needed to investigate the mechanisms whereby iNKT cells remain quiescent in order to maintain pregnancy until term.

Late preterm neonates survive, yet are at a higher risk for morbidity and mortality than term neonates (271, 272). In our model of α-GalCer-induced late PTB, we consistently showed that pups did not die *in utero*; yet, they were bradycardic and died shortly after birth. This finding indicated that fetal compromise was occurring simultaneously with the process of preterm labor rather than as a direct cause of prematurity. Because NKT cells appear at day 5 after birth (273), we are confident that the adverse neonatal outcomes are due to the effects of α-GalCer administration on the maternal immune system and at the maternal-fetal interface rather than as a direct effect on the pups.

Herein, we demonstrated for the first time that α-GalCer inhibits PPARγ activation at the maternal-fetal interface, which is concordant with a previous study demonstrating that PPARγ expression is reduced in intrauterine tissues in term parturition (274). These data suggest that PPARγ activation, a suppression of inflammatory genes, is required for late pregnancy maintenance and its inhibition participates in the normal and pathological processes of labor. Conversely, rosiglitazone causes PPARγ activation and prevents α-GalCer-induced late PTB. Our

unpublished results demonstrated that this PPARγ agonist also prevents endotoxin-induced PTB (275). Therefore, targeting the PPARγ pathway could represent a new strategy to prevent both sterile and microbial inflammation-related preterm labor/birth.

An expansion of decidual iNKT cells was observed shortly after α-GalCer administration. This is consistent with a previous study demonstrating that iNKT-cell activation is observed only 4 hours post-αGalCer administration (241). A systemic expansion of iNKT cells occurs 2-3 days after α-GalCer administration (276), which explains why in our study we did not observe such an event. We also demonstrated that treatment with rosiglitazone attenuated the α-GalCer-induced iNKT-cell expansion in decidual tissues. It is likely that rosiglitazone is interfering with iNKT-cell development instead of causing cell death, since this drug did not reduce cell viability in decidual cells (Figure 40); yet, it caused a reduction of iNKT cells in the liver (Figure 31A). The previous hypothesis is supported by the fact that PPARγ activation regulates CD1d molecules (242, 277), which are constitutively expressed by APCs (278, 279) and can modulate iNKT-cell responses (220, 280). Therefore, it is probable that indirect suppression of iNKT-cell expansion and activation is the primary mechanism whereby rosiglitazone prevents PTB in our model. Consequently, we investigated whether rosiglitazone could be suppressing activation/maturation of T cells, macrophages, neutrophils, and DCs, all of which are implicated in the pathophysiology of preterm labor/birth (281-283).

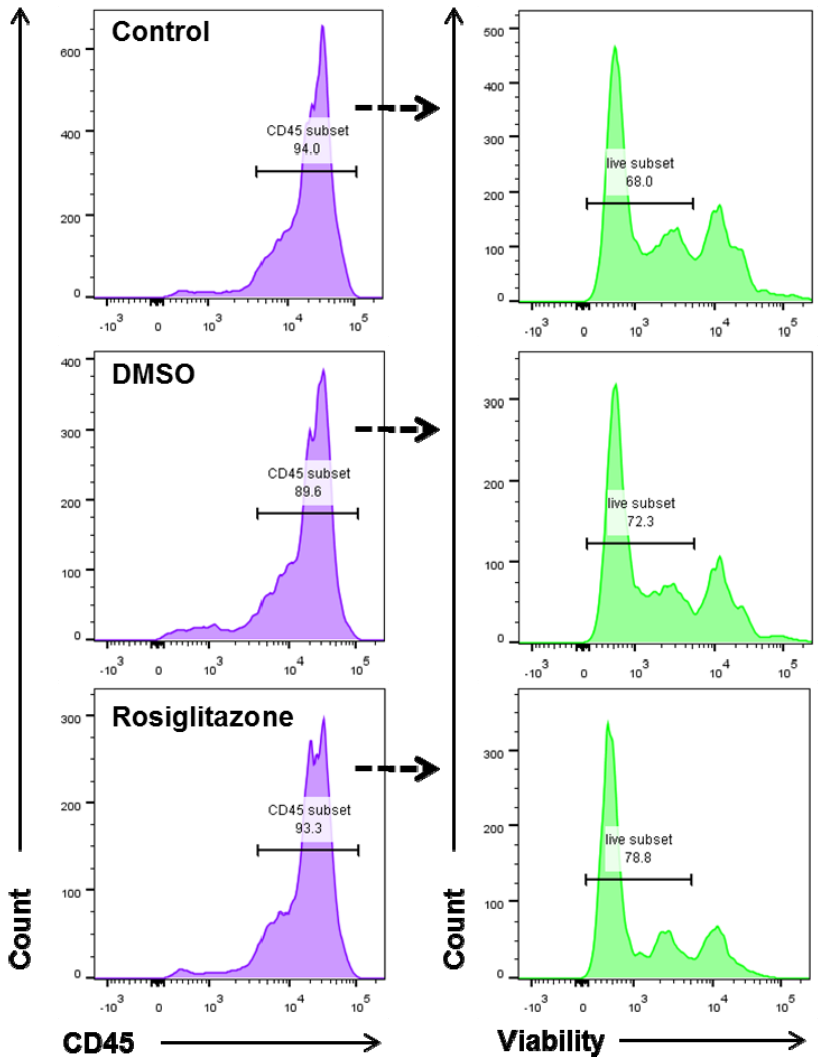

Figure 40: Viability of decidual cells after treatment with rosiglitazone. Cell viability of decidual leukocytes ($CD45^+$ cells) was determined by flow cytometry after 6 hrs of incubation with DMSO (rosiglitazone vehicle), rosiglitazone, or without either treatment (control).

T cells seem to be implicated in the process of preterm parturition (282). This concept was based on the fact that mice deficient in T and B cells (*Rag1*$^{-/-}$) are more susceptible to endotoxin-induced PTB than wild type mice, and this susceptibility is reversed upon transfer of $CD4^+$ T cells (284). These findings led us to suggest that $CD4^+$ T cells play a regulatory role in late pregnancy (282); however, their function has not been established by depleting these cells prior to preterm labor. Recently, we proposed that the activation of effector $CD4^+$ T cells is involved in the physiological process of parturition (9, 10, 285). Herein, we provide further evidence to this

hypothesis by demonstrating that activation of $CD4^+$ T cells occurs prior to αGalCer-induced PTB. We also demonstrated that rosiglitazone reduced αGalCer-induced T-cell activation. This finding is consistent with previous studies demonstrating that pretreatment with PPARγ ligands reduces T-cell activation and proliferation *in vitro* (286, 287). Taken together, these data support the hypothesis that $CD4^+$ T cell activation participates in the physiological and pathological processes of parturition and suggests that targeting the PPARγ pathway attenuates activation of the adaptive limb of immunity, rescuing preterm labor/birth.

The role of macrophages in the mechanisms that lead to preterm labor is well-established since the depletion of these innate cells protects mice from endotoxin-induced PTB (15). The study herein demonstrated increased macrophage activation prior to αGalCer-induced PTB, which supports a central role for these innate immune cells in the pro-inflammatory milieu that accompanies the sterile processes of preterm parturition. We also demonstrated that treatment with rosiglitazone inhibits macrophage activation in decidual tissues. Prior research, in line with our study, has shown that PPARγ expression is up-regulated in activated macrophages and that treatment with rosiglitazone, or natural PPARγ agonists, down-regulates the expression of iNOS, inhibits migration, and suppresses the release of inflammatory cytokines by these cells (224, 288, 289).

Unlike macrophages, the depletion of neutrophils does not prevent endotoxin-induced PTB; yet, it ameliorates the pro-inflammatory response in the uterine-placental tissues (290). Herein, we demonstrated that activation of neutrophils occurs prior to αGalCer-induced preterm birth, which suggests that although neutrophils are not essential, they participate in the pro-inflammatory milieu that accompanies the

pathological process of preterm parturition. We also found that treatment with rosiglitazone reduced α-GalCer-induced neutrophil activation. This is in accord with a previous *in vitro* study which demonstrated that PPARγ agonists (troglitazone and 15-deoxy-$\Delta^{12,14}$ prostaglandin J_2) diminished the chemotactic response of neutrophils and suppressed their production of pro-inflammatory cytokines (291).

In addition, administration of α-GalCer resulted in the expression of IFNγ by mature decidual DCs. These innate immune cells seem to contribute to the initiation of T cell responses during the physiological and pathological processes of parturition (282, 284, 285, 292, 293). Herein, we provide evidence to support this hypothesis by demonstrating that mature DCs participate in the inflammatory process that leads to inflammation-related preterm labor/birth. We also showed that treatment with rosiglitazone blunted the α-Galcer-induced IFNγ expression in mature DCs but did not interfere in their maturation. This is consistent with a previous study demonstrating that rosiglitazone does not interfere with the maturation of DCs *in vitro* nor affects their ability to activate T cells *in vivo*; however, this PPARγ agonist modifies DC differentiation by reducing their secretion of cytokines (294).

Collectively, our results demonstrated that prior to α-Galcer-induced PTB there was an activation of innate immune cells at the maternal-fetal interface, which were suppressed by PPARγ activation, rescuing inflammation-related preterm labor/birth. Besides regulating immune cell activation at the maternal-fetal interface, rosiglitazone attenuated the expression of pro-inflammatory cytokine/chemokines implicated in the pathophysiology of inflammation-related preterm labor (295-303). The suppressive effect of PPARγ agonists on cytokine expression has been previously demonstrated *in vitro* (304). These data demonstrate that PPARγ activation regulates the local pro-

inflammatory milieu associated with preterm labor/birth.

The systemic anti-inflammatory activity of rosiglitazone was also demonstrated in this study. This finding is in concordance with our unpublished data showing that treatment with rosiglitazone increases the serum concentration of IL5 and CXCL9 in dams injected with an endotoxin (Yi Xu, et al; unpublished data). The immunomodulatory action of rosiglitazone through the up-regulation of anti-inflammatory cytokines was previously demonstrated when PMA-stimulated THP-1 cells were incubated with PPARγ agonists and an increased production of IL1RA was observed (305). In our study, the anti-inflammatory effect of rosiglitazone was observed at 24h, but not at 6h, after α-GalCer administration, suggesting that said effect takes place after regulating the local microenvironment.

To conclude, we identified activated iNKT-like cells at the human maternal-fetal interface in term and preterm gestations. Activated iNKT-like cells were more abundant in the decidual basalis of women who underwent preterm labor than in those who delivered preterm without labor, suggesting that these cells are localized in a fetal antigenic site. The majority (92%) of our samples came from women who underwent spontaneous preterm labor and did not present intra-amniotic infection, which further supports the hypothesis that activated iNKT-like cells are implicated in the sterile process of inflammation that leads to preterm labor/birth.

In summary, this study demonstrates that *in vivo* iNKT-cell activation leads to late preterm labor/birth by activating innate and adaptive immune cells as well as decidual and myometrial cells at the maternal-fetal interface. We also showed that iNKT-cell activation exerts this effect by inducing a maternal systemic pro-inflammatory response. Finally, we demonstrated that PPARγ activation prevents prematurity by modulating the

local and systemic inflammatory milieu that accompanies preterm labor. Further exploration of the PPARγ pathway and its regulation in pregnancy complications may lead to novel therapeutic approaches that can improve neonatal outcomes.

CHAPTER 7 - THE ROLE OF SENESCENCE IN THE PATHOPHYSIOLOGY OF STERILE INFLAMMATION

Introduction

Cellular senescence, first described in 1965 as limited replicative capacity of a normal cell (306), is characterized by growth arrest, resistance to apoptosis, altered gene expression and, in some cases, by formation of heterochromatic foci, telomere shortening, and increased secretion of signaling molecules (307). Under physiological conditions, senescence cells, immuno-recognized by T helper cells (308), are thought to recruit phagocytes, promoting clearance and regeneration that occur during tissue remodeling in embryogenesis and upon tissue damage (309). However, persistence or deficient clearance of senescent cells can lead to accumulation of cellular damage, which is associated with multiple disorders (309).

The initial observation that uterine-specific p53 deficiency leads to uterine senescence and causes preterm delivery in 50% of mice (310) provided the first indication of senescence-associated preterm birth. The follow-up studies showed that increased mTORC1 signaling (31) and oxidative stress (311) predispose these mice to preterm birth, which reaches 100% with a mild inflammatory insult (312). Additionally, deciduae obtained from women who underwent preterm labor stained positive for senescence-associated β-galactosidase (SA- β-gal) and exhibited higher immunoreactivity for the mTORC1 signaling marker pS6 as well as for labor-promoting enzyme cyclooxygenase 2 (COX2) when compared to term labor cases and non-labor controls (312). It has been proposed that, in addition to decidual senescence, senescence of the chorioamniotic membranes may promote labor (313). Although senescence of the chorioamniotic membranes was documented in preterm prelabor

rupture of membranes (pPROM) (314), it requires clearer characterization in the context of spontaneous preterm labor. The evidence presented herein stipulates that the chorioamniotic membranes of patients who undergo spontaneous preterm labor exhibit both exaggerated senescence, as confirmed by the expression of senescence-associated genes and increased reactivity of SA- β-gal, and up-regulated mTOR signaling, as indicated by elevation of pS6 in the chorioamniotic membranes.

Materials and Methods

Human subjects, clinical specimens, and definitions

The chorioamniotic membrane samples were collected at the Perinatology Research Branch, an intramural program of the Eunice Kennedy Shriver National Institute of Child Health and Human Development, National Institutes of Health, U. S. Department of Health and Human Services (NICHD/NIH/DHHS), Wayne State University (Detroit, MI, USA), and the Detroit Medical Center (Detroit, MI, USA). All participants provided written informed consent.

Table 9: Demographical characteristics of the patients whose samples were used for RT-PCR in the Senescence study

	TNL (n=28)	TIL (n=28)	PTNL (n=27)	PTL (n=26)	p value
Age, y	26.5 (22.8-29.3)	22.5 (20-25)	24 (21-27)	23 (20-25)	0.047
Body mass index, kg/m^2	28.3 (25.3-35.4)	22.7 (19.8-25.9)	27.3 (23.9-34.1)	22.1 (20-25.2)	0.001
Gestational age at delivery, wk	39.3 (39-39.7)	39.7 (39.2-40.2)	32.9 (29.8-34.2)	33.8 (31.3-35.3)	<0.001
Birth weight, g	3293 (3104-3633)	3238 (3076-3490)	1480 (908-1865)	1980 (1558-2155)	<0.001
Race					
African-American	22 (78.5%)	22 (78.5%)	26 (96.2%)	24 (92.3%)	
Caucasian	3 (10.7%)	2 (7.1%)	0 (0%)	1 (3.8%)	
Hispanic	1 (3.6%)	3 (11%)	0 (0%)	0 (0%)	NS
Other	2 (7.1%)	1 (3.6 %)	1 (3.7%)	1 (3.8%)	
Primiparity	1 (3.6%)	5 (17.8%)	4 (14.8%)	2 (8%)	NS
C-section	28 (100%)	0 (0%)	27 (100%)	8 (31%)	<0.001
Acute Chorioamnionitis	0 (0%)	0 (0%)	0 (0%)	0 (0%)	NA

Maternal age, body mass index, gestational age at delivery, birth weight, race, Primiparity, C-section, and acute chorioamnionitis are listed as mean (range) or n (%). Either Kruskal-Wallis test or Chi-square test was used to analyze the statistical differences between the study groups (TNL, TIL, PTNL, and PTL).

The collection and utilization of biological materials was approved by the Institutional Review Boards of the NICHD and Wayne State University. The collected samples were categorized based on the labor status of the patients: 1) spontaneous term labor (TIL) (n=40); 2) term delivery without labor (TNL) (n=35); 3) spontaneous preterm labor (PTL) (n=37); and 4) preterm delivery without labor (PTNL) (n=36). The demographic characteristics of these patients are shown in Tables 9 & 10. Labor was defined as the presence of regular uterine contractions at a minimum frequency of two every 10 minutes associated with cervical changes leading to delivery (315, 316).

Table 10: Demographical characteristics of the patients whose samples were used for expression array and SA-β-gal assays in the Senescence study

	TNL (n=7)	TIL (n=8)	PTNL (n=8)	PTL (n=9)	p value
Age, y	29 (26-29)	22 (18.8-24.3)	29 (25.5-35.3)	23 (19-27)	NS
Body mass index, kg/m2	34.1 (30.2-36.6)	23.5 (21.3-24.3)	27.6 (22.1-45.8)	25.2 (23.4-32)	NS
Gestational age at delivery, wk	39.3 (39.2-39.7)	39.4 (39.2-39.6)	30.2 (29.3-30.7)	34 (33.6-36)	<0.001
Birth weight, g	3820 (3603-3898)	3256 (3156-3390)	1117 (816.3-1233.8)	2330 (1795-2655)	<0.001
Race African-American Caucasian Hispanic Other	 5 (71.4%) 2 (28.6%) 0 (0%) 0 (0%)	 8 (100%) 0 (0%) 0 (0%) 0 (0%)	 6 (75%) 0 (0%) 0 (0%) 2 (25%)	 9 (100%) 0 (0%) 0 (0%) 0 (0%)	NS
Primiparity	0 (0%)	3 (37.8%)	0 (0%)	1 (11.1%)	NS
C-section	7 (100%)	0 (0%)	8 (100%)	4 (44.4%)	<0.001
Acute Chorioamnionitis	0 (0%)	0 (0%)	0 (0%)	0 (0%)	NA

Maternal age, body mass index, gestational age at delivery, birth weight, race, Primiparity, C-section, and acute chorioamnionitis are listed as mean (range) or n (%). Either Kruskal-Wallis test or Chi-square test was used to analyze the statistical differences between the study groups (TNL, TIL, PTNL, and PTL).

Gene Expression Determination

Frozen chorioamniotic membranes were treated with TRI Reagent ® Solution (Ambion, Carlsbad, CA, USA), and RNA extraction was performed with RNeasy Mini

Kits (Qiagen,Valencia, CA, USA), QIAshredders (Qiagen), and RNase-Free DNase Sets (Qiagen).

Table 11: List of primers used for RT-PCR in the Senescence study

Symbol	Gene Name	Assay ID	Lot
P53	Tumor Protein p53	Hs01034249_m1	1366180
CDKN1A (*P21*)	Cyclin-Dependent Kinase Inhibitor 1A	Hs00355782_m1	1347306
AKT1	V-akt Murine Thymoma Viral Oncogene Homolog 1	Hs00178289_m1	1349271
AGF1	AT-Hook Protein of GA Feedback 1	Hs00153126_m1	731440
IFNG	Interferon Gamma	Hs00989291_m1	1099507
CCNE1	Cyclin E1	Hs01026536_m1	1320002
CCNA2	Cyclin A2	Hs00996788_m1	1351631
CCNB1	Cyclin B1	Hs01030099_m1	1323891
CDK2	Cyclin-Dependent Kinase 2	Hs01548894_m1	1356790
FN1	Fibronectin 1	Hs01549940_m1	1221289
COL1A1	Collagen, Type I, Alpha 1	Hs00164004_m1	1078329
RPLP0	Ribosomal Protein, Large, P0	Hs99999902_m1	1347306
BACT	Beta-Actin	Hs99999903_m1	1086982
GAPDH	Glyceraldehyde-3-Phosphate Dehydrogenase	Hs99999905_m1	1335169

Gene symbol, gene name, assay ID, and lot are listed.

NanoDrop 1000 spectrophotometer (Thermo Scientific, Wilmington, DE, USA) was used to analyze the extracted RNA for concentration and purity whereas the Bioanalyzer 2100 (Agilent Technologies, Wilmington, DE, USA) was used to assess the RNA integrity. The RT^2 First Strand Kits (Qiagen) were utilized to synthesize cDNA. RT^2 Profiler PCR Array (Qiagen) was used to determine expression of 84 senescence-associated genes and 6 reference genes (n=7-9). Based on the pathway analysis results, gene expression of the selected candidates was confirmed by RT-PCR (n=25-28). The RT-PCR experiments were performed on BioMark™ High-throughput qRT-PCR system (Fluidigm, San Francisco, CA, USA) and on an ABI 7500 FAST Real-Time PCR System (Applied Biosystems, Life Technologies Corporation, Foster City, CA, USA) with TaqMan® gene expression assays (Applied Biosystems) (Table III).

Western Blot

The immunoblotting was performed as described in Chapter 2. For detecting phosphorylated S6, 1:500 mouse pS6 Ribosomal Protein (S235/236) (Catalog #2211S, Cell Signal Technology, Danvers, MA, USA) was used. The housekeeping gene was probed with 1:5000 β-actin antibody (Catalog # A5316, Clone AC-74, Sigma Aldrich, Saint Louis, MO). Images were semi-quantified using ImageJ 1.44p software (National Institute of Health, USA).

Immunohistochemistry

Five-µm-thick sections of formalin-fixed, paraffin-embedded chorioamniotic membrane tissues (n=7-8) were placed on salinized slides. Anti-Cox2 antibody (1:100, catalog # NB100-689, Novus Biologicals, Littleton, CO, USA) was used to perform immunostaining on Leica Bond Max automatic staining system (Leica Microsystems, Wetzlar, Germany). Antigen retrieval was performed for 10 min with citrate-based Bond TM Epitope Retrieval Solution I (Leica Microsystems). Chromogenic reaction of horseradish peroxidase was detected with Bond™ Polymer Refine Detection Kit (Leica Microsystems). A PerkinElmer Pannoramic MIDI slide scanner (PerkinElmer, Waltham, MA, USA) was used to assess the intensity of staining (a semi-quantitative method of analysis).

Senescence-associated β-galactosidase (SA-β-gal) staining

To detect the presence of SA-β-gala in the fetal membranes, positive cells were identified as described by Dimri et al. with minor modifications. Fetal membrane roll sections were frozen in a 25mm x 20mm x 5mm cryomold (Sakura, Torrance, CA, USA) with O.C.T. Compound (Fisher Scientific, Hampton, NH, USA); from these blocks, 10µm thick sections were cut using a Leica CM3050 cryostat (Leica Biosystems, Buffalo

Grove, IL, USA) and mounted on FisherBrand Superfrost microscope slides (Fisher Scientific, Hampton, NH, USA). Newly prepared slides were fixed with a cytology fixative (Leica Biosystems, Buffalo Grove, IL, USA) and kept frozen at -20° C. Sections were fixed in 0.5% glutaraldehyde in PBS (Life Technology, Carlsbad, CA, USA) (pH 5.5) at room temperature for 15 minutes. The slides were then washed twice in 1mM $MgCl_2$ in PBS (pH 6.0) for 5 minutes each. After last wash, staining solution containing 1mg/ml X-gal, 1mM $MgCl_2$, 5mM potassium ferricyanide, and 5mM potassium ferrocyanide in PBS (pH 6.0) was added. Slides were then incubated at 37° C for 24 hours. After incubation, slides were washed twice in 1mM $MgCl_2$ in PBS (pH 7.4), followed by an additional 30-minute wash with tap water to remove any crystals/precipitates from the staining solution. Slides were dehydrated with a graded alcohol bath, counterstained with eosin, mounted with xylene, and cover slipped by Tissue-Tek SCA (Sakura, Torrance, CA, USA). The slides were scanned using the Pannoramic MIDI Digital Slide Scanner (PerkinElmer, Inc., Waltham, MA, USA); and annotations were made by laboratory personnel who then utilized 3DHISTECH software (3DHISTECH Kft., Budapest, Hungary) to assess the intensity of the SA-β-gal staining.

ELISA

ELISA was performed as described in Chapter 2. PathScan® Total S6 Ribosomal Protein Sandwich ELISA Kit (Cell Signaling, catalog # 7225C) was used.

Statistical analysis

For senescence-associated gene expression array, Ct values over technical replicates were averaged, and gene expressions relative to reference (*ACTB*, *B2M*, *GAPDH*, *HPRT1*, *RPLP0*) were quantified by subtracting target gene Ct values from mean reference gene Ct values within the same sample. Group comparisons were

conducted via t-test from a linear model. Hierarchical clustering on genes was applied on the group mean expressions using 1-Pearson correlation as distance metric and average linkage. Gene set analysis was performed for PTL vs TIL. Gene sets (GO and KEGG signaling and metabolic pathways) were extracted from R Bioconductor package "gageData", and gene symbol to Entrez ID mapping was obtained from package "org.Hs.eg.db". The list of genes (ranked by the p value from differential expression comparison PTL vs TIL), the expression data, the sample classification and the gene sets are formatted as input to Gene Set Enrichment Analysis (GSEA: http://www.broadinstitute.org/gsea/index.jsp) (317). For confirmatory RT-PCR, Ct values over technical replicates were averaged, and gene expressions relative to reference (*BACT*, *GAPDH*, *RPLPO*) were quantified by subtracting target gene Ct values from mean reference gene Ct values within the same sample. Wilcoxon rank sum test was used for group comparison. All expression analyses were performed in R statistical computing environment (http://www.R-project.org/). Western blot and immunohistochemistry data were analyzed by Mann-Whitney U test in GraphPad Prism 6 (GraphPad Software, Inc., La Jolla, CA, USA). Patient demographics data was performed using Chi-square test for proportions as well as the Kruskal-Wallis test for non-normally distributed continuous variables in SPSS Statistics 19 (IBM Corporation, Armonk, NY, USA). A p-value < 0.05 was set as a threshold of statistical significance.

Results

Expression of the senescence-associated genes is dysregulated in preterm spontaneous labor

To determine whether senescence-associated genes are dysregulated in preterm labor, we utilized commercially available RT^2 Profiler PCR Array (Qiagen). The patient

demographics for this experiment are listed in Table 10. Each of the four labor group tested (preterm labor, term labor, and respective no-labor controls) had a unique expression profile (Figure 41). Interestingly, the no-labor groups (PTNL and TNL) exhibited up-regulation of multiple senescence-associated genes. Additionally, we assessed the expression of two labor groups (term and preterm) complicated by acute infection/inflammation of the chorioamniotic membranes (chorioamnionitis). We found that the cases with chorioamnionitis exhibited striking increase in expression of senescence-associated genes (data not shown). However, we aimed to determine whether senescence contributes to the pathophysiology of sterile, or infection-free, inflammation in preterm labor. Therefore, we used the Senescence RT^2 Profiler PCR Array data to perform more detailed comparison in gene expression between normal term labor (TIL) and pathological preterm labor (PTL).

When comparing expression patterns between preterm and term labor groups by gene set enrichment analysis (317), we found significant differences between the groups ($p=0.0036$), with all of the core enrichment genes being up-regulated in PTL (Figure 42). We also used the Senescence Array data for pathway analysis to identify which of the senescence-associated cellular pathways is differentially expressed between PTL and TIL. We found that the greatest difference in expression ($p=0.038$) between term and preterm labor occurred in genes of the p53 pathway (Figure 43).

Considering that disruption of *P53* gene induces preterm delivery in mice (310), it was reassuring to find that preterm labor cases exhibited dysregulated expression of several genes in the P53 pathway.

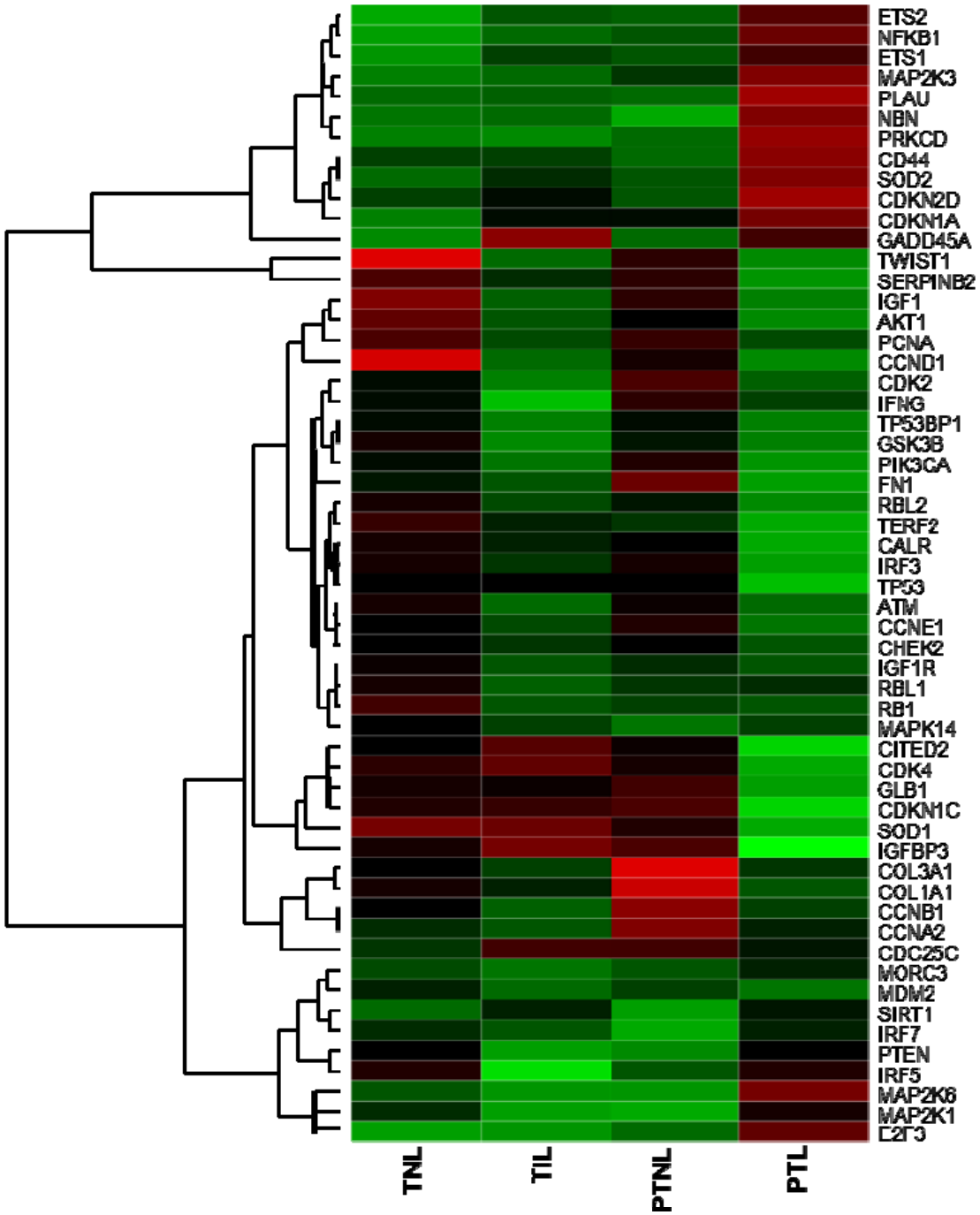

Figure 41: Heat map analysis of the senescence expression array. The chorioamniotic membranes obtained from women who either delivered at term (TIL and TNL) or preterm (PTL and PTNL) with or without labor, respectively, were subjected to the Senescence RT^2 Profiler PCR Array (Qiagen). Heat map compares the expression patterns of senescence-associated genes between the labor groups (n=7-9 per group).

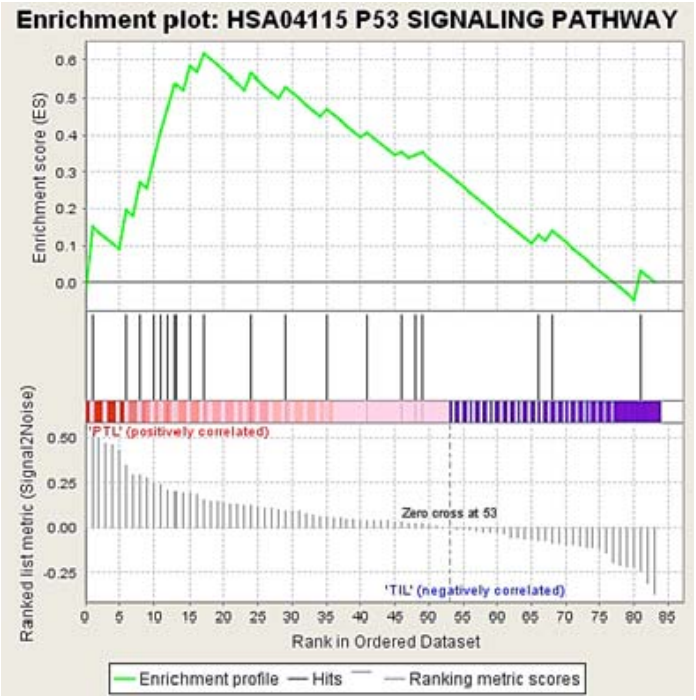

Figure 42: Gene set enrichment analysis to compare senescence-associated gene expression between preterm and term labor. Senescence RT^2 Profiler PCR Array data was further analyzed by set enrichment analysis to compare gene expression patterns between PTL (marked in red) and TIL (marked in blue). Nine out of nine core enrichment genes and seven out of ten non-core enrichment genes were up-regulated in PTL (p=0.0036).

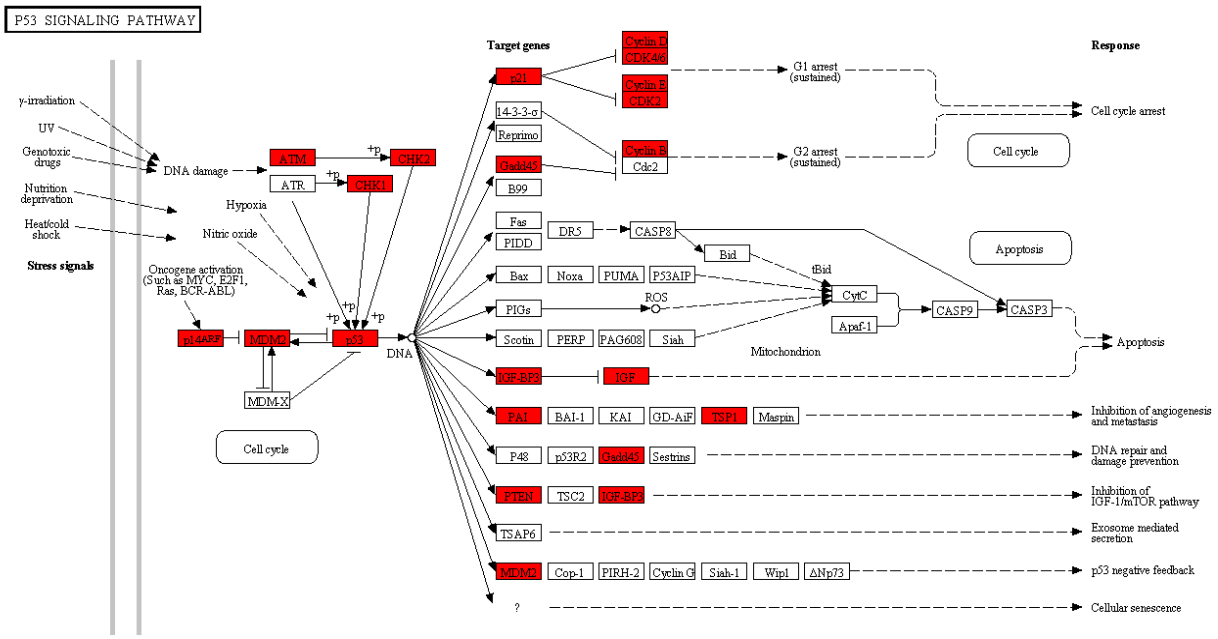

Figure 43: P53 pathway is differentially expressed between preterm and term labor. Pathway analysis revealed significant differences in the P53 signaling pathway between PTL and TIL groups (p=0.038). Genes highlighted in red were found to be differentially expressed.

Taken together, these data show that preterm labor is characterized by up-regulation of the senescence-associated genes, including the genes in the P53 pathway, when compared to term labor.

Based on our expression array findings, we selected several candidate genes for expression confirmation using conventional RT-PCR with a greater number of samples per group (n=25-28). We found that the expression of P53 was significantly down-regulated in both preterm and term labor when compared to non-labor controls (p=0.007 and 0.001, respectively) and tended to be down-regulated in preterm labor when compared to term labor (Figure 44). Inversely, expression of *P21* is significantly increased in both preterm (p<0.001) and term (p<0.001) labor when compared to the non-labor controls (Figure 44). P21, also referred to as cyclin-dependent kinase inhibitor 1, is known to inhibit such cell cycle progression genes as cyclin-dependent kinase 2 (*CDK2*), cyclin-A2 (*CCNA2*), G2/mitotic-specific cyclin-B1 (*CCNB1*), and G1/S-specific cyclin-E1 (*CCNE1*) (318, 319). Correspondingly, the expression of *CDK2*, *CCNA2*, *CCNB1*, and *CCNE1* was significantly decreased (p=0.018, <0.001, <0.001, <0.001, respectively) in preterm labor when compared to preterm delivery without labor (Figure 44). Additionally, expression of *CCNA2* and *CCNB1* is down-regulated (p=0.02 and 0.009, respectively) in preterm labor when compared to term labor (Figure 44).

Therefore, preterm labor is associated with decreased expression of *P53* as well as increased expression of the cell cycle inhibitor *P21* and subsequent decreased expression of several cell cycle progression genes.

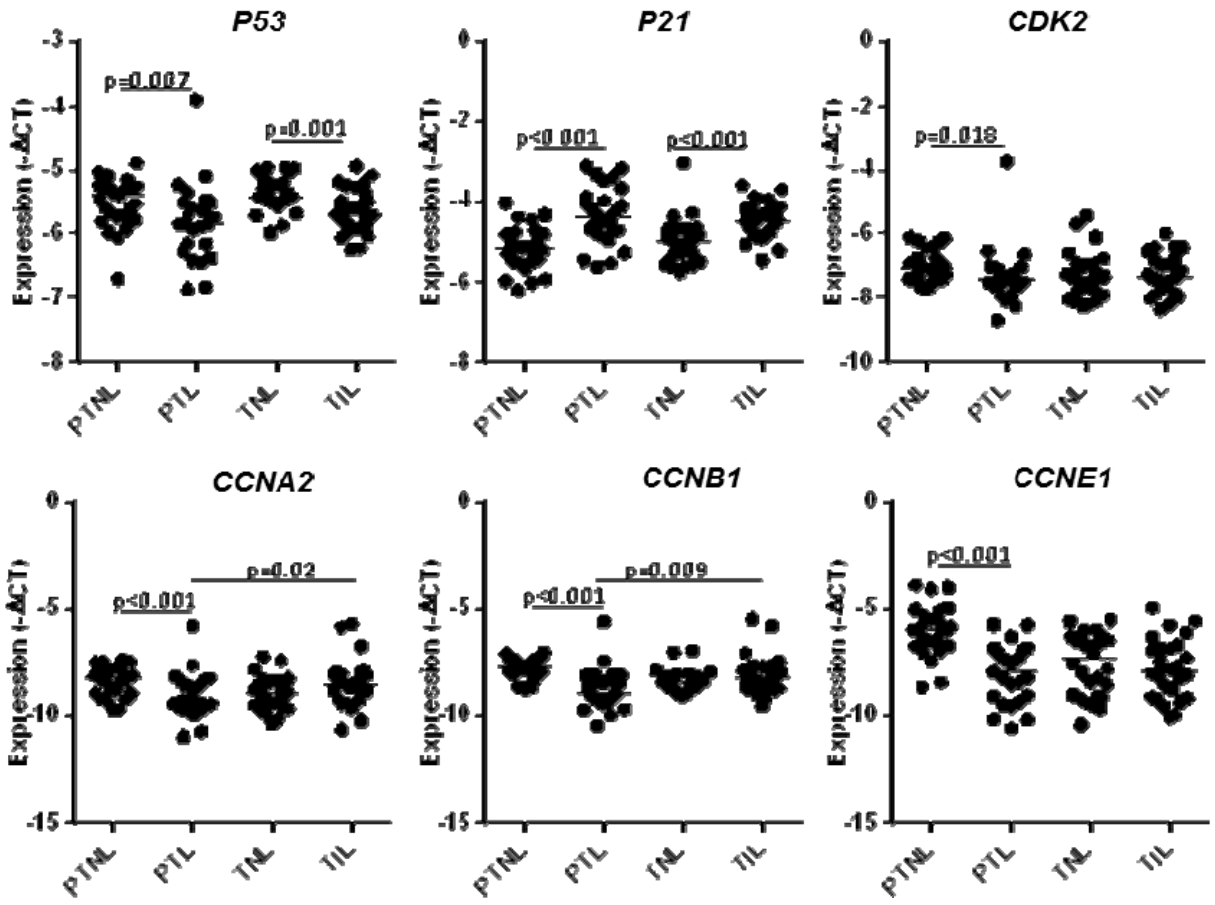

Figure 44: Expression of *P53*, *P21*, and several cycle-progression genes is dysregulated in preterm labor. The confirmatory RT-PCR (n=25-28) was performed to compare expression of P53, P21, CDK2, CCNA2, CCNB1, and CCNE1 in the chorioamniotic membranes between four labor groups (PTNL, PTL, TNL, and TIL).

Senescence-Associated β-galactosidase is more prominent in preterm labor

To determine localization of the senescent cells in the chorioamniotic membranes, we utilized senescence-associated β-galactosidase staining (SA-β-gal) which specifically marks senescent cells blue.

We found that the senescent cells were mostly localized to choriodecidua, which some staining present in the mesenchyme layer as well (Figure 45A). This suggests that the senescence initiates from the maternal compartment rather than from the fetus. When we semi-quantified the intensity of the blue signal, we found that the SA-β-gal

mean intensity was greater in the preterm labor group when compared to term labor (p=0.0006) or preterm delivery without labor (p=0.06) (Figure 45B). These findings provide further evidence that preterm labor is associated with pathological senescence of the chorioamniotic membranes.

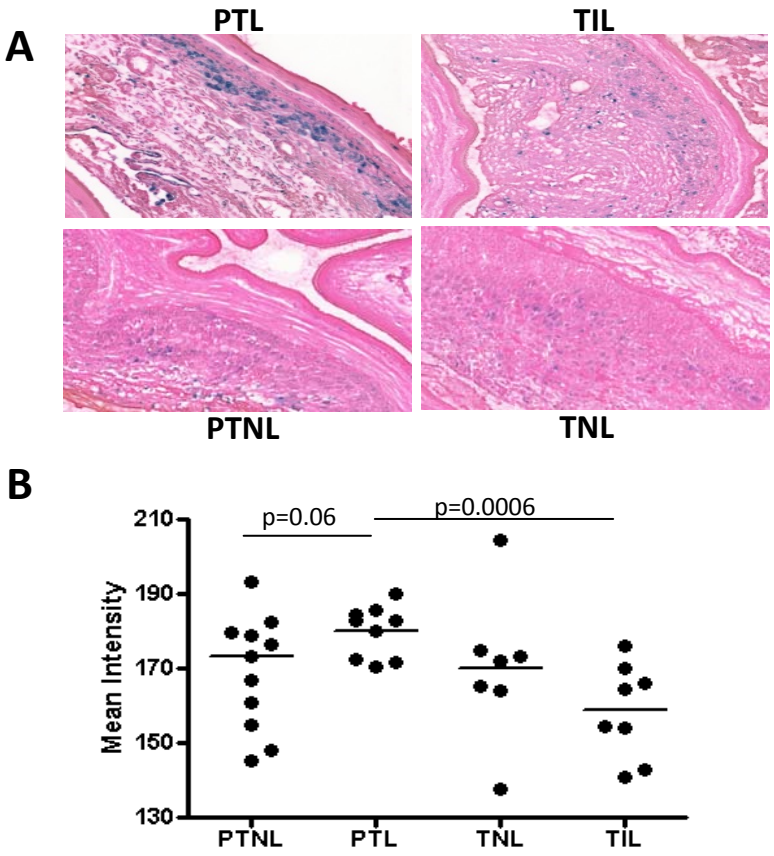

Figure 45: SA-β-gal is increased in preterm labor. Senescence-associated β-galactosidase staining was performed on the chorioamniotic membranes from four labor groups (n=7-11 per group). Only senescent cells stain blue (A). Staining intensity was semi-quantified (B).

Heightened mTORC signaling in preterm labor

Next, we aimed to determine whether senescence-induced phenotype of the chorioamniotic membranes is due to increased mTOR singling, as previously proposed by Hirota et al. (31). S6 kinase is a down-stream enzyme in mTOR signaling (320); thus phosphorylated S6 (pS6) is a marker of mTOR activity. We found that, when compared to the term labor group, the chorioamniotic membranes obtained from women who

underwent preterm labor contained significantly increased concentration of pS6 (p=0.0047) as determined by ELISA (Figure 46A). Surprisingly, term labor membranes exhibited significantly higher concentration of pS6 (p=0.0002) than the membranes that were collected from women who underwent elective Caesarian section at term without labor, but no significant differences were observed between preterm labor and its corresponding non-labor control (Figure 46A). When we attempted to confirm this finding by Western blot, the identical trend was reveled, although no statistical significance was reached (Figure 46B).

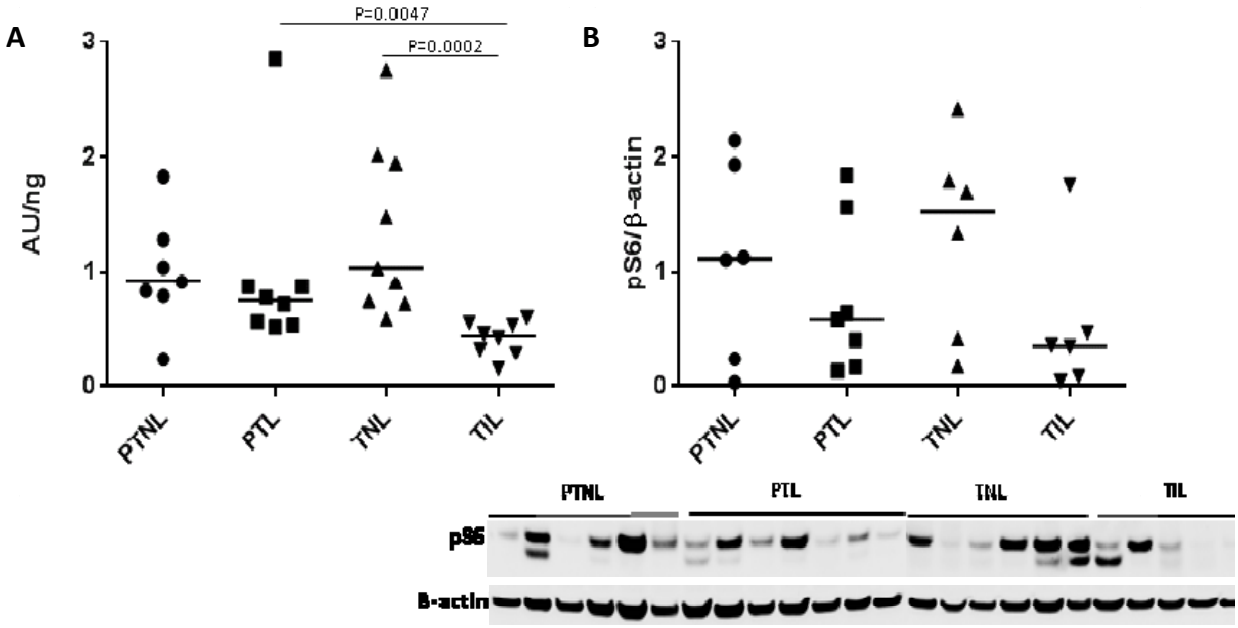

Figure 46: Heightened mTOR signaling in preterm labor. Phosphorylated S6 protein (pS6) was measured by ELISA (A) and by Western blot (B) in the chorioamniotic membranes from four labor groups (PTNL, PTL, TNL, and TIL).

Cox2 expression is increased in preterm labor

With uterine-specific p53 deficiency in mice, senescence-associated preterm birth is reversed by oral administration of the selective Cox2 inhibitor celecoxib (310). Rapamycin is another chemical agent that attenuates senescence, decreases the levels of Cox2, and rescues preterm birth in this animal model (31). Thus, it was hypothesized

that senescence promotes labor via activation of Cox-2-dependent prostaglandin secretion (321). We semi-quantified the immunoreactivity of Cox2 in the chorioamniotic membranes and found that Cox2 is significantly elevated in preterm and term labor when compared to non-labor controls, as expected (Figure 47). It is possible that senescent cells induce preterm labor by releasing pro-inflammatory mediators, such as alarmins, which are known to up-regulate expression of Cox2.

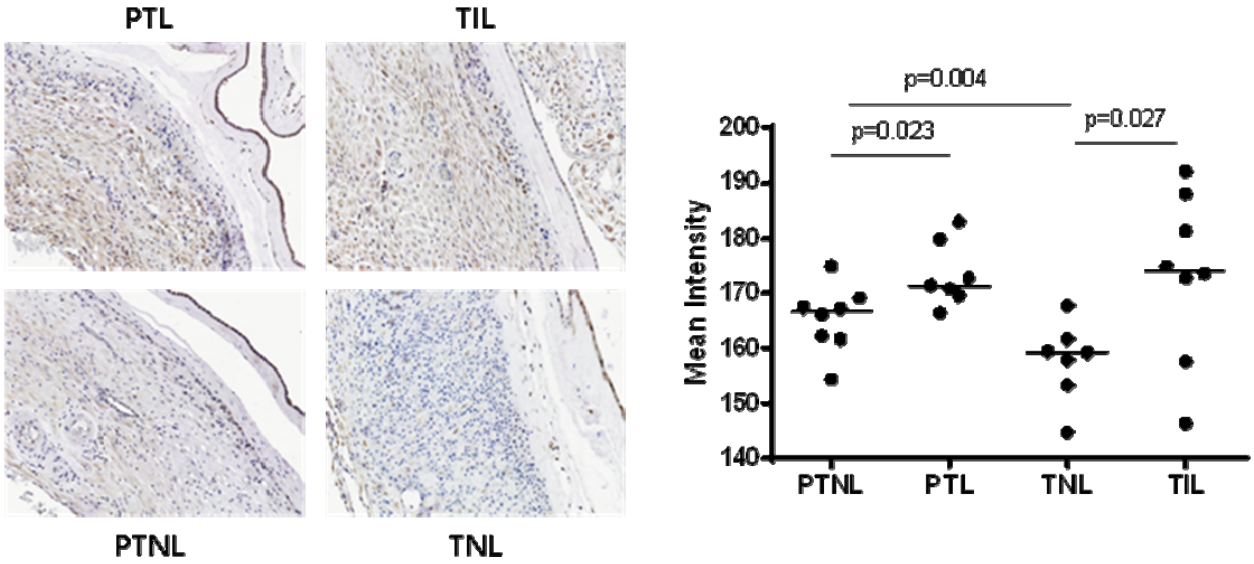

Figure 47: Cox2 expression is increased in preterm labor. Cox2 immunostaining was performed on the chorioamniotic membranes, followed by semi-quantification of the staining intensity (n=7-8 per group).

Discussion

Major findings of the study

Major findings of the study herein are: 1) Preterm labor is characterized by dysregulated expression of the senescence-associated genes; 2) The expression of senescence-associated genes, including the genes in the P53 pathway tends to be elevated in preterm labor when compared to term labor; 3) *P53* gene itself is down-regulated in preterm labor, whereas cell cycle inhibitor *P21* is up-regulated, while numerous cell cycle progression genes are down-regulated; 4) SA-β-gal localizes

senescent cells to choriodecidua and is elevated in preterm labor; 5) mTOR signaling is heightened in preterm labor when compared to term labor, as determined by concentration of pS6; 6) Chorioamniotic membranes from patients who underwent preterm labor exhibit higher immunoreactivity for Cox2 enzyme when compared to non-labor controls.

Preterm labor is characterized by dysregulated expression of senescence-associated genes in the chorioamniotic membranes

Our findings demonstrate that dysregulated gene expression characteristic of the senescent cells occurs in the chorioamniotic membranes of those patients who underwent spontaneous preterm labor. Pathological senescence of preterm labor differs from the natural processes of term labor, as confirmed by differential expression of multiple senescence-associated genes (Figure 42), including those in the p53 pathway (Figure 43). P53 is best known for being mutated in over half of all cancers, as it functions to induce cell cycle arrest or apoptosis when the cells get exposed to DNA damage signals (322). Paradoxically, P53 is actually capable of both inducing senescence and of suppressing it (323, 324). The precise regulation of senescence by P53 is still under investigation, but both up-regulation and down-regulation of P53 as well as its post-transcriptional modifications can promote senescence (325-327). In the mouse model of senescence-induced preterm birth, P53 deletion in the uterus causes senescent phenotype and ultimately leads to labor (310). We find that P53 is significantly down-regulated in the chorioamniotic membranes of the patients who underwent preterm labor when compared to preterm delivery without labor (Figure 44). Down-regulation of *P53* occurs simultaneously with up-regulation of cell cycle inhibitor *P21* and inhibition of its targets *CDK2*, *CCNA2*, *CCNB1*, and *CCNE1* (Figure 44).

Interestingly, it was previously found that knocking out *P21* in the animal model of senescent-induced preterm labor rescues preterm birth (31, 328). Taken together, our findings confirm that senescence-associated transcription occurs in the chorioamniotic membranes of patients that eventually undergo preterm birth.

SA-β-gal and mTOR signaling are elevated in the chorioamniotic membranes of patients who undergo preterm labor

Our findings reveal that the chorioamniotic membranes of patients who undergo preterm labor are more reactive to SA-β-gal staining that localizes the senescent cells predominantly to choriodecidua (Figures 45A and B). The senescent phenotype occurs with heightened mTOR signaling, as evidenced by increased concentration of pS6 in the chorioamniotic membranes from patients that undergo preterm labor when compared to labor at term (Figure 46A). Additionally, preterm labor samples also exhibit increased immunostaining for Cox2 enzyme when compared to no-labor controls, although no significant differences between preterm labor and term labor in terms of Cox2 concentrations were observed (Figure 47). We hypothesize that increased mTOR signaling promotes senescent-associated secretory phenotype (SASP) which leads to secretion of pro-inflammatory alarmins that activate various immune cells including iNKTs and ultimately initiate the final pathway of parturition that involves Cox2-mediated heightened uterine contractility. In support of our hypothesis, p53 was found to promote the release of prototypical alarmin HMGB1 (28, 329), and both placental membrane aging and HMGB1 signaling were found to be associated with human parturition (330). Interestingly, the relationship between senescence and sterile inflammation may be of mutual causation – senescence is known to promote local inflammation and emergent evidence suggests that inflammation promotes senescence.

For instance, pro-inflammatory transcription factor NF-κB inducible by alarmins was shown to trigger SASP in the senescent cells (331) and heat shock protein 60 (an alarmin) was found to induce senescence in monocytes (332). Further research is required to sort out the complexities of interaction between senescence, sterile intraamniotic inflammation, and labor.

CHAPTER 8 - CONCLUSION

The studies described herein demonstrate that sterile inflammation of the chorioamniotic membranes can be initiated by such alarmins as HMGB1 (Figure 2), S100A12 (Figure 8), MSU (Figure 15), and HSP70 (Figure 21) as evidenced by increased expression/ secretion of IL-1β and numerous other pro-inflammatory mediators, after *in vitro* treatment. Although most of the alarmins tested promote inflammation by NF-κB-dependent up-regulation of the inflammasome components, particularly *NLRP3* (Figures 4, 9, & 16), HSP70 seems to act via inflammasome-independent pathway (Figure 23).

Alarmins have been shown to activate various immune cells, including iNKT cells (212, 213). We found that activation of iNKT cells in late gestation in turn induces activation of $CD4^+$ and $CD8^+$ T cells (Figure 34) as well as innate immune cells (Figures 35 & 36) establishing pro-inflammatory microenvironment at the maternal-fetal interface (Figure 37) and ultimately leading to preterm birth (Figure 27). Therefore, alarmins set in motion a complex multi-directional immune response that is exaggerated by positive feedback regulation (Figures 6 & 12), cross-talk between innate and adaptive immunity (Chapter 6), and mutual causation (Chapter 7).

The alarmins are released during tissue/ cell stress or injury (333). In pregnancy, the sources of tissue injury and the subsequent release of alarmins can vary from microbial infection (334-336) to physical trauma (337), maternal stress (338), environmental exposure/ pollution (339), oxidative damage (340), and cellular senescence (341). Such range of alarmin-releasing conditions coincides with the mutli-factorial nature of preterm parturition syndrome (180). The studies detailed in Chapter 7 provide evidence for cellular senescence as a potential etiology for preterm birth.

Specifically, we show that the chorioamniotic membranes obtained from patients who undergo preterm birth are characterized by dysregulated expression of senescence-associated genes (Figures 41, 42, 43, & 44), increases SA-β-gal staining in the choriodecidua (Figure 45), heightened mTOR signaling (Figure 46), and increased immunoreactivity for Cox2 (Figure 47). Therefore, senescence of the chorioamniotic membranes may contribute to the release of alarmin at the maternal-fetal interface and the ensued sterile inflammation characteristic of preterm labor.

In summary, we found that the release of alarmins at the maternal-fetal interface from senescent, stressed, or injured cells initiates multifaceted pro-inflammatory cascade that involves activation of both innate and adaptive immune cells including iNKTs and the release of a multitude of pro-inflammatory cytokines, most notably IL-1β. This exaggerated inflammatory response initiates the final pathway of parturition that involves up-regulation of prostaglandin synthase-2 (Figures 13, 19, & 47) and increased activity of matrix metalloproteinases (Figures 7, 13, & 25) and culminates in preterm birth (Figure 27) and adverse neonatal outcomes (Figures 14 and 26). More detailed elucidation of the mechanisms of sterile intraamniotic inflammation will allow us to search for new therapeutic agents, such as PPARγ agonist rosiglitazone (Chapter 6).

APPENDIX A

IACUC Protocol Approval Letter

WAYNE STATE UNIVERSITY

INSTITUTIONAL ANIMAL
CARE AND USE COMMITTEE
87 E. Canfield, Second Floor
Detroit, MI 48201-2011
Telephone: (313) 577-1629
Fax Number: (313) 577-1941

ANIMAL WELFARE ASSURANCE # A 3310-01

PROTOCOL # A 09-08-12

Protocol Effective Period: October 25, 2012 – September 30, 2015

TO: Dr. Nardhy Gomez-Lopez
Perinatology Research Branch
305 Perinatology Research Branch

FROM: Lisa Anne Polin, Ph.D.
Chairperson
Institutional Animal Care and Use Committee

SUBJECT: Approval of Protocol # A 09-08-12
"Immunological tolerance during normal and preterm birth"

DATE: October 25, 2012

Your animal research protocol has been reviewed by the Wayne State University Institutional Animal Care and Use Committee, and given final approval for the period effective **October 25, 2012** through **September 30, 2015**. The listed source of funding for the protocol is **Internal Funds**. The species and number of animals approved for the duration of this protocol are listed below.

Species	Strain	Qty.	USDA Cat.
MICE	M. musculus, BALB/cByJ, MALE, 6 weeks	10	B
MICE	M. musculus, BALB/cByJ, FEMALE, 6 weeks	20	B
MICE	M. musculus, C57BL/6J, MALE, 6 weeks	10	B
MICE	M. musculus, C57BL/6J, FEMALE	20	B
MICE	M. musculus, C57BL/6-Tg(CAG-OVA)916Jen/J, MALE, 6 weeks	20	B
MICE	M. musculus, C57BL/6-Tg(Foxp3-DTR/EGFP)23.2Spar/Mmjax, MALE, 6 weeks	6	B
MICE	M. musculus, C57BL/6-Tg(Foxp3-DTR/EGFP)23.2Spar/Mmjax, FEMALE, 6 weeks	6	B
*To be purchased			
MICE	M. musculus C57BL/6J MALE	201	B
MICE	M. musculus C57BL/6J FEMALE	150	B
MICE	M. musculus C57BL/6J FEMALE	1425	D
MICE	M. musculus BALB/cByJ MALES	205	B
MICE	M. musculus BALB/cByJ FEMALES	150	B
MICE	M. musculus BALB/cByJ FEMALES	1023	D
MICE	M. musculus C57BL/6-Tg(Foxp3-DTR/EGFP)23.2Spar/Mmjax MALES	75	B
MICE	M. musculus C57BL/6-Tg(Foxp3-DTR/EGFP)23.2Spar/Mmjax FEMALES	150	B
MICE	M. musculus C57BL/6-Tg(Foxp3-DTR/EGFP)23.2Spar/Mmjax FEMALES	1000	D
MICE	M. musculus C57BL/6J / C57BL/6J MALE	1380	D
MICE	M. musculus C57BL/6J / C57BL/6J FEMALE	1380	D
MICE	M. musculus C57BL/6J / BALB/cByJ MALE	1380	D
MICE	M. musculus C57BL/6J / BALB/cByJ FEMALE	1380	D
MICE	M. musculus C57BL/ 6-Tg(CAG-OVA)916Jen/J / C57BL/6J MALE	630	D
MICE	M. musculus C57BL/ 6-Tg(CAG-OVA)916Jen/J / C57BL/6J FEMALE	630	D
MICE	M. musculus C57BL/ 6-Tg(CAG-OVA)916Jen/J / BALB/cByJ MALE	630	D
MICE	M. musculus C57BL/ 6-Tg(CAG-OVA)916Jen/J / BALB/cByJ FEMALE	630	D
MICE	M. musculus C57BL/6J / C57BL / 6-Tg(Foxp3-DTR/EGFP)23.2Spar/Mmjax MALE	1200	D

MICE ...M. musculus C57BL/6J / C57BL / 6-Tg(Foxp3-DTR/EGFP)23.2Spar/Mmjax FEMALE1200 ..D
MICE ...M. musculus BALB/cByJ / 6-Tg(Foxp3-DTR/EGFP)23.2Spar/Mmjax MALE .....1200 ..D
MICE ...M. musculus BALB/cByJ / 6-Tg(Foxp3-DTR/EGFP)23.2Spar/Mmjax FEMALE.....1200 ..D
**To be bred in-house

Be advised that this protocol must be reviewed by the IACUC on an annual basis to remain active. Any change in procedures, change in lab personnel, change in species, or additional numbers of animals requires prior approval by the IACUC. Any animal work on this research protocol beyond the expiration date will require the submission of a new IACUC protocol form and full committee review.

The Guide for the Care and Use of Laboratory Animals is the primary reference used for standards of animal care at Wayne State University. The University has submitted an appropriate assurance statement to the Office for Laboratory Animal Welfare (OLAW) of the National Institutes of Health. The animal care program at Wayne State University is accredited by the Association for Assessment and Accreditation of Laboratory Animal Care International (AAALAC).

APPENDIX B

HIC IRB Approval Letter

WAYNE STATE UNIVERSITY

IRB Administration Office
87 East Canfield, Second Floor
Detroit, Michigan 48201
Phone: (313) 577-1628
FAX: (313) 993-7122
http://irb.wayne.edu

NOTICE OF FULL BOARD CONTINUATION APPROVAL

To: Sonia Hassan
Perinatology Research
3990 John R

From: James Chinarian, M.D. or designee J. Chinarian MP/pm
Chairperson, Medical/Pediatric Institutional Review Board (MP2)

Date: May 14, 2015

RE: IRB #: 082403MP2F(5R)

Protocol Title: Establishment of a Clinical Perinatal Database and a Bank of Biological Materials

Funding Source: Sponsor: NATIONAL INSTITUTE OF CHILD HEALTH AND HUMAN DEV.
Sponsor: NATIONAL INSTITUTES OF HEALTH

Protocol #: 1011008995

Expiration Date: May 13, 2016

Risk Level / Category: Pediatric: 45 CFR 46.404 - Research not involving greater than minimal risk
Adult: Research not involving greater than minimal risk

Continuation for the above-referenced protocol and items listed below (if applicable) were **APPROVED** following Full Board review by the Wayne State University Institutional Review Board (MP2) for the period of 05/14/2015 through 05/13/2016. This approval does not replace any departmental or other approvals that may be required.

- Actively accruing participants.
- Medical Research Informed Consent Form-Maternal Consent with HIPAA Authorization (revision dated 2/25/2015)
- Medical Research Informed Consent Form Non-Pregnant Control Consent with HIPAA Authorization (revision dated 2/28/2013)
- Medical Research Informed Consent Form-Father's Consent with HIPAA Authorization (revision dated 2/28/2013)
- Medical Documentation of Adolescent Assent Form Ages 15-17 (revision dated 2/25/2015)

- Federal regulations require that all research be reviewed at least annually. You *may* receive a *"Continuation Renewal Reminder"* approximately two months prior to the expiration date; however, it is the Principal Investigator's responsibility to obtain review and continued approval ***before*** the expiration date. Data collected during a period of lapsed approval is unapproved research and can *never* be reported or published as research data.
- All changes or amendments to the above-referenced protocol require review and approval by the IRB **BEFORE** implementation.
- Adverse Reactions/Unexpected Events (AR/UE) must be submitted on the appropriate form within the timeframe specified in the IRB Administration Office Policy (http://www.irb.wayne.edu/policies-human-research.php).

NOTE:

1. Upon notification of an impending regulatory site visit, hold notification, and/or external audit the IRB Administration Office must be contacted immediately.
2. Forms should be downloaded from the IRB website at **each** use.

APPENDIX C

Copyright License Agreement for Chapter 6

April 12, 2016

Olesya Plazo
Wayne State University
475 E. Hancock
Detroit, MI 48201
United States
Email: oplazyo@med.wayne.edu

Dear Dr. Plazo,

The American Association of Immunologists, Inc., grants permission to reproduce the article, "Invariant NKT Cell Activation Induces Late Preterm Birth That Is Attenuated by Rosiglitazone," published in *The Journal of Immunology*, vol. 196, pp. 1044-1059, 2016, in your thesis, contingent on the following conditions:

1. That you give proper credit to the authors and to *The Journal of Immunology*, including in your citation the volume, date, and page numbers.

2. That you include the statement:

   Copyright 2016. The American Association of Immunologists, Inc.

3. That permission is granted for one-time use only for print and electronic format. Permission must be requested separately for future editions, revisions, derivative works, and promotional pieces. Reproduction of any content, other than figures and figure legends, from *The Journal of Immunology* is permitted in English only.

Thank you for your interest in *The Journal of Immunology*.

Sincerely,

Gene Bailey
Senior Editorial Manager
The Journal of Immunology

REFERENCES

1. Goldenberg RL, Culhane JF, Iams JD, Romero R. Epidemiology and causes of preterm birth. Lancet. 2008;371(9606):75-84. Epub 2008/01/08.
2. Martin JA, Hamilton BE, Osterman MJ, Curtin SC, Matthews TJ. Births: final data for 2013. National vital statistics reports : from the Centers for Disease Control and Prevention, National Center for Health Statistics, National Vital Statistics System. 2015;64(1):1-65. Epub 2015/01/21.
3. Liu L, Oza S, Hogan D, Perin J, Rudan I, Lawn JE, et al. Global, regional, and national causes of child mortality in 2000-13, with projections to inform post-2015 priorities: an updated systematic analysis. Lancet. 2015;385(9966):430-40. Epub 2014/10/05.
4. Manuck TA, Sheng X, Yoder BA, Varner MW. Correlation between initial neonatal and early childhood outcomes following preterm birth. American journal of obstetrics and gynecology. 2014;210(5):426 e1-9. Epub 2014/05/06.
5. Lubow JM, How HY, Habli M, Maxwell R, Sibai BM. Indications for delivery and short-term neonatal outcomes in late preterm as compared with term births. American journal of obstetrics and gynecology. 2009;200(5):e30-3. Epub 2009/01/13.
6. Mwaniki MK, Atieno M, Lawn JE, Newton CR. Long-term neurodevelopmental outcomes after intrauterine and neonatal insults: a systematic review. Lancet. 2012;379(9814):445-52. Epub 2012/01/17.
7. Murray CJ, Vos T, Lozano R, Naghavi M, Flaxman AD, Michaud C, et al. Disability-adjusted life years (DALYs) for 291 diseases and injuries in 21 regions, 1990-2010: a systematic analysis for the Global Burden of Disease Study 2010.

Lancet. 2012;380(9859):2197-223. Epub 2012/12/19.

8. Romero R, Dey SK, Fisher SJ. Preterm labor: one syndrome, many causes. Science. 2014;345(6198):760-5. Epub 2014/08/16.

9. Gomez-Lopez N, Vadillo-Perez L, Hernandez-Carbajal A, Godines-Enriquez M, Olson DM, Vadillo-Ortega F. Specific inflammatory microenvironments in the zones of the fetal membranes at term delivery. American journal of obstetrics and gynecology. 2011;205(3):235 e15-24. Epub 2011/07/19.

10. Gomez-Lopez N, Vega-Sanchez R, Castillo-Castrejon M, Romero R, Cubeiro-Arreola K, Vadillo-Ortega F. Evidence for a role for the adaptive immune response in human term parturition. American journal of reproductive immunology. 2013;69(3):212-30. Epub 2013/01/26.

11. Gomez-Lopez N, Estrada-Gutierrez G, Jimenez-Zamudio L, Vega-Sanchez R, Vadillo-Ortega F. Fetal membranes exhibit selective leukocyte chemotaxic activity during human labor. Journal of reproductive immunology. 2009;80(1-2):122-31. Epub 2009/05/02.

12. Gotsch F, Gotsch F, Romero R, Erez O, Vaisbuch E, Kusanovic JP, et al. The preterm parturition syndrome and its implications for understanding the biology, risk assessment, diagnosis, treatment and prevention of preterm birth. The journal of maternal-fetal & neonatal medicine : the official journal of the European Association of Perinatal Medicine, the Federation of Asia and Oceania Perinatal Societies, the International Society of Perinatal Obstet. 2009;22 Suppl 2:5-23. Epub 2009/12/03.

13. Athayde N, Romero R, Gomez R, Maymon E, Pacora P, Mazor M, et al. Matrix metalloproteinases-9 in preterm and term human parturition. The Journal of

maternal-fetal medicine. 1999;8(5):213-9. Epub 1999/09/04.

14. Kim SM, Romero R, Lee J, Chaemsaithong P, Lee MW, Chaiyasit N, et al. About one-half of early spontaneous preterm deliveries can be identified by a rapid matrix metalloproteinase-8 (MMP-8) bedside test at the time of mid-trimester genetic amniocentesis. The journal of maternal-fetal & neonatal medicine : the official journal of the European Association of Perinatal Medicine, the Federation of Asia and Oceania Perinatal Societies, the International Society of Perinatal Obstet. 2015:1-9. Epub 2015/12/09.

15. Gonzalez JM, Franzke CW, Yang F, Romero R, Girardi G. Complement activation triggers metalloproteinases release inducing cervical remodeling and preterm birth in mice. The American journal of pathology. 2011;179(2):838-49. Epub 2011/08/02.

16. Sorokin Y, Romero R, Mele L, Wapner RJ, Iams JD, Dudley DJ, et al. Maternal serum interleukin-6, C-reactive protein, and matrix metalloproteinase-9 concentrations as risk factors for preterm birth <32 weeks and adverse neonatal outcomes. American journal of perinatology. 2010;27(8):631-40. Epub 2010/03/03.

17. Park CW, Lee SM, Park JS, Jun JK, Romero R, Yoon BH. The antenatal identification of funisitis with a rapid MMP-8 bedside test. Journal of perinatal medicine. 2008;36(6):497-502. Epub 2009/01/08.

18. Nien JK, Yoon BH, Espinoza J, Kusanovic JP, Erez O, Soto E, et al. A rapid MMP-8 bedside test for the detection of intra-amniotic inflammation identifies patients at risk for imminent preterm delivery. American journal of obstetrics and gynecology. 2006;195(4):1025-30. Epub 2006/09/27.

19. Park JY, Romero R, Lee J, Chaemsaithong P, Chaiyasit N, Yoon BH. An elevated amniotic fluid prostaglandin F concentration is associated with intra-amniotic inflammation/infection, and clinical and histologic chorioamnionitis, as well as impending preterm delivery in patients with preterm labor and intact membranes. The journal of maternal-fetal & neonatal medicine : the official journal of the European Association of Perinatal Medicine, the Federation of Asia and Oceania Perinatal Societies, the International Society of Perinatal Obstet. 2015:1-10. Epub 2015/12/17.

20. Hong JS, Romero R, Lee DC, Than NG, Yeo L, Chaemsaithong P, et al. Umbilical cord prostaglandins in term and preterm parturition. The journal of maternal-fetal & neonatal medicine : the official journal of the European Association of Perinatal Medicine, the Federation of Asia and Oceania Perinatal Societies, the International Society of Perinatal Obstet. 2016;29(4):523-31. Epub 2015/03/12.

21. Romero R, Miranda J, Chaiworapongsa T, Korzeniewski SJ, Chaemsaithong P, Gotsch F, et al. Prevalence and Clinical Significance of Sterile Intra-amniotic Inflammation in Patients with Preterm Labor and Intact Membranes. American journal of reproductive immunology. 2014;72(5):458-72. Epub 2014/08/01.

22. Chen GY, Nunez G. Sterile inflammation: sensing and reacting to damage. Nature reviews Immunology. 2010;10(12):826-37. Epub 2010/11/23.

23. Rubartelli A, Lotze MT. Inside, outside, upside down: damage-associated molecular-pattern molecules (DAMPs) and redox. Trends in immunology. 2007;28(10):429-36. Epub 2007/09/12.

24. Oppenheim JJ, Yang D. Alarmins: chemotactic activators of immune responses.

Current opinion in immunology. 2005;17(4):359-65. Epub 2005/06/16.

25. Zelenay S, Reis e Sousa C. Adaptive immunity after cell death. Trends in immunology. 2013;34(7):329-35. Epub 2013/04/24.

26. Pouwels SD, Heijink IH, ten Hacken NH, Vandenabeele P, Krysko DV, Nawijn MC, et al. DAMPs activating innate and adaptive immune responses in COPD. Mucosal immunology. 2014;7(2):215-26. Epub 2013/10/24.

27. Brennan PJ, Tatituri RV, Brigl M, Kim EY, Tuli A, Sanderson JP, et al. Invariant natural killer T cells recognize lipid self antigen induced by microbial danger signals. Nature immunology. 2011;12(12):1202-11. Epub 2011/11/01.

28. Davalos AR, Kawahara M, Malhotra GK, Schaum N, Huang J, Ved U, et al. p53-dependent release of Alarmin HMGB1 is a central mediator of senescent phenotypes. The Journal of cell biology. 2013;201(4):613-29. Epub 2013/05/08.

29. Menon R, Behnia F, Polettini J, Saade GR, Campisi J, Velarde M. Placental membrane aging and HMGB1 signaling associated with human parturition. Aging. 2016. Epub 2016/02/07.

30. Cannizzo ES, Clement CC, Sahu R, Follo C, Santambrogio L. Oxidative stress, inflamm-aging and immunosenescence. Journal of proteomics. 2011;74(11):2313-23. Epub 2011/07/02.

31. Hirota Y, Cha J, Yoshie M, Daikoku T, Dey SK. Heightened uterine mammalian target of rapamycin complex 1 (mTORC1) signaling provokes preterm birth in mice. Proceedings of the National Academy of Sciences of the United States of America. 2011;108(44):18073-8. Epub 2011/10/26.

32. Matzinger P. An innate sense of danger. Seminars in immunology. 1998;10(5):399-415. Epub 1998/12/05.

33. Abrahams VM. Pattern recognition at the maternal-fetal interface. Immunological investigations. 2008;37(5):427-47. Epub 2008/08/22.

34. Pineles BL RR, Montenegro D, Tarca AL, Than NG, Hassan S, Gotsch F, Draghici S, Espinoza J, Kim CJ. "The inflammasome" in human parturition. Reproductive Sciences. 2007;14(59A).

35. Ogura Y, Sutterwala FS, Flavell RA. The inflammasome: first line of the immune response to cell stress. Cell. 2006;126(4):659-62. Epub 2006/08/23.

36. Mariathasan S, Monack DM. Inflammasome adaptors and sensors: intracellular regulators of infection and inflammation. Nature reviews Immunology. 2007;7(1):31-40. Epub 2006/12/23.

37. Schroder K, Tschopp J. The inflammasomes. Cell. 2010;140(6):821-32. Epub 2010/03/23.

38. Martinon F, Burns K, Tschopp J. The inflammasome: a molecular platform triggering activation of inflammatory caspases and processing of proIL-beta. Molecular cell. 2002;10(2):417-26. Epub 2002/08/23.

39. Franchi L, Eigenbrod T, Munoz-Planillo R, Nunez G. The inflammasome: a caspase-1-activation platform that regulates immune responses and disease pathogenesis. Nature immunology. 2009;10(3):241-7. Epub 2009/02/18.

40. Romero R, Xu Y, Plazyo O, Chaemsaithong P, Chaiworapongsa T, Unkel R, et al. A Role for the Inflammasome in Spontaneous Labor at Term. American journal of reproductive immunology. 2016.

41. Gotsch F, Romero R, Chaiworapongsa T, Erez O, Vaisbuch E, Espinoza J, et al. Evidence of the involvement of caspase-1 under physiologic and pathologic cellular stress during human pregnancy: a link between the inflammasome and

parturition. The journal of maternal-fetal & neonatal medicine : the official journal of the European Association of Perinatal Medicine, the Federation of Asia and Oceania Perinatal Societies, the International Society of Perinatal Obstet. 2008;21(9):605-16. Epub 2008/10/02.

42. Romero R, Brody DT, Oyarzun E, Mazor M, Wu YK, Hobbins JC, et al. Infection and labor. III. Interleukin-1: a signal for the onset of parturition. American journal of obstetrics and gynecology. 1989;160(5 Pt 1):1117-23. Epub 1989/05/01.

43. Romero R, Parvizi ST, Oyarzun E, Mazor M, Wu YK, Avila C, et al. Amniotic fluid interleukin-1 in spontaneous labor at term. The Journal of reproductive medicine. 1990;35(3):235-8. Epub 1990/03/01.

44. Romero R, Mazor M, Brandt F, Sepulveda W, Avila C, Cotton DB, et al. Interleukin-1 alpha and interleukin-1 beta in preterm and term human parturition. American journal of reproductive immunology. 1992;27(3-4):117-23. Epub 1992/04/01.

45. Romero R, Sepulveda W, Mazor M, Brandt F, Cotton DB, Dinarello CA, et al. The natural interleukin-1 receptor antagonist in term and preterm parturition. American journal of obstetrics and gynecology. 1992;167(4 Pt 1):863-72. Epub 1992/10/01.

46. Lotze MT, Tracey KJ. High-mobility group box 1 protein (HMGB1): nuclear weapon in the immune arsenal. Nature reviews Immunology. 2005;5(4):331-42. Epub 2005/04/02.

47. Park JS, Gamboni-Robertson F, He Q, Svetkauskaite D, Kim JY, Strassheim D, et al. High mobility group box 1 protein interacts with multiple Toll-like receptors. American journal of physiology Cell physiology. 2006;290(3):C917-24. Epub

2005/11/04.

48. Hori O, Brett J, Slattery T, Cao R, Zhang J, Chen JX, et al. The receptor for advanced glycation end products (RAGE) is a cellular binding site for amphoterin. Mediation of neurite outgrowth and co-expression of rage and amphoterin in the developing nervous system. The Journal of biological chemistry. 1995;270(43):25752-61. Epub 1995/10/27.

49. Andersson U, Wang H, Palmblad K, Aveberger AC, Bloom O, Erlandsson-Harris H, et al. High mobility group 1 protein (HMG-1) stimulates proinflammatory cytokine synthesis in human monocytes. The Journal of experimental medicine. 2000;192(4):565-70. Epub 2000/08/22.

50. Park JS, Arcaroli J, Yum HK, Yang H, Wang H, Yang KY, et al. Activation of gene expression in human neutrophils by high mobility group box 1 protein. American journal of physiology Cell physiology. 2003;284(4):C870-9. Epub 2003/03/07.

51. Orlova VV, Choi EY, Xie C, Chavakis E, Bierhaus A, Ihanus E, et al. A novel pathway of HMGB1-mediated inflammatory cell recruitment that requires Mac-1-integrin. The EMBO journal. 2007;26(4):1129-39. Epub 2007/02/03.

52. Messmer D, Yang H, Telusma G, Knoll F, Li J, Messmer B, et al. High mobility group box protein 1: an endogenous signal for dendritic cell maturation and Th1 polarization. Journal of immunology. 2004;173(1):307-13. Epub 2004/06/24.

53. Fiuza C, Bustin M, Talwar S, Tropea M, Gerstenberger E, Shelhamer JH, et al. Inflammation-promoting activity of HMGB1 on human microvascular endothelial cells. Blood. 2003;101(7):2652-60. Epub 2002/11/29.

54. Stephen GL, Lui S, Hamilton SA, Tower CL, Harris LK, Stevens A, et al.

Transcriptomic profiling of human choriodecidua during term labor: inflammation as a key driver of labor. American journal of reproductive immunology. 2015;73(1):36-55. Epub 2014/10/07.

55. Romero R, Chaiworapongsa T, Savasan ZA, Hussein Y, Dong Z, Kusanovic JP, et al. Clinical chorioamnionitis is characterized by changes in the expression of the alarmin HMGB1 and one of its receptors, sRAGE. The journal of maternal-fetal & neonatal medicine : the official journal of the European Association of Perinatal Medicine, the Federation of Asia and Oceania Perinatal Societies, the International Society of Perinatal Obstet. 2012;25(6):558-67. Epub 2012/05/15.

56. Romero R, Chaiworapongsa T, Alpay Savasan Z, Xu Y, Hussein Y, Dong Z, et al. Damage-associated molecular patterns (DAMPs) in preterm labor with intact membranes and preterm PROM: a study of the alarmin HMGB1. The journal of maternal-fetal & neonatal medicine : the official journal of the European Association of Perinatal Medicine, the Federation of Asia and Oceania Perinatal Societies, the International Society of Perinatal Obstet. 2011;24(12):1444-55. Epub 2011/10/01.

57. Dubicke A, Andersson P, Fransson E, Andersson E, Sioutas A, Malmstrom A, et al. High-mobility group box protein 1 and its signalling receptors in human preterm and term cervix. Journal of reproductive immunology. 2010;84(1):86-94. Epub 2009/12/08.

58. Yang LL, Sun ZM, Liu X, Zhu XY, Wang XB, Wang J. [Extracellular HMGB1 promotes the migration of cord Blood CD34(+) cells via SDF-1/CXCR-4 axis]. Zhongguo shi yan xue ye xue za zhi / Zhongguo bing li sheng li xue hui = Journal of experimental hematology / Chinese Association of Pathophysiology.

2014;22(5):1415-21. Epub 2014/10/24.

59. Aghai ZH, Saslow JG, Meniru C, Porter C, Eydelman R, Bhat V, et al. High-mobility group box-1 protein in tracheal aspirates from premature infants: relationship with bronchopulmonary dysplasia and steroid therapy. Journal of perinatology : official journal of the California Perinatal Association. 2010;30(9):610-5. Epub 2010/02/26.

60. Gomez-Lopez N, et al. Intra-amniotic Administration of HMGB1 Induces Spontaneous Preterm Labor and Birth. American journal of reproductive immunology. 2015.

61. Bredeson S, Papaconstantinou J, Deford JH, Kechichian T, Syed TA, Saade GR, et al. HMGB1 promotes a p38MAPK associated non-infectious inflammatory response pathway in human fetal membranes. PloS one. 2014;9(12):e113799. Epub 2014/12/04.

62. Sen R, Baltimore D. Multiple nuclear factors interact with the immunoglobulin enhancer sequences. Cell. 1986;46(5):705-16. Epub 1986/08/29.

63. Lindstrom TM, Bennett PR. The role of nuclear factor kappa B in human labour. Reproduction. 2005;130(5):569-81. Epub 2005/11/03.

64. Vora S, Abbas A, Kim CJ, Summerfield TL, Kusanovic JP, Iams JD, et al. Nuclear factor-kappa B localization and function within intrauterine tissues from term and preterm labor and cultured fetal membranes. Reproductive biology and endocrinology : RB&E. 2010;8:8. Epub 2010/01/27.

65. Belt AR, Baldassare JJ, Molnar M, Romero R, Hertelendy F. The nuclear transcription factor NF-kappaB mediates interleukin-1beta-induced expression of cyclooxygenase-2 in human myometrial cells. American journal of obstetrics and

gynecology. 1999;181(2):359-66. Epub 1999/08/24.

66. Kim YG, Park JH, Shaw MH, Franchi L, Inohara N, Nunez G. The cytosolic sensors Nod1 and Nod2 are critical for bacterial recognition and host defense after exposure to Toll-like receptor ligands. Immunity. 2008;28(2):246-57. Epub 2008/02/12.

67. Mulla MJ, Yu AG, Cardenas I, Guller S, Panda B, Abrahams VM. Regulation of Nod1 and Nod2 in first trimester trophoblast cells. American journal of reproductive immunology. 2009;61(4):294-302. Epub 2009/03/06.

68. Cardenas I, Mulla MJ, Myrtolli K, Sfakianaki AK, Norwitz ER, Tadesse S, et al. Nod1 activation by bacterial iE-DAP induces maternal-fetal inflammation and preterm labor. Journal of immunology. 2011;187(2):980-6. Epub 2011/06/17.

69. Franchi L, Warner N, Viani K, Nunez G. Function of Nod-like receptors in microbial recognition and host defense. Immunological reviews. 2009;227(1):106-28. Epub 2009/01/06.

70. Creagh EM, Conroy H, Martin SJ. Caspase-activation pathways in apoptosis and immunity. Immunological reviews. 2003;193:10-21. Epub 2003/05/20.

71. Martinon F, Tschopp J. Inflammatory caspases: linking an intracellular innate immune system to autoinflammatory diseases. Cell. 2004;117(5):561-74. Epub 2004/05/28.

72. Martinon F, Tschopp J. Inflammatory caspases and inflammasomes: master switches of inflammation. Cell death and differentiation. 2007;14(1):10-22. Epub 2006/09/16.

73. Schmitz J, Owyang A, Oldham E, Song Y, Murphy E, McClanahan TK, et al. IL-33, an interleukin-1-like cytokine that signals via the IL-1 receptor-related protein

ST2 and induces T helper type 2-associated cytokines. Immunity. 2005;23(5):479-90. Epub 2005/11/16.

74. Meylan E, Tschopp J, Karin M. Intracellular pattern recognition receptors in the host response. Nature. 2006;442(7098):39-44. Epub 2006/07/11.

75. Cerretti DP, Kozlosky CJ, Mosley B, Nelson N, Van Ness K, Greenstreet TA, et al. Molecular cloning of the interleukin-1 beta converting enzyme. Science. 1992;256(5053):97-100. Epub 1992/04/03.

76. Fantuzzi G, Dinarello CA. Interleukin-18 and interleukin-1 beta: two cytokine substrates for ICE (caspase-1). Journal of clinical immunology. 1999;19(1):1-11. Epub 1999/03/18.

77. Thornberry NA, Bull HG, Calaycay JR, Chapman KT, Howard AD, Kostura MJ, et al. A novel heterodimeric cysteine protease is required for interleukin-1 beta processing in monocytes. Nature. 1992;356(6372):768-74. Epub 1992/04/30.

78. van Beijnum JR, Buurman WA, Griffioen AW. Convergence and amplification of toll-like receptor (TLR) and receptor for advanced glycation end products (RAGE) signaling pathways via high mobility group B1 (HMGB1). Angiogenesis. 2008;11(1):91-9. Epub 2008/02/12.

79. Choi SJ, Oh S, Kim JH, Roh CR. Changes of nuclear factor kappa B (NF-kappaB), cyclooxygenase-2 (COX-2) and matrix metalloproteinase-9 (MMP-9) in human myometrium before and during term labor. European journal of obstetrics, gynecology, and reproductive biology. 2007;132(2):182-8. Epub 2006/10/03.

80. Vadillo-Ortega F, Gonzalez-Avila G, Furth EE, Lei H, Muschel RJ, Stetler-Stevenson WG, et al. 92-kd type IV collagenase (matrix metalloproteinase-9) activity in human amniochorion increases with labor. The American journal of

pathology. 1995;146(1):148-56. Epub 1995/01/01.

81. Xu P, Alfaidy N, Challis JR. Expression of matrix metalloproteinase (MMP)-2 and MMP-9 in human placenta and fetal membranes in relation to preterm and term labor. The Journal of clinical endocrinology and metabolism. 2002;87(3):1353-61. Epub 2002/03/13.

82. Maymon E, Romero R, Pacora P, Gervasi MT, Gomez R, Edwin SS, et al. Evidence of in vivo differential bioavailability of the active forms of matrix metalloproteinases 9 and 2 in parturition, spontaneous rupture of membranes, and intra-amniotic infection. American journal of obstetrics and gynecology. 2000;183(4):887-94. Epub 2000/10/18.

83. Athayde N, Edwin SS, Romero R, Gomez R, Maymon E, Pacora P, et al. A role for matrix metalloproteinase-9 in spontaneous rupture of the fetal membranes. American journal of obstetrics and gynecology. 1998;179(5):1248-53. Epub 1998/11/20.

84. Romero R, Chaiworapongsa T, Espinoza J, Gomez R, Yoon BH, Edwin S, et al. Fetal plasma MMP-9 concentrations are elevated in preterm premature rupture of the membranes. American journal of obstetrics and gynecology. 2002;187(5):1125-30. Epub 2002/11/20.

85. Librach CL, Feigenbaum SL, Bass KE, Cui TY, Verastas N, Sadovsky Y, et al. Interleukin-1 beta regulates human cytotrophoblast metalloproteinase activity and invasion in vitro. The Journal of biological chemistry. 1994;269(25):17125-31. Epub 1994/06/24.

86. Fortunato SJ, Menon R, Lombardi SJ. Role of tumor necrosis factor-alpha in the premature rupture of membranes and preterm labor pathways. American journal

of obstetrics and gynecology. 2002;187(5):1159-62. Epub 2002/11/20.

87. Calfee CS, Matthay MA. Clinical immunology: Culprits with evolutionary ties. Nature. 2010;464(7285):41-2. Epub 2010/03/06.

88. Bianchi ME. HMGB1 loves company. Journal of leukocyte biology. 2009;86(3):573-6. Epub 2009/05/06.

89. Regan JK, Kannan PS, Kemp MW, Kramer BW, Newnham JP, Jobe AH, et al. Damage-Associated Molecular Pattern and Fetal Membrane Vascular Injury and Collagen Disorganization in Lipopolysaccharide-Induced Intra-amniotic Inflammation in Fetal Sheep. Reprod Sci. 2015. Epub 2015/07/15.

90. Buhimschi CS, Baumbusch MA, Dulay AT, Oliver EA, Lee S, Zhao G, et al. Characterization of RAGE, HMGB1, and S100beta in inflammation-induced preterm birth and fetal tissue injury. The American journal of pathology. 2009;175(3):958-75. Epub 2009/08/15.

91. Franchi L, Eigenbrod T, Nunez G. Cutting edge: TNF-alpha mediates sensitization to ATP and silica via the NLRP3 inflammasome in the absence of microbial stimulation. Journal of immunology. 2009;183(2):792-6. Epub 2009/06/23.

92. Bauernfeind FG, Horvath G, Stutz A, Alnemri ES, MacDonald K, Speert D, et al. Cutting edge: NF-kappaB activating pattern recognition and cytokine receptors license NLRP3 inflammasome activation by regulating NLRP3 expression. Journal of immunology. 2009;183(2):787-91.

93. Sutterwala FS, Haasken S, Cassel SL. Mechanism of NLRP3 inflammasome activation. Annals of the New York Academy of Sciences. 2014;1319:82-95. Epub 2014/05/21.

94. Guo H, Callaway JB, Ting JP. Inflammasomes: mechanism of action, role in disease, and therapeutics. Nature medicine. 2015;21(7):677-87. Epub 2015/06/30.

95. Black RA, Kronheim SR, Merriam JE, March CJ, Hopp TP. A pre-aspartate-specific protease from human leukocytes that cleaves pro-interleukin-1 beta. The Journal of biological chemistry. 1989;264(10):5323-6. Epub 1989/04/05.

96. Kostura MJ, Tocci MJ, Limjuco G, Chin J, Cameron P, Hillman AG, et al. Identification of a monocyte specific pre-interleukin 1 beta convertase activity. Proceedings of the National Academy of Sciences of the United States of America. 1989;86(14):5227-31. Epub 1989/07/01.

97. Gu Y, Kuida K, Tsutsui H, Ku G, Hsiao K, Fleming MA, et al. Activation of interferon-gamma inducing factor mediated by interleukin-1beta converting enzyme. Science. 1997;275(5297):206-9. Epub 1997/01/10.

98. Ghayur T, Banerjee S, Hugunin M, Butler D, Herzog L, Carter A, et al. Caspase-1 processes IFN-gamma-inducing factor and regulates LPS-induced IFN-gamma production. Nature. 1997;386(6625):619-23. Epub 1997/04/10.

99. Dinarello CA. Interleukin-1 beta, interleukin-18, and the interleukin-1 beta converting enzyme. Annals of the New York Academy of Sciences. 1998;856:1-11. Epub 1999/01/26.

100. Sansonetti PJ, Phalipon A, Arondel J, Thirumalai K, Banerjee S, Akira S, et al. Caspase-1 activation of IL-1beta and IL-18 are essential for Shigella flexneri-induced inflammation. Immunity. 2000;12(5):581-90. Epub 2000/06/08.

101. Kahlenberg JM, Lundberg KC, Kertesy SB, Qu Y, Dubyak GR. Potentiation of caspase-1 activation by the P2X7 receptor is dependent on TLR signals and

requires NF-kappaB-driven protein synthesis. Journal of immunology. 2005;175(11):7611-22. Epub 2005/11/23.

102. Cayrol C, Girard JP. The IL-1-like cytokine IL-33 is inactivated after maturation by caspase-1. Proceedings of the National Academy of Sciences of the United States of America. 2009;106(22):9021-6. Epub 2009/05/15.

103. Luthi AU, Cullen SP, McNeela EA, Duriez PJ, Afonina IS, Sheridan C, et al. Suppression of interleukin-33 bioactivity through proteolysis by apoptotic caspases. Immunity. 2009;31(1):84-98. Epub 2009/06/30.

104. Talabot-Ayer D, Lamacchia C, Gabay C, Palmer G. Interleukin-33 is biologically active independently of caspase-1 cleavage. The Journal of biological chemistry. 2009;284(29):19420-6. Epub 2009/05/26.

105. Netea MG, van de Veerdonk FL, van der Meer JW, Dinarello CA, Joosten LA. Inflammasome-Independent Regulation of IL-1-Family Cytokines. Annual review of immunology. 2014. Epub 2014/12/11.

106. von Moltke J, Trinidad NJ, Moayeri M, Kintzer AF, Wang SB, van Rooijen N, et al. Rapid induction of inflammatory lipid mediators by the inflammasome in vivo. Nature. 2012;490(7418):107-11. Epub 2012/08/21.

107. Wu D, Choi JC, Coselli J, Shen YH, LeMaire SA. NLRP3 Inflammasome Activates Matrix Metalloproteinase-9: Potential Role in Smooth Muscle Cell Dysfunction in Thoracic Aortic Disease. Journal of Surgical Research. 2013;179(2):204.

108. Romero R, Durum S, Dinarello CA, Oyarzun E, Hobbins JC, Mitchell MD. Interleukin-1 stimulates prostaglandin biosynthesis by human amnion. Prostaglandins. 1989;37(1):13-22. Epub 1989/01/01.

109. Hertelendy F, Romero R, Molnar M, Todd H, Baldassare JJ. Cytokine-initiated signal transduction in human myometrial cells. American journal of reproductive immunology. 1993;30(2-3):49-57. Epub 1993/09/01.

110. Hertelendy F, Rastogi P, Molnar M, Romero R. Interleukin-1beta-induced prostaglandin E2 production in human myometrial cells: role of a pertussis toxin-sensitive component. American journal of reproductive immunology. 2001;45(3):142-7. Epub 2001/03/29.

111. Watari M, Watari H, DiSanto ME, Chacko S, Shi GP, Strauss JF, 3rd. Pro-inflammatory cytokines induce expression of matrix-metabolizing enzymes in human cervical smooth muscle cells. The American journal of pathology. 1999;154(6):1755-62. Epub 1999/06/11.

112. Romero R, Mazor M, Tartakovsky B. Systemic administration of interleukin-1 induces preterm parturition in mice. American journal of obstetrics and gynecology. 1991;165(4 Pt 1):969-71. Epub 1991/10/01.

113. Gravett MG, Witkin SS, Haluska GJ, Edwards JL, Cook MJ, Novy MJ. An experimental model for intraamniotic infection and preterm labor in rhesus monkeys. American journal of obstetrics and gynecology. 1994;171(6):1660-7. Epub 1994/12/01.

114. Witkin SS, Gravett MG, Haluska GJ, Novy MJ. Induction of interleukin-1 receptor antagonist in rhesus monkeys after intraamniotic infection with group B streptococci or interleukin-1 infusion. American journal of obstetrics and gynecology. 1994;171(6):1668-72. Epub 1994/12/01.

115. Baggia S, Gravett MG, Witkin SS, Haluska GJ, Novy MJ. Interleukin-1 beta intra-amniotic infusion induces tumor necrosis factor-alpha, prostaglandin production,

and preterm contractions in pregnant rhesus monkeys. Journal of the Society for Gynecologic Investigation. 1996;3(3):121-6. Epub 1996/05/01.

116. Vadillo-Ortega F, Sadowsky DW, Haluska GJ, Hernandez-Guerrero C, Guevara-Silva R, Gravett MG, et al. Identification of matrix metalloproteinase-9 in amniotic fluid and amniochorion in spontaneous labor and after experimental intrauterine infection or interleukin-1 beta infusion in pregnant rhesus monkeys. American journal of obstetrics and gynecology. 2002;186(1):128-38. Epub 2002/01/26.

117. Sadowsky DW, Adams KM, Gravett MG, Witkin SS, Novy MJ. Preterm labor is induced by intraamniotic infusions of interleukin-1beta and tumor necrosis factor-alpha but not by interleukin-6 or interleukin-8 in a nonhuman primate model. American journal of obstetrics and gynecology. 2006;195(6):1578-89. Epub 2006/11/30.

118. Aagaard K, Ganu R, Ma J, Hu M, Miller L, Jobe AH, et al. Intraamniotic interleukin-1 (IL1β) induces histological choriamnionitis and alters the microbiome in a primate model of inflammatory preterm birth. American journal of obstetrics and gynecology. 2014;208(1):S218.

119. Prince A, Ma J, Miller L, Hu M, Jobe AH, Chougnet CA, et al. Chorioamnionitis induced by intraamniotic injection of IL1, LPS or *Ureaplasma parvum* is associated with an altered microbiome in a primate model of inflammatory preterm birth. American journal of obstetrics and gynecology. 2014;212(1):S153.

120. Presicce P, Senthamaraikannan P, Alvarez M, Rueda CM, Cappelletti M, Miller LA, et al. Neutrophil recruitment and activation in decidua with intra-amniotic IL-1beta in the preterm rhesus macaque. Biology of reproduction. 2015;92(2):56. Epub 2014/12/30.

121. Gomez-Lopez N, Romero R, Plazyo O, Panaitescu B, Furcron AE, Miller D, et al. Intra-Amniotic Administration of HMGB1 Induces Spontaneous Preterm Labor and Birth. American journal of reproductive immunology. 2016;75(1):3-7. Epub 2016/01/20.

122. Santamaria-Kisiel L, Rintala-Dempsey AC, Shaw GS. Calcium-dependent and -independent interactions of the S100 protein family. The Biochemical journal. 2006;396(2):201-14. Epub 2006/05/11.

123. Donato R. RAGE: a single receptor for several ligands and different cellular responses: the case of certain S100 proteins. Current molecular medicine. 2007;7(8):711-24. Epub 2008/03/12.

124. Zhou Y, Yang W, Kirberger M, Lee HW, Ayalasomayajula G, Yang JJ. Prediction of EF-hand calcium-binding proteins and analysis of bacterial EF-hand proteins. Proteins. 2006;65(3):643-55. Epub 2006/09/19.

125. Foell D, Wittkowski H, Vogl T, Roth J. S100 proteins expressed in phagocytes: a novel group of damage-associated molecular pattern molecules. Journal of leukocyte biology. 2007;81(1):28-37. Epub 2006/09/01.

126. Donato R, Cannon BR, Sorci G, Riuzzi F, Hsu K, Weber DJ, et al. Functions of S100 proteins. Current molecular medicine. 2013;13(1):24-57. Epub 2012/07/28.

127. Odink K, Cerletti N, Bruggen J, Clerc RG, Tarcsay L, Zwadlo G, et al. Two calcium-binding proteins in infiltrate macrophages of rheumatoid arthritis. Nature. 1987;330(6143):80-2. Epub 1987/11/05.

128. Dell'Angelica EC, Schleicher CH, Santome JA. Primary structure and binding properties of calgranulin C, a novel S100-like calcium-binding protein from pig granulocytes. The Journal of biological chemistry. 1994;269(46):28929-36. Epub

1994/11/18.

129. Vogl T, Propper C, Hartmann M, Strey A, Strupat K, van den Bos C, et al. S100A12 is expressed exclusively by granulocytes and acts independently from MRP8 and MRP14. The Journal of biological chemistry. 1999;274(36):25291-6. Epub 1999/08/28.

130. Robinson MJ, Hogg N. A comparison of human S100A12 with MRP-14 (S100A9). Biochemical and biophysical research communications. 2000;275(3):865-70. Epub 2000/09/07.

131. Gottsch JD, Li Q, Ashraf F, O'Brien TP, Stark WJ, Liu SH. Cytokine-induced calgranulin C expression in keratocytes. Clinical immunology. 1999;91(1):34-40. Epub 1999/04/29.

132. Foell D, Wittkowski H, Kessel C, Luken A, Weinhage T, Varga G, et al. Proinflammatory S100A12 can activate human monocytes via Toll-like receptor 4. American journal of respiratory and critical care medicine. 2013;187(12):1324-34. Epub 2013/04/25.

133. Ingels C, Derese I, Wouters PJ, Van den Berghe G, Vanhorebeek I. Soluble RAGE and the RAGE ligands HMGB1 and S100A12 in critical illness: impact of glycemic control with insulin and relation with clinical outcome. Shock. 2015;43(2):109-16. Epub 2014/11/14.

134. Herold K, Moser B, Chen Y, Zeng S, Yan SF, Ramasamy R, et al. Receptor for advanced glycation end products (RAGE) in a dash to the rescue: inflammatory signals gone awry in the primal response to stress. Journal of leukocyte biology. 2007;82(2):204-12. Epub 2007/05/22.

135. Foell D, Kane D, Bresnihan B, Vogl T, Nacken W, Sorg C, et al. Expression of

the pro-inflammatory protein S100A12 (EN-RAGE) in rheumatoid and psoriatic arthritis. Rheumatology. 2003;42(11):1383-9. Epub 2003/07/02.

136. Hou F, Wang L, Wang H, Gu J, Li M, Zhang J, et al. Elevated gene expression of S100A12 is correlated with the predominant clinical inflammatory factors in patients with bacterial pneumonia. Molecular medicine reports. 2015;11(6):4345-52. Epub 2015/02/05.

137. Ma D, Li X, Zhang L, Deng C, Zhang T, Wang L, et al. S100A12 expression in patients with primary biliary cirrhosis. Immunological investigations. 2015;44(1):13-22. Epub 2014/10/15.

138. Sharma R, Macy S, Richardson K, Lokhnygina Y, Laskowitz DT. A blood-based biomarker panel to detect acute stroke. Journal of stroke and cerebrovascular diseases : the official journal of National Stroke Association. 2014;23(5):910-8. Epub 2013/10/15.

139. Tyden H, Lood C, Gullstrand B, Jonsen A, Nived O, Sturfelt G, et al. Increased serum levels of S100A8/A9 and S100A12 are associated with cardiovascular disease in patients with inactive systemic lupus erythematosus. Rheumatology. 2013;52(11):2048-55. Epub 2013/08/15.

140. Buhimschi IA, Zhao G, Pettker CM, Bahtiyar MO, Magloire LK, Thung S, et al. The receptor for advanced glycation end products (RAGE) system in women with intraamniotic infection and inflammation. American journal of obstetrics and gynecology. 2007;196(2):181 e1-13. Epub 2007/02/20.

141. Yamaoka M, Maeda N, Nakamura S, Mori T, Inoue K, Matsuda K, et al. Gene expression levels of S100 protein family in blood cells are associated with insulin resistance and inflammation (Peripheral blood S100 mRNAs and metabolic

syndrome). Biochemical and biophysical research communications. 2013;433(4):450-5. Epub 2013/03/19.

142. Naruse K, Sado T, Noguchi T, Tsunemi T, Yoshida S, Akasaka J, et al. Peripheral RAGE (receptor for advanced glycation endproducts)-ligands in normal pregnancy and preeclampsia: novel markers of inflammatory response. Journal of reproductive immunology. 2012;93(2):69-74. Epub 2012/03/03.

143. Buhimschi CS, Bhandari V, Han YW, Dulay AT, Baumbusch MA, Madri JA, et al. Using proteomics in perinatal and neonatal sepsis: hopes and challenges for the future. Current opinion in infectious diseases. 2009;22(3):235-43. Epub 2009/04/28.

144. Dabritz J, Foell D, Wirth S, Jenke A. Fecal S100A12: identifying intestinal distress in very-low-birth-weight infants. Journal of pediatric gastroenterology and nutrition. 2013;57(2):204-10. Epub 2013/04/04.

145. Buhimschi IA, Christner R, Buhimschi CS. Proteomic biomarker analysis of amniotic fluid for identification of intra-amniotic inflammation. BJOG : an international journal of obstetrics and gynaecology. 2005;112(2):173-81. Epub 2005/01/25.

146. Romero R, Tartakovsky B. The natural interleukin-1 receptor antagonist prevents interleukin-1-induced preterm delivery in mice. American journal of obstetrics and gynecology. 1992;167(4 Pt 1):1041-5. Epub 1992/10/01.

147. Chellan B, Yan L, Sontag TJ, Reardon CA, Hofmann Bowman MA. IL-22 is induced by S100/calgranulin and impairs cholesterol efflux in macrophages by downregulating ABCG1. Journal of lipid research. 2014;55(3):443-54. Epub 2013/12/25.

148. Cunden LS, Gaillard A, Nolan EM. Calcium Ions Tune the Zinc-Sequestering Properties and Antimicrobial Activity of Human S100A12. Chemical science (Royal Society of Chemistry : 2010). 2016;7(2):1338-48.

149. Haley KP, Delgado AG, Piazuelo MB, Mortensen BL, Correa P, Damo SM, et al. The Human Antimicrobial Protein Calgranulin C Participates in Control of Helicobacter pylori Growth and Regulation of Virulence. Infection and immunity. 2015;83(7):2944-56. Epub 2015/05/13.

150. Foell D, Wittkowski H, Kessel C, Lüken A, Weinhage T, Varga G, et al. Proinflammatory S100A12 Can Activate Human Monocytes via Toll-like Receptor 4. American journal of respiratory and critical care medicine. 2013;187(12):1324-34.

151. Cogswell JP, Godlevski MM, Wisely GB, Clay WC, Leesnitzer LM, Ways JP, et al. NF-kappa B regulates IL-1 beta transcription through a consensus NF-kappa B binding site and a nonconsensus CRE-like site. Journal of immunology. 1994;153(2):712-23. Epub 1994/07/15.

152. http://www.bu.edu/nf-kb/gene-resources/target-genes/. Boston University Biology.

153. Park JH, Kim YG, McDonald C, Kanneganti TD, Hasegawa M, Body-Malapel M, et al. RICK/RIP2 mediates innate immune responses induced through Nod1 and Nod2 but not TLRs. Journal of immunology. 2007;178(4):2380-6. Epub 2007/02/06.

154. Li J, Schmidt AM. Characterization and functional analysis of the promoter of RAGE, the receptor for advanced glycation end products. The Journal of biological chemistry. 1997;272(26):16498-506. Epub 1997/06/27.

155. Wang T, Lafuse WP, Zwilling BS. NFkappaB and Sp1 elements are necessary for maximal transcription of toll-like receptor 2 induced by Mycobacterium avium. Journal of immunology. 2001;167(12):6924-32. Epub 2001/12/12.

156. Abderrazak A, Syrovets T, Couchie D, El Hadri K, Friguet B, Simmet T, et al. NLRP3 inflammasome: From a danger signal sensor to a regulatory node of oxidative stress and inflammatory diseases. Redox Biology. 2015;4:296-307.

157. Allport VC, Pieber D, Slater DM, Newton R, White JO, Bennett PR. Human labour is associated with nuclear factor-kappaB activity which mediates cyclo-oxygenase-2 expression and is involved with the 'functional progesterone withdrawal'. Molecular human reproduction. 2001;7(6):581-6. Epub 2001/06/01.

158. Soloff MS, Cook DL, Jr., Jeng YJ, Anderson GD. In situ analysis of interleukin-1-induced transcription of cox-2 and il-8 in cultured human myometrial cells. Endocrinology. 2004;145(3):1248-54. Epub 2003/12/03.

159. Martillo MA, Nazzal L, Crittenden DB. The Crystallization of Monosodium Urate. Current rheumatology reports. 2014;16(2):400-.

160. Grassi W, De Angelis R. Clinical features of gout. Reumatismo. 2011;63(4):238-45. Epub 2012/02/04.

161. Laughon SK, Catov J, Powers RW, Roberts JM, Gandley RE. First trimester uric acid and adverse pregnancy outcomes. American journal of hypertension. 2011;24(4):489-95. Epub 2011/01/22.

162. Roberts JM, Bodnar LM, Lain KY, Hubel CA, Markovic N, Ness RB, et al. Uric acid is as important as proteinuria in identifying fetal risk in women with gestational hypertension. Hypertension. 2005;46(6):1263-9. Epub 2005/10/26.

163. Hawkins TL, Roberts JM, Mangos GJ, Davis GK, Roberts LM, Brown MA.

Plasma uric acid remains a marker of poor outcome in hypertensive pregnancy: a retrospective cohort study. BJOG : an international journal of obstetrics and gynaecology. 2012;119(4):484-92. Epub 2012/01/19.

164. Vazquez-Rodriguez JG, Rico-Trejo EI. [Role of uric acid in preeclampsia-eclampsia]. Ginecologia y obstetricia de Mexico. 2011;79(5):292-7. Epub 2011/10/05. Papel del acido urico en la preeclampsia-eclampsia.

165. Amini E, Sheikh M, Hantoushzadeh S, Shariat M, Abdollahi A, Kashanian M. Maternal hyperuricemia in normotensive singleton pregnancy, a prenatal finding with continuous perinatal and postnatal effects, a prospective cohort study. BMC pregnancy and childbirth. 2014;14:104. Epub 2014/03/19.

166. Gao T, Zablith NR, Burns DH, Skinner CD, Koski KG. Second trimester amniotic fluid transferrin and uric acid predict infant birth outcomes. Prenatal diagnosis. 2008;28(9):810-4. Epub 2008/07/23.

167. Washburn LK, Nixon PA, Russell GB, Snively BM, O'Shea TM. Preterm Birth Is Associated with Higher Uric Acid Levels in Adolescents. The Journal of pediatrics. 2015;167(1):76-80. Epub 2015/04/15.

168. Girard S, Heazell AE, Derricott H, Allan SM, Sibley CP, Abrahams VM, et al. Circulating cytokines and alarmins associated with placental inflammation in high-risk pregnancies. American journal of reproductive immunology. 2014;72(4):422-34. Epub 2014/05/29.

169. Eleftheriadis T, Pissas G, Antoniadi G, Makri P, Liakopoulos V, Stefanidis I. Urate crystals induce NLRP3 inflammasome-dependent IL-1beta secretion and proliferation in isolated primary human T-cells. Hippokratia. 2015;19(1):41-6. Epub 2015/10/06.

170. Gicquel T, Robert S, Loyer P, Victoni T, Bodin A, Ribault C, et al. IL-1beta production is dependent on the activation of purinergic receptors and NLRP3 pathway in human macrophages. FASEB journal : official publication of the Federation of American Societies for Experimental Biology. 2015;29(10):4162-73. Epub 2015/06/28.

171. Wu J, Yan Z, Schwartz DE, Yu J, Malik AB, Hu G. Activation of NLRP3 inflammasome in alveolar macrophages contributes to mechanical stretch-induced lung inflammation and injury. Journal of immunology. 2013;190(7):3590-9. Epub 2013/02/26.

172. Licandro G, Ling Khor H, Beretta O, Lai J, Derks H, Laudisi F, et al. The NLRP3 inflammasome affects DNA damage responses after oxidative and genotoxic stress in dendritic cells. European journal of immunology. 2013;43(8):2126-37. Epub 2013/04/27.

173. Zheng SC, Zhu XX, Xue Y, Zhang LH, Zou HJ, Qiu JH, et al. Role of the NLRP3 inflammasome in the transient release of IL-1beta induced by monosodium urate crystals in human fibroblast-like synoviocytes. Journal of inflammation. 2015;12:30. Epub 2015/04/22.

174. Jhang JJ, Cheng YT, Ho CY, Yen GC. Monosodium urate crystals trigger Nrf2- and heme oxygenase-1-dependent inflammation in THP-1 cells. Cellular & molecular immunology. 2015;12(4):424-34. Epub 2014/08/12.

175. Mulla MJ, Salmon JE, Chamley LW, Brosens JJ, Boeras CM, Kavathas PB, et al. A role for uric acid and the Nalp3 inflammasome in antiphospholipid antibody-induced IL-1beta production by human first trimester trophoblast. PloS one. 2013;8(6):e65237. Epub 2013/06/14.

176. Mulla MJ, Myrtolli K, Potter J, Boeras C, Kavathas PB, Sfakianaki AK, et al. Uric acid induces trophoblast IL-1beta production via the inflammasome: implications for the pathogenesis of preeclampsia. American journal of reproductive immunology. 2011;65(6):542-8. Epub 2011/03/01.

177. Xiao J, Fu C, Zhang X, Zhu D, Chen W, Lu Y, et al. Soluble monosodium urate, but not its crystal, induces toll like receptor 4-dependent immune activation in renal mesangial cells. Molecular Immunology. 2015;66(2):310-8.

178. Chen DP, Wong CK, Tam LS, Li EK, Lam CWK. Activation of human fibroblast-like synoviocytes by uric acid crystals in rheumatoid arthritis. Cellular & molecular immunology. 2011;8(6):469-78.

179. Xiao J, Zhang XL, Fu C, Han R, Chen W, Lu Y, et al. Soluble uric acid increases NALP3 inflammasome and interleukin-1beta expression in human primary renal proximal tubule epithelial cells through the Toll-like receptor 4-mediated pathway. International journal of molecular medicine. 2015;35(5):1347-54. Epub 2015/03/31.

180. Romero R, Espinoza J, Kusanovic JP, Gotsch F, Hassan S, Erez O, et al. The preterm parturition syndrome. BJOG : an international journal of obstetrics and gynaecology. 2006;113 Suppl 3:17-42. Epub 2007/01/09.

181. Mayer MP, Bukau B. Hsp70 chaperones: Cellular functions and molecular mechanism. Cellular and Molecular Life Sciences. 2005;62(6):670-84.

182. Asea A. Chaperokine-Induced Signal Transduction Pathways. Exercise immunology review. 2003;9:25-33.

183. Calderwood SK, Mambula SS, Gray PJ, Jr., Theriault JR. Extracellular heat shock proteins in cell signaling. FEBS letters. 2007;581(19):3689-94. Epub

2007/05/15.

184. Samborski P, Grzymislawski M. The Role of HSP70 Heat Shock Proteins in the Pathogenesis and Treatment of Inflammatory Bowel Diseases. Advances in clinical and experimental medicine : official organ Wroclaw Medical University. 2015;24(3):525-30. Epub 2015/10/16.

185. Banecka-Majkutewicz Z, Grabowski M, Kadzinski L, Papkov A, Wegrzyn A, Banecki B. Increased levels of antibodies against heat shock proteins in stroke patients. Acta biochimica Polonica. 2014;61(2):379-83. Epub 2014/06/07.

186. Yadav AK, Kumar V, Jha V. Heat shock proteins 60 and 70 specific proinflammatory and cytotoxic response of CD4+CD28null cells in chronic kidney disease. Mediators of inflammation. 2013;2013:384807. Epub 2013/12/19.

187. Alexiou GA, Karamoutsios A, Lallas G, Ragos V, Goussia A, Kyritsis AP, et al. Expression of heat shock proteins in brain tumors. Turkish neurosurgery. 2014;24(5):745-9. Epub 2014/10/01.

188. Srivastava K, Narang R, Bhatia J, Saluja D. Expression of Heat Shock Protein 70 Gene and Its Correlation with Inflammatory Markers in Essential Hypertension. PloS one. 2016;11(3):e0151060. Epub 2016/03/19.

189. Mathur S, Walley KR, Wang Y, Indrambarya T, Boyd JH. Extracellular heat shock protein 70 induces cardiomyocyte inflammation and contractile dysfunction via TLR2. Circulation journal : official journal of the Japanese Circulation Society. 2011;75(10):2445-52. Epub 2011/08/06.

190. Martin-Murphy BV, Holt MP, Ju C. The role of damage associated molecular pattern molecules in acetaminophen-induced liver injury in mice. Toxicology letters. 2010;192(3):387-94. Epub 2009/11/26.

191. Chaiworapongsa T, Erez O, Kusanovic JP, Vaisbuch E, Mazaki-Tovi S, Gotsch F, et al. Amniotic fluid heat shock protein 70 concentration in histologic chorioamnionitis, term and preterm parturition. The journal of maternal-fetal & neonatal medicine : the official journal of the European Association of Perinatal Medicine, the Federation of Asia and Oceania Perinatal Societies, the International Society of Perinatal Obstet. 2008;21(7):449-61. Epub 2008/06/24.

192. Chang A, Zhang Z, Jia L, Zhang L, Gao Y, Zhang L. Alteration of heat shock protein 70 expression levels in term and preterm delivery. The journal of maternal-fetal & neonatal medicine : the official journal of the European Association of Perinatal Medicine, the Federation of Asia and Oceania Perinatal Societies, the International Society of Perinatal Obstet. 2013;26(16):1581-5. Epub 2013/04/16.

193. Pozo E, Mesa F, Ikram MH, Puertas A, Torrecillas-Martinez L, Ortega-Oller I, et al. Preterm birth and/or low birth weight are associated with periodontal disease and the increased placental immunohistochemical expression of inflammatory markers. Histology and histopathology. 2016;31(2):231-7. Epub 2015/10/03.

194. Timmermans K, Kox M, Vaneker M, van den Berg M, John A, van Laarhoven A, et al. Plasma levels of danger-associated molecular patterns are associated with immune suppression in trauma patients. Intensive care medicine. 2016;42(4):551-61. Epub 2016/02/26.

195. Prakken BJ, Wendling U, van der Zee R, Rutten VP, Kuis W, van Eden W. Induction of IL-10 and inhibition of experimental arthritis are specific features of microbial heat shock proteins that are absent for other evolutionarily conserved immunodominant proteins. Journal of immunology. 2001;167(8):4147-53. Epub

2001/10/10.

196. Borges TJ, Wieten L, van Herwijnen MJC, Broere F, van der Zee R, Bonorino C, et al. The anti-inflammatory mechanisms of Hsp70. Frontiers in Immunology. 2012;3:95.

197. Genc MR, Karasahin E, Onderdonk AB, Bongiovanni AM, Delaney ML, Witkin SS, et al. Association between vaginal 70-kd heat shock protein, interleukin-1 receptor antagonist, and microbial flora in mid trimester pregnant women. American journal of obstetrics and gynecology. 2005;192(3):916-21. Epub 2005/03/05.

198. van Eden W, Spiering R, Broere F, van der Zee R. A case of mistaken identity: HSPs are no DAMPs but DAMPERs. Cell stress & chaperones. 2012;17(3):281-92. Epub 2011/12/06.

199. Krause M, Heck TG, Bittencourt A, Scomazzon SP, Newsholme P, Curi R, et al. The chaperone balance hypothesis: the importance of the extracellular to intracellular HSP70 ratio to inflammation-driven type 2 diabetes, the effect of exercise, and the implications for clinical management. Mediators of inflammation. 2015;2015:249205. Epub 2015/03/31.

200. Wang R, Kovalchin JT, Muhlenkamp P, Chandawarkar RY. Exogenous heat shock protein 70 binds macrophage lipid raft microdomain and stimulates phagocytosis, processing, and MHC-II presentation of antigens. Blood. 2005;107(4):1636-42.

201. Asea A, Kraeft SK, Kurt-Jones EA, Stevenson MA, Chen LB, Finberg RW, et al. HSP70 stimulates cytokine production through a CD14-dependant pathway, demonstrating its dual role as a chaperone and cytokine. Nature medicine.

2000;6(4):435-42. Epub 2000/03/31.

202. Luong M, Zhang Y, Chamberlain T, Zhou T, Wright JF, Dower K, et al. Stimulation of TLR4 by recombinant HSP70 requires structural integrity of the HSP70 protein itself. Journal of inflammation. 2012;9:11. Epub 2012/03/28.

203. Johnson AD, Berberian PA, Tytell M, Bond MG. Differential distribution of 70-kD heat shock protein in atherosclerosis. Its potential role in arterial SMC survival. Arteriosclerosis, thrombosis, and vascular biology. 1995;15(1):27-36. Epub 1995/01/01.

204. Wachstein J, Tischer S, Figueiredo C, Limbourg A, Falk C, Immenschuh S, et al. HSP70 Enhances Immunosuppressive Function of CD4⁺CD25⁺FoxP3⁺ T Regulatory Cells and Cytotoxicity in CD4⁺CD25[?] T Cells. PloS one. 2012;7(12):e51747.

205. Lukens JR, Gross JM, Calabrese C, Iwakura Y, Lamkanfi M, Vogel P, et al. Critical role for inflammasome-independent IL-1beta production in osteomyelitis. Proceedings of the National Academy of Sciences of the United States of America. 2014;111(3):1066-71. Epub 2014/01/08.

206. Netea MG, van de Veerdonk FL, van der Meer JW, Dinarello CA, Joosten LA. Inflammasome-independent regulation of IL-1-family cytokines. Annual review of immunology. 2015;33:49-77. Epub 2014/12/11.

207. Provoost S, Maes T, Pauwels NS, Vanden Berghe T, Vandenabeele P, Lambrecht BN, et al. NLRP3/caspase-1-independent IL-1beta production mediates diesel exhaust particle-induced pulmonary inflammation. Journal of immunology. 2011;187(6):3331-7. Epub 2011/08/17.

208. Mayer-Barber KD, Barber DL, Shenderov K, White SD, Wilson MS, Cheever A, et al. Caspase-1 independent IL-1beta production is critical for host resistance to mycobacterium tuberculosis and does not require TLR signaling in vivo. Journal of immunology. 2010;184(7):3326-30. Epub 2010/03/05.

209. Gomez-Lopez N, Romero R, Plazyo O, Panaitescu B, Furcron AE, Miller D, et al. Intra-amniotic administration of HMGB1 induces spontaneous preterm labor and birth American journal of reproductive immunology. 2015:In press.

210. Topping V, Romero R, Than NG, Tarca AL, Xu Z, Kim SY, et al. Interleukin-33 in the human placenta. The journal of maternal-fetal & neonatal medicine : the official journal of the European Association of Perinatal Medicine, the Federation of Asia and Oceania Perinatal Societies, the International Society of Perinatal Obstet. 2013;26(4):327-38. Epub 2012/10/09.

211. Kim CJ, Romero R, Chaemsaithong P, Chaiyasit N, Yoon BH, Kim YM. Acute chorioamnionitis and funisitis: definition, pathologic features, and clinical significance. American journal of obstetrics and gynecology. 2015;213(4 Suppl):S29-52. Epub 2015/10/03.

212. Bourgeois E, Van LP, Samson M, Diem S, Barra A, Roga S, et al. The pro-Th2 cytokine IL-33 directly interacts with invariant NKT and NK cells to induce IFN-gamma production. European journal of immunology. 2009;39(4):1046-55. Epub 2009/03/07.

213. Smithgall MD, Comeau MR, Yoon BR, Kaufman D, Armitage R, Smith DE. IL-33 amplifies both Th1- and Th2-type responses through its activity on human basophils, allergen-reactive Th2 cells, iNKT and NK cells. International immunology. 2008;20(8):1019-30. Epub 2008/06/14.

214. Kitamura H, Iwakabe K, Yahata T, Nishimura S, Ohta A, Ohmi Y, et al. The natural killer T (NKT) cell ligand alpha-galactosylceramide demonstrates its immunopotentiating effect by inducing interleukin (IL)-12 production by dendritic cells and IL-12 receptor expression on NKT cells. The Journal of experimental medicine. 1999;189(7):1121-8. Epub 1999/04/06.

215. Tomura M, Yu WG, Ahn HJ, Yamashita M, Yang YF, Ono S, et al. A novel function of Valpha14+CD4+NKT cells: stimulation of IL-12 production by antigen-presenting cells in the innate immune system. Journal of immunology. 1999;163(1):93-101. Epub 1999/06/29.

216. Fujii S, Shimizu K, Kronenberg M, Steinman RM. Prolonged IFN-gamma-producing NKT response induced with alpha-galactosylceramide-loaded DCs. Nature immunology. 2002;3(9):867-74. Epub 2002/08/03.

217. Brigl M, Bry L, Kent SC, Gumperz JE, Brenner MB. Mechanism of CD1d-restricted natural killer T cell activation during microbial infection. Nature immunology. 2003;4(12):1230-7. Epub 2003/10/28.

218. Oki S, Chiba A, Yamamura T, Miyake S. The clinical implication and molecular mechanism of preferential IL-4 production by modified glycolipid-stimulated NKT cells. The Journal of clinical investigation. 2004;113(11):1631-40. Epub 2004/06/03.

219. Sag D, Krause P, Hedrick CC, Kronenberg M, Wingender G. IL-10-producing NKT10 cells are a distinct regulatory invariant NKT cell subset. The Journal of clinical investigation. 2014;124(9):3725-40. Epub 2014/07/26.

220. Bendelac A, Savage PB, Teyton L. The biology of NKT cells. Annual review of immunology. 2007;25(0):297-336. Epub 2006/12/08.

221. Kawano T, Cui J, Koezuka Y, Toura I, Kaneko Y, Motoki K, et al. CD1d-restricted and TCR-mediated activation of valpha14 NKT cells by glycosylceramides. Science. 1997;278(5343):1626-9. Epub 1997/12/31.

222. Sidobre S, Naidenko OV, Sim BC, Gascoigne NR, Garcia KC, Kronenberg M. The V alpha 14 NKT cell TCR exhibits high-affinity binding to a glycolipid/CD1d complex. Journal of immunology. 2002;169(3):1340-8. Epub 2002/07/23.

223. Lehmann JM, Moore LB, Smith-Oliver TA, Wilkison WO, Willson TM, Kliewer SA. An antidiabetic thiazolidinedione is a high affinity ligand for peroxisome proliferator-activated receptor gamma (PPAR gamma). The Journal of biological chemistry. 1995;270(22):12953-6. Epub 1995/06/02.

224. Ricote M, Li AC, Willson TM, Kelly CJ, Glass CK. The peroxisome proliferator-activated receptor-gamma is a negative regulator of macrophage activation. Nature. 1998;391(6662):79-82. Epub 1998/01/09.

225. Chinetti G, Griglio S, Antonucci M, Torra IP, Delerive P, Majd Z, et al. Activation of proliferator-activated receptors alpha and gamma induces apoptosis of human monocyte-derived macrophages. The Journal of biological chemistry. 1998;273(40):25573-80.

226. Delerive P, Martin-Nizard F, Chinetti G, Trottein F, Fruchart JC, Najib J, et al. Peroxisome proliferator-activated receptor activators inhibit thrombin-induced endothelin-1 production in human vascular endothelial cells by inhibiting the activator protein-1 signaling pathway. Circulation research. 1999;85(5):394-402. Epub 1999/09/04.

227. McCarthy FP, Delany AC, Kenny LC, Walsh SK. PPAR-gamma -- a possible drug target for complicated pregnancies. British journal of pharmacology.

2013;168(5):1074-85. Epub 2012/11/29.

228. Forman BM, Tontonoz P, Chen J, Brun RP, Spiegelman BM, Evans RM. 15-Deoxy-delta 12, 14-prostaglandin J2 is a ligand for the adipocyte determination factor PPAR gamma. Cell. 1995;83(5):803-12. Epub 1995/12/01.

229. Kliewer SA, Lenhard JM, Willson TM, Patel I, Morris DC, Lehmann JM. A prostaglandin J2 metabolite binds peroxisome proliferator-activated receptor gamma and promotes adipocyte differentiation. Cell. 1995;83(5):813-9. Epub 1995/12/01.

230. Pirianov G, Waddington SN, Lindstrom TM, Terzidou V, Mehmet H, Bennett PR. The cyclopentenone 15-deoxy-delta 12,14-prostaglandin J(2) delays lipopolysaccharide-induced preterm delivery and reduces mortality in the newborn mouse. Endocrinology. 2009;150(2):699-706. Epub 2008/10/11.

231. Arenas-Hernandez M, Sanchez-Rodriguez EN, Mial NT, Robertson SA, Gomez-Lopez N. Isolation of leukocytes from the murine tissues at the maternal-fetal interface. J Vis Exp. 2015;99(0):e52866.

232. ACOG Practice Bulletin Number 49, December 2003: Dystocia and augmentation of labor. Obstetrics and gynecology. 2003;102(6):1445-54. Epub 2003/12/10.

233. Redline RW. Placental pathology: a systematic approach with clinical correlations. Placenta. 2008;29 Suppl A:S86-91. Epub 2007/10/24.

234. Kim CJ, Romero R, Kusanovic JP, Yoo W, Dong Z, Topping V, et al. The frequency, clinical significance, and pathological features of chronic chorioamnionitis: a lesion associated with spontaneous preterm birth. Modern pathology : an official journal of the United States and Canadian Academy of Pathology, Inc. 2010;23(7):1000-11. Epub 2010/03/30.

235. Xu Y, Plazyo O, Romero R, Hassan SS, Gomez-Lopez N. Isolation of leukocytes from the human maternal-fetal interface. J Vis Exp. 2015;99:e52863.

236. Rochelson BL, Schulman H, Fleischer A, Farmakides G, Bracero L, Ducey J, et al. The clinical significance of Doppler umbilical artery velocimetry in the small for gestational age fetus. American journal of obstetrics and gynecology. 1987;156(5):1223-6. Epub 1987/05/01.

237. Schulman H. The clinical implications of Doppler ultrasound analysis of the uterine and umbilical arteries. American journal of obstetrics and gynecology. 1987;156(4):889-93. Epub 1987/04/01.

238. ACOG technical bulletin. Fetal heart rate patterns: monitoring, interpretation, and management. Number 207--July 1995 (replaces No. 132, September 1989). International journal of gynaecology and obstetrics: the official organ of the International Federation of Gynaecology and Obstetrics. 1995;51(1):65-74. Epub 1995/10/01.

239. Electronic fetal heart rate monitoring: research guidelines for interpretation. The National Institute of Child Health and Human Development Research Planning Workshop. Journal of obstetric, gynecologic, and neonatal nursing : JOGNN / NAACOG. 1997;26(6):635-40. Epub 1997/12/13.

240. Boyson JE, Nagarkatti N, Nizam L, Exley MA, Strominger JL. Gestation stage-dependent mechanisms of invariant natural killer T cell-mediated pregnancy loss. Proceedings of the National Academy of Sciences of the United States of America. 2006;103(12):4580-5.

241. Ito K, Karasawa M, Kawano T, Akasaka T, Koseki H, Akutsu Y, et al. Involvement of decidual Valpha14 NKT cells in abortion. Proceedings of the

National Academy of Sciences of the United States of America. 2000;97(2):740-4.

242. Szatmari I, Gogolak P, Im JS, Dezso B, Rajnavolgyi E, Nagy L. Activation of PPARgamma specifies a dendritic cell subtype capable of enhanced induction of iNKT cell expansion. Immunity. 2004;21(1):95-106.

243. Frohnert BI, Hui TY, Bernlohr DA. Identification of a functional peroxisome proliferator-responsive element in the murine fatty acid transport protein gene. The Journal of biological chemistry. 1999;274(7):3970-7. Epub 1999/02/06.

244. Chiu YH, Jayawardena J, Weiss A, Lee D, Park SH, Dautry-Varsat A, et al. Distinct subsets of CD1d-restricted T cells recognize self-antigens loaded in different cellular compartments. The Journal of experimental medicine. 1999;189(1):103-10. Epub 1999/01/05.

245. Crowe NY, Coquet JM, Berzins SP, Kyparissoudis K, Keating R, Pellicci DG, et al. Differential antitumor immunity mediated by NKT cell subsets in vivo. The Journal of experimental medicine. 2005;202(9):1279-88. Epub 2005/11/09.

246. Terabe M, Swann J, Ambrosino E, Sinha P, Takaku S, Hayakawa Y, et al. A nonclassical non-Valpha14Jalpha18 CD1d-restricted (type II) NKT cell is sufficient for down-regulation of tumor immunosurveillance. The Journal of experimental medicine. 2005;202(12):1627-33. Epub 2005/12/21.

247. Zheng Q, Zhou L, Mi QS. MicroRNA miR-150 is involved in Valpha14 invariant NKT cell development and function. Journal of immunology. 2012;188(5):2118-26. Epub 2012/01/31.

248. Taniguchi M, Seino K, Nakayama T. The NKT cell system: bridging innate and acquired immunity. Nature immunology. 2003;4(12):1164-5. Epub 2003/11/26.

249. Carnaud C, Lee D, Donnars O, Park SH, Beavis A, Koezuka Y, et al. Cutting edge: Cross-talk between cells of the innate immune system: NKT cells rapidly activate NK cells. Journal of immunology. 1999;163(9):4647-50.

250. Singh N, Hong S, Scherer DC, Serizawa I, Burdin N, Kronenberg M, et al. Cutting edge: activation of NK T cells by CD1d and alpha-galactosylceramide directs conventional T cells to the acquisition of a Th2 phenotype. Journal of immunology. 1999;163(5):2373-7. Epub 1999/08/24.

251. Nishimura T, Kitamura H, Iwakabe K, Yahata T, Ohta A, Sato M, et al. The interface between innate and acquired immunity: glycolipid antigen presentation by CD1d-expressing dendritic cells to NKT cells induces the differentiation of antigen-specific cytotoxic T lymphocytes. International immunology. 2000;12(7):987-94. Epub 2000/07/06.

252. Kitamura H, Ohta A, Sekimoto M, Sato M, Iwakabe K, Nakui M, et al. alpha-galactosylceramide induces early B-cell activation through IL-4 production by NKT cells. Cellular immunology. 2000;199(1):37-42. Epub 2000/02/17.

253. Wang H, Feng D, Park O, Yin S, Gao B. Invariant NKT cell activation induces neutrophil accumulation and hepatitis: opposite regulation by IL-4 and IFN-gamma. Hepatology. 2013;58(4):1474-85. Epub 2013/05/21.

254. Fujii S, Shimizu K, Smith C, Bonifaz L, Steinman RM. Activation of natural killer T cells by alpha-galactosylceramide rapidly induces the full maturation of dendritic cells in vivo and thereby acts as an adjuvant for combined CD4 and CD8 T cell immunity to a coadministered protein. The Journal of experimental medicine. 2003;198(2):267-79. Epub 2003/07/23.

255. Xue J, Schmidt SV, Sander J, Draffehn A, Krebs W, Quester I, et al.

Transcriptome-based network analysis reveals a spectrum model of human macrophage activation. Immunity. 2014;40(2):274-88. Epub 2014/02/18.

256. Murray PJ, Allen JE, Biswas SK, Fisher EA, Gilroy DW, Goerdt S, et al. Macrophage activation and polarization: nomenclature and experimental guidelines. Immunity. 2014;41(1):14-20. Epub 2014/07/19.

257. Mills CD, Kincaid K, Alt JM, Heilman MJ, Hill AM. M-1/M-2 macrophages and the Th1/Th2 paradigm. Journal of immunology. 2000;164(12):6166-73. Epub 2000/06/08.

258. Mantovani A, Sozzani S, Locati M, Allavena P, Sica A. Macrophage polarization: tumor-associated macrophages as a paradigm for polarized M2 mononuclear phagocytes. Trends in immunology. 2002;23(11):549-55. Epub 2002/10/29.

259. Biswas SK, Mantovani A. Macrophage plasticity and interaction with lymphocyte subsets: cancer as a paradigm. Nature immunology. 2010;11(10):889-96. Epub 2010/09/22.

260. Sica A, Mantovani A. Macrophage plasticity and polarization: in vivo veritas. The Journal of clinical investigation. 2012;122(3):787-95. Epub 2012/03/02.

261. Ellis TN, Beaman BL. Murine polymorphonuclear neutrophils produce interferon-gamma in response to pulmonary infection with Nocardia asteroides. Journal of leukocyte biology. 2002;72(2):373-81. Epub 2002/08/01.

262. Ethuin F, Gerard B, Benna JE, Boutten A, Gougereot-Pocidalo MA, Jacob L, et al. Human neutrophils produce interferon gamma upon stimulation by interleukin-12. Laboratory investigation; a journal of technical methods and pathology. 2004;84(10):1363-71. Epub 2004/06/29.

263. Boyson JE, Rybalov B, Koopman LA, Exley M, Balk SP, Racke FK, et al. CD1d

and invariant NKT cells at the human maternal-fetal interface. Proceedings of the National Academy of Sciences of the United States of America. 2002;99(21):13741-6.

264. Romero R, Miranda J, Chaemsaithong P, Chaiworapongsa T, Kusanovic JP, Dong Z, et al. Sterile and microbial-associated intra-amniotic inflammation in preterm prelabor rupture of membranes. The journal of maternal-fetal & neonatal medicine : the official journal of the European Association of Perinatal Medicine, the Federation of Asia and Oceania Perinatal Societies, the International Society of Perinatal Obstet. 2015;28(12):1394-409. Epub 2014/09/06.

265. Li LP, Fang YC, Dong GF, Lin Y, Saito S. Depletion of invariant NKT cells reduces inflammation-induced preterm delivery in mice. Journal of immunology. 2012;188(9):4681-9. Epub 2012/04/03.

266. Li L, Yang J, Jiang Y, Tu J, Schust DJ. Activation of decidual invariant natural killer T cells promotes lipopolysaccharide-induced preterm birth. Molecular human reproduction. 2015;21(4):369-81. Epub 2015/01/16.

267. Mattner J, Debord KL, Ismail N, Goff RD, Cantu C, 3rd, Zhou D, et al. Exogenous and endogenous glycolipid antigens activate NKT cells during microbial infections. Nature. 2005;434(7032):525-9. Epub 2005/03/26.

268. Aluvihare VR, Kallikourdis M, Betz AG. Regulatory T cells mediate maternal tolerance to the fetus. Nature immunology. 2004;5(3):266-71.

269. Rowe JH, Ertelt JM, Xin L, Way SS. Pregnancy imprints regulatory memory that sustains anergy to fetal antigen. Nature. 2012;490(7418):102-6.

270. Shima T, Sasaki Y, Itoh M, Nakashima A, Ishii N, Sugamura K, et al. Regulatory T cells are necessary for implantation and maintenance of early pregnancy but

not late pregnancy in allogeneic mice. Journal of reproductive immunology. 2010;85(2):121-9. Epub 2010/05/05.

271. Wang ML, Dorer DJ, Fleming MP, Catlin EA. Clinical outcomes of near-term infants. Pediatrics. 2004;114(2):372-6. Epub 2004/08/03.

272. Raju TN, Higgins RD, Stark AR, Leveno KJ. Optimizing care and outcome for late-preterm (near-term) infants: a summary of the workshop sponsored by the National Institute of Child Health and Human Development. Pediatrics. 2006;118(3):1207-14. Epub 2006/09/05.

273. Pellicci DG, Hammond KJ, Uldrich AP, Baxter AG, Smyth MJ, Godfrey DI. A natural killer T (NKT) cell developmental pathway iInvolving a thymus-dependent NK1.1(-)CD4(+) CD1d-dependent precursor stage. The Journal of experimental medicine. 2002;195(7):835-44. Epub 2002/04/03.

274. Dunn-Albanese LR, Ackerman WEt, Xie Y, Iams JD, Kniss DA. Reciprocal expression of peroxisome proliferator-activated receptor-gamma and cyclooxygenase-2 in human term parturition. American journal of obstetrics and gynecology. 2004;190(3):809-16. Epub 2004/03/26.

275. Mial NT, Kadam L, Romero R, Drewlo S, Gomez-Lopez N. Rosiglitazone treatment rapidly controls the systemic pro-inflammatory response and reduces the rate of infection-induced preterm birth. Reprod Sci. 2015;22(Suppl 1):137A.

276. Crowe NY, Uldrich AP, Kyparissoudis K, Hammond KJ, Hayakawa Y, Sidobre S, et al. Glycolipid antigen drives rapid expansion and sustained cytokine production by NK T cells. Journal of immunology. 2003;171(8):4020-7. Epub 2003/10/08.

277. Szatmari I, Pap A, Ruhl R, Ma JX, Illarionov PA, Besra GS, et al. PPARgamma

controls CD1d expression by turning on retinoic acid synthesis in developing human dendritic cells. The Journal of experimental medicine. 2006;203(10):2351-62. Epub 2006/09/20.

278. Brossay L, Jullien D, Cardell S, Sydora BC, Burdin N, Modlin RL, et al. Mouse CD1 is mainly expressed on hemopoietic-derived cells. Journal of immunology. 1997;159(3):1216-24. Epub 1997/08/01.

279. Roark JH, Park SH, Jayawardena J, Kavita U, Shannon M, Bendelac A. CD1.1 expression by mouse antigen-presenting cells and marginal zone B cells. Journal of immunology. 1998;160(7):3121-7. Epub 1998/04/08.

280. Bendelac A. Positive selection of mouse NK1+ T cells by CD1-expressing cortical thymocytes. The Journal of experimental medicine. 1995;182(6):2091-6. Epub 1995/12/01.

281. Gomez-Lopez N, Guilbert LJ, Olson DM. Invasion of the leukocytes into the fetal-maternal interface during pregnancy. Journal of leukocyte biology. 2010;88(4):625-33. Epub 2010/06/04.

282. Gomez-Lopez N, StLouis D, Lehr MA, Sanchez-Rodriguez EN, Arenas-Hernandez M. Immune cells in term and preterm labor. Cellular & molecular immunology. 2014. Epub 2014/06/24.

283. Arenas-Hernandez M, Romero R, St Louis D, Hassan SS, Kaye EB, Gomez-Lopez N. An imbalance between innate and adaptive immune cells at the maternal-fetal interface occurs prior to endotoxin-induced preterm birth. Cellular & molecular immunology. 2015:In press. Epub 2015/04/08.

284. Bizargity P, Del Rio R, Phillippe M, Teuscher C, Bonney EA. Resistance to lipopolysaccharide-induced preterm delivery mediated by regulatory T cell

function in mice. Biology of reproduction. 2009;80(5):874-81. Epub 2009/01/16.

285. Gomez-Lopez N, Olson DM, Robertson SA. Interleukin-6 controls uterine Th9 cells and CD8 T regulatory cells to accelerate parturition in mice. Immunology and cell biology. 2015. Epub 2015/06/16.

286. Marx N, Kehrle B, Kohlhammer K, Grub M, Koenig W, Hombach V, et al. PPAR activators as antiinflammatory mediators in human T lymphocytes: implications for atherosclerosis and transplantation-associated arteriosclerosis. Circulation research. 2002;90(6):703-10.

287. Yang XY, Wang LH, Chen T, Hodge DR, Resau JH, DaSilva L, et al. Activation of human T lymphocytes is inhibited by peroxisome proliferator-activated receptor gamma (PPARgamma) agonists. PPARgamma co-association with transcription factor NFAT. The Journal of biological chemistry. 2000;275(7):4541-4.

288. Jiang C, Ting AT, Seed B. PPAR-gamma agonists inhibit production of monocyte inflammatory cytokines. Nature. 1998;391(6662):82-6. Epub 1998/01/09.

289. Kintscher U, Goetze S, Wakino S, Kim S, Nagpal S, Chandraratna RA, et al. Peroxisome proliferator-activated receptor and retinoid X receptor ligands inhibit monocyte chemotactic protein-1-directed migration of monocytes. European journal of pharmacology. 2000;401(3):259-70.

290. Rinaldi SF, Catalano RD, Wade J, Rossi AG, Norman JE. Decidual neutrophil infiltration is not required for preterm birth in a mouse model of infection-induced preterm labor. Journal of immunology. 2014;192(5):2315-25. Epub 2014/02/07.

291. Reddy RC, Narala VR, Keshamouni VG, Milam JE, Newstead MW, Standiford TJ. Sepsis-induced inhibition of neutrophil chemotaxis is mediated by activation of peroxisome proliferator-activated receptor-{gamma}. Blood.

2008;112(10):4250-8. Epub 2008/06/07.

292. Blois SM, Alba Soto CD, Tometten M, Klapp BF, Margni RA, Arck PC. Lineage, maturity, and phenotype of uterine murine dendritic cells throughout gestation indicate a protective role in maintaining pregnancy. Biology of reproduction. 2004;70(4):1018-23. Epub 2003/12/19.

293. Bizargity P, Bonney EA. Dendritic cells: a family portrait at mid-gestation. Immunology. 2009;126(4):565-78. Epub 2008/09/10.

294. Faveeuw C, Fougeray S, Angeli V, Fontaine J, Chinetti G, Gosset P, et al. Peroxisome proliferator-activated receptor gamma activators inhibit interleukin-12 production in murine dendritic cells. FEBS letters. 2000;486(3):261-6.

295. Romero R, Manogue KR, Mitchell MD, Wu YK, Oyarzun E, Hobbins JC, et al. Infection and labor. IV. Cachectin-tumor necrosis factor in the amniotic fluid of women with intraamniotic infection and preterm labor. American journal of obstetrics and gynecology. 1989;161(2):336-41. Epub 1989/08/01.

296. Casey ML, Cox SM, Beutler B, Milewich L, MacDonald PC. Cachectin/tumor necrosis factor-alpha formation in human decidua. Potential role of cytokines in infection-induced preterm labor. The Journal of clinical investigation. 1989;83(2):430-6. Epub 1989/02/01.

297. Romero R, Mazor M, Sepulveda W, Avila C, Copeland D, Williams J. Tumor necrosis factor in preterm and term labor. American journal of obstetrics and gynecology. 1992;166(5):1576-87. Epub 1992/05/01.

298. Jacobsson B, Holst RM, Wennerholm UB, Andersson B, Lilja H, Hagberg H. Monocyte chemotactic protein-1 in cervical and amniotic fluid: relationship to microbial invasion of the amniotic cavity, intra-amniotic inflammation, and

preterm delivery. American journal of obstetrics and gynecology. 2003;189(4):1161-7. Epub 2003/10/31.

299. Esplin MS, Peltier MR, Hamblin S, Smith S, Fausett MB, Dildy GA, et al. Monocyte chemotactic protein-1 expression is increased in human gestational tissues during term and preterm labor. Placenta. 2005;26(8-9):661-71. Epub 2005/08/09.

300. Esplin MS, Romero R, Chaiworapongsa T, Kim YM, Edwin S, Gomez R, et al. Monocyte chemotactic protein-1 is increased in the amniotic fluid of women who deliver preterm in the presence or absence of intra-amniotic infection. The journal of maternal-fetal & neonatal medicine : the official journal of the European Association of Perinatal Medicine, the Federation of Asia and Oceania Perinatal Societies, the International Society of Perinatal Obstet. 2005;17(6):365-73. Epub 2005/07/13.

301. Tornblom SA, Klimaviciute A, Bystrom B, Chromek M, Brauner A, Ekman-Ordeberg G. Non-infected preterm parturition is related to increased concentrations of IL-6, IL-8 and MCP-1 in human cervix. Reproductive biology and endocrinology : RB&E. 2005;3(39):1-10. Epub 2005/08/27.

302. Shynlova O, Tsui P, Dorogin A, Lye SJ. Monocyte chemoattractant protein-1 (CCL-2) integrates mechanical and endocrine signals that mediate term and preterm labor. Journal of immunology. 2008;181(2):1470-9. Epub 2008/07/09.

303. Romero R, Grivel JC, Tarca AL, Chaemsaithong P, Xu Z, Fitzgerald W, et al. Evidence of perturbations of the cytokine network in preterm labor. American journal of obstetrics and gynecology. 2015. Epub 2015/08/02.

304. Lappas M, Permezel M, Georgiou HM, Rice GE. Regulation of proinflammatory

cytokines in human gestational tissues by peroxisome proliferator-activated receptor-gamma: effect of 15-deoxy-Delta(12,14)-PGJ(2) and troglitazone. The Journal of clinical endocrinology and metabolism. 2002;87(10):4667-72. Epub 2002/10/05.

305. Meier CA, Chicheportiche R, Juge-Aubry CE, Dreyer MG, Dayer JM. Regulation of the interleukin-1 receptor antagonist in THP-1 cells by ligands of the peroxisome proliferator-activated receptor gamma. Cytokine. 2002;18(6):320-8. Epub 2002/08/06.

306. Hayflick L. The Limited in Vitro Lifetime of Human Diploid Cell Strains. Experimental cell research. 1965;37:614-36. Epub 1965/03/01.

307. Campisi J, d'Adda di Fagagna F. Cellular senescence: when bad things happen to good cells. Nature reviews Molecular cell biology. 2007;8(9):729-40. Epub 2007/08/02.

308. Kang TW, Yevsa T, Woller N, Hoenicke L, Wuestefeld T, Dauch D, et al. Senescence surveillance of pre-malignant hepatocytes limits liver cancer development. Nature. 2011;479(7374):547-51. Epub 2011/11/15.

309. Munoz-Espin D, Serrano M. Cellular senescence: from physiology to pathology. Nature reviews Molecular cell biology. 2014;15(7):482-96. Epub 2014/06/24.

310. Hirota Y, Daikoku T, Tranguch S, Xie H, Bradshaw HB, Dey SK. Uterine-specific p53 deficiency confers premature uterine senescence and promotes preterm birth in mice. The Journal of clinical investigation. 2010;120(3):803-15. Epub 2010/02/04.

311. Burnum KE, Hirota Y, Baker ES, Yoshie M, Ibrahim YM, Monroe ME, et al. Uterine deletion of Trp53 compromises antioxidant responses in the mouse

decidua. Endocrinology. 2012;153(9):4568-79. Epub 2012/07/05.

312. Cha J, Bartos A, Egashira M, Haraguchi H, Saito-Fujita T, Leishman E, et al. Combinatory approaches prevent preterm birth profoundly exacerbated by gene-environment interactions. The Journal of clinical investigation. 2013;123(9):4063-75. Epub 2013/08/28.

313. Behnia F, Taylor BD, Woodson M, Kacerovsky M, Hawkins H, Fortunato SJ, et al. Chorioamniotic membrane senescence: a signal for parturition? American journal of obstetrics and gynecology. 2015. Epub 2015/05/31.

314. Menon R, Boldogh I, Hawkins HK, Woodson M, Polettini J, Syed TA, et al. Histological evidence of oxidative stress and premature senescence in preterm premature rupture of the human fetal membranes recapitulated in vitro. The American journal of pathology. 2014;184(6):1740-51. Epub 2014/05/17.

315. American College of O, Gynecology Committee on Practice B-O. ACOG Practice Bulletin Number 49, December 2003: Dystocia and augmentation of labor. Obstetrics and gynecology. 2003;102(6):1445-54. Epub 2003/12/10.

316. Macones GA, Hankins GD, Spong CY, Hauth J, Moore T. The 2008 National Institute of Child Health and Human Development workshop report on electronic fetal monitoring: update on definitions, interpretation, and research guidelines. Obstetrics and gynecology. 2008;112(3):661-6. Epub 2008/09/02.

317. Subramanian A, Tamayo P, Mootha VK, Mukherjee S, Ebert BL, Gillette MA, et al. Gene set enrichment analysis: a knowledge-based approach for interpreting genome-wide expression profiles. Proceedings of the National Academy of Sciences of the United States of America. 2005;102(43):15545-50. Epub 2005/10/04.

318. Munoz-Espin D, Serrano M. Cellular senescence: from physiology to pathology. Nature reviews Molecular cell biology. 2014;15(7):482-96.

319. Abbas T, Dutta A. p21 in cancer: intricate networks and multiple activities. Nature reviews Cancer. 2009;9(6):400-14.

320. Hay N, Sonenberg N. Upstream and downstream of mTOR. Genes & development. 2004;18(16):1926-45. Epub 2004/08/18.

321. Cha J, Hirota Y, Dey SK. Sensing senescence in preterm birth. Cell cycle. 2012;11(2):205-6. Epub 2011/12/23.

322. Brady CA, Jiang D, Mello SS, Johnson TM, Jarvis LA, Kozak MM, et al. Distinct p53 transcriptional programs dictate acute DNA-damage responses and tumor suppression. Cell. 2011;145(4):571-83. Epub 2011/05/14.

323. Demidenko ZN, Korotchkina LG, Gudkov AV, Blagosklonny MV. Paradoxical suppression of cellular senescence by p53. Proceedings of the National Academy of Sciences of the United States of America. 2010;107(21):9660-4. Epub 2010/05/12.

324. Sui X, Fang Y, Lou H, Wang K, Zheng Y, Lou F, et al. p53 suppresses stress-induced cellular senescence via regulation of autophagy under the deprivation of serum. Molecular medicine reports. 2015;11(2):1214-20. Epub 2014/11/06.

325. Li T, Kon N, Jiang L, Tan M, Ludwig T, Zhao Y, et al. Tumor suppression in the absence of p53-mediated cell-cycle arrest, apoptosis, and senescence. Cell. 2012;149(6):1269-83. Epub 2012/06/12.

326. Valente LJ, Gray DH, Michalak EM, Pinon-Hofbauer J, Egle A, Scott CL, et al. p53 efficiently suppresses tumor development in the complete absence of its cell-cycle inhibitory and proapoptotic effectors p21, Puma, and Noxa. Cell reports.

2013;3(5):1339-45. Epub 2013/05/15.

327. Meek DW. P53 levels govern the choice between senescence and quiescence. Aging. 2010;2(10):637-8.

328. Foley JF. Provoking Preterm Birth. Science Signaling. 2011;4(198):ec311-ec.

329. Yan HX, Wu HP, Zhang HL, Ashton C, Tong C, Wu H, et al. p53 promotes inflammation-associated hepatocarcinogenesis by inducing HMGB1 release. Journal of hepatology. 2013;59(4):762-8. Epub 2013/05/30.

330. Menon R, Behnia F, Polettini J, Saade GR, Campisi J, Velarde M. Placental membrane aging and HMGB1 signaling associated with human parturition. Aging. 2016;8(2):216-30. Epub 2016/02/07.

331. Salminen A, Kauppinen A, Kaarniranta K. Emerging role of NF-kappaB signaling in the induction of senescence-associated secretory phenotype (SASP). Cellular signalling. 2012;24(4):835-45. Epub 2011/12/21.

332. Kamalakannan V, Shiny A, Babu S, Narayanan RB. Autophagy protects monocytes from Wolbachia heat shock protein 60-induced apoptosis and senescence. PLoS neglected tropical diseases. 2015;9(4):e0003675. Epub 2015/04/08.

333. Pugin J. How tissue injury alarms the immune system and causes a systemic inflammatory response syndrome. Annals of Intensive Care. 2012;2:27-.

334. Goncalves LF, Chaiworapongsa T, Romero R. Intrauterine infection and prematurity. Mental retardation and developmental disabilities research reviews. 2002;8(1):3-13. Epub 2002/03/29.

335. Romero R, Espinoza J, Chaiworapongsa T, Kalache K. Infection and prematurity and the role of preventive strategies. Seminars in neonatology : SN.

2002;7(4):259-74. Epub 2002/10/29.

336. Romero R, Chaiworapongsa T, Espinoza J. Micronutrients and intrauterine infection, preterm birth and the fetal inflammatory response syndrome. The Journal of nutrition. 2003;133(5 Suppl 2):1668S-73S. Epub 2003/05/06.

337. Cheng HT, Wang YC, Lo HC, Su LT, Lin CH, Sung FC, et al. Trauma during pregnancy: a population-based analysis of maternal outcome. World journal of surgery. 2012;36(12):2767-75. Epub 2012/09/04.

338. Dole N, Savitz DA, Hertz-Picciotto I, Siega-Riz AM, McMahon MJ, Buekens P. Maternal stress and preterm birth. American journal of epidemiology. 2003;157(1):14-24. Epub 2002/12/31.

339. DeFranco E, Moravec W, Xu F, Hall E, Hossain M, Haynes EN, et al. Exposure to airborne particulate matter during pregnancy is associated with preterm birth: a population-based cohort study. Environmental Health. 2016;15(1):1-8.

340. Dutta EH, Behnia F, Boldogh I, Saade GR, Taylor BD, Kacerovsky M, et al. Oxidative stress damage-associated molecular signaling pathways differentiate spontaneous preterm birth and preterm premature rupture of the membranes. Molecular human reproduction. 2016;22(2):143-57. Epub 2015/12/23.

341. Behnia F, Taylor BD, Woodson M, Kacerovsky M, Hawkins H, Fortunato SJ, et al. Chorioamniotic membrane senescence: a signal for parturition? American journal of obstetrics and gynecology. 2015;213(3):359 e1-16. Epub 2015/05/31.

ABSTRACT

THE ROLE OF ALARMINS, INVARIANT NKT CELLS AND SENESCENCE IN THE PATHOPHYSIOLOGY OF STERILE INTRA-AMNIOTIC INFLAMMATION

by

OLESYA PLAZYO

August 2016

Advisor: Nardhy Gomez-Lopez, Ph.D.

Major: Physiology (Reproductive Sciences Concentration)

Degree: Doctor of Philosophy

Preterm birth is defined as the delivery of a live baby prior to the 37th week of gestation. It is the leading cause of neonatal mortality worldwide. Preterm neonates are at a higher risk for short- and long-term complications, and prematurity places significant burden on our society. Elucidation of the mechanisms that lead to spontaneous preterm labor will enable development of therapies to prevent this syndrome. We aimed to study pathological inflammation that is implicated in the pathophysiology of spontaneous preterm labor.

Pathological inflammation can be initiated by the activation of innate immunity either by microorganisms or alarmins, which are endogenous danger signals derived cellular stress or injury. The inflammatory process initiated by alarmins in the amniotic cavity is referred to as sterile intraamniotic inflammation because it occurs in the absence of detectable microbial infection. Sterile intra-amniotic inflammation is more common than microbial-associated intra-amniotic inflammation in patients with intact chorioamniotic membranes who undergo spontaneous preterm labor, and administration of such alarmins as IL1α or HMGB1 was shown to induce preterm birth.

Our major aim was to determine whether HMGB1 and three additional alarmins (S100A12, monosodium urate, and HSP70) are capable of inducing sterile inflammation of the chorioamniotic membranes and by what molecular mechanism.

Our findings show that HMGB1, S100A12, monosodium urate, and HSP70 greatly increase secretion of pro-inflammatory cytokine IL-1β from the chorioamniotic membranes and up-regulate other pro-inflammatory pathways leading to collagen remodeling and synthesis of labor promoting enzyme prostaglandin synthase 2. We also found that activation of iNKT cells, which was shown to occur via stimulation with alarmins, induces preterm birth in mice by activating $CD4^+$ and $CD8^+$ T cells as well as innate immune cells and by establishing pro-inflammatory microenvironment at the maternal-fetal interface. We also identified rosiglitazone, an anti-inflammatory drug that dampens iNKT-dependent inflammation, as a potent treatment for preterm labor in mice. Finally, our data demonstrates that preterm labor is associated with dysregulated expression of senescence-associated genes and accumulation of senescence markers. Cellular senescence is characterized by release of pro-inflammatory mediators, including alarmins, and thus may provide a source of inflammatory signaling in a subset of patients who undergo preterm parturition.

AUTOBIOGRAPHICAL STATEMENT

Olesya Plazyo

Education

Ph.D. in Physiology (Reproductive Sciences Concentration) – Wayne State University, School of Medicine, Department of Physiology, Detroit, MI (2013-present)

M.S. in Molecular Biology, Wayne State University, Detroit, MI (2012)

B.A. in Biological Sciences, Wayne State University, Detroit, MI (2006)

Peer Reviewed Publications

1. Romero R, Xu Y, **Plazyo O**, Chaemsaithong P, Chaiworapongsa T, Unkel R, Than NG, Chiang PJ, Dong Z, Xu Z, Tarca A, Abrahams V, Hassan SS, Yeo L, Gomez-Lopez N. A role for the inflammasome in spontaneous labor at term. Am J Reprod Immunol. 2016 Mar 8. doi: 10.1111/aji.12440. PMID: 26952361
2. Xu Y, Romero R, Miller D, Kadam L, Mial TN, **Plazyo O**, Garcia-Flores V, Hassan SS, Xu Z, Tarca AL, Drewlo S, Gomez-Lopez N. An M1-like Macrophage Polarization in Decidual Tissue during Spontaneous Preterm Labor That Is Attenuated by Rosiglitazone Treatment. J Immunol. 2016 Mar 15;196(6):2476-91. doi: 10.4049/jimmunol.1502055. Epub 2016 Feb 17; PMID: 26889045
3. Gomez-Lopez N, Romero R, **Plazyo O**, Panaitescu B, Furcron AE, Miller D, Roumayah T, Flom E, Hassan SS. Intra-Amniotic Administration of HMGB1 Induces Spontaneous Preterm Labor and Birth. Am J Reprod Immunol. 2016 Jan;75(1):3-7. doi: 10.1111/aji.12443; PMID: 26781934
4. St Louis D, Romero R, **Plazyo O***, Arenas-Hernandez M, , Panaitescu B, Xu Y, Milovic T, Xu Z, Bhatti G, Mi QS, Drewlo S, Tarca AL, Hassan SS, Gomez-Lopez N. Invariant NKT Cell Activation Induces Late Preterm Birth That Is Attenuated by Rosiglitazone. J Immunol. 2016 Feb 1; 196(3):1044-59. doi: 10.4049/jimmunol.1501962; PMID: 26740111
5. Furcron AE, Romero R, **Plazyo O**, Unkel R, Xu Y, Hassan SS, Chaemsaithong P, Mahajan A, Gomez-Lopez N. Vaginal progesterone, but not 17α-hydroxyprogesterone caproate, has antiinflammatory effects at the murine maternal-fetal interface. Am J Obstet Gynecol. 2015 Dec;213(6):846.e1-846.e19. doi: 10.1016/j.ajog.2015.08.010; PMID: 26264823
6. Xu Y, **Plazyo O**, Romero R, Hassan SS, Gomez-Lopez N. Isolation of Leukocytes from the Human Maternal-fetal Interface. J Vis Exp. 2015 May 21;(99):e52863. doi: 10.3791/52863; PMID: 26067211
7. Szalai G, Romero R, Chaiworapongsa T, Xu Y, Wang B, Ahn H, Xu Z, Chiang PJ, Sundell B, Wang R, Jiang Y, **Plazyo O**, Olive M, Tarca AL, Dong Z, Qureshi F, Papp Z, Hassan SS, Hernandez-Andrade E, Than NG. Full-length human placental sFlt-1-e15a isoform induces distinct maternal phenotypes of preeclampsia in mice. PLoS One. 2015 Apr 10;10(4):e0119547. doi: 10.1371/journal.pone.0119547; PMID: 25860260
8. Szalai G, Xu Y, Romero R, Chaiworapongsa T, Xu Z, Chiang PJ, Ahn H, Sundell B, **Plazyo O**, Jiang Y, Olive M, Wang B, Jacques SM, Qureshi F, Tarca AL, Erez O, Dong Z, Papp Z, Hassan SS, Hernandez-Andrade E, Than NG. *In vivo* experiments reveal the good, the bad and the ugly faces of sFlt-1 in pregnancy. PLoS One. 2014 Nov 13;9(11):e110867. doi: 10.1371/journal.pone.0110867; PMID: 25393290